 65-13,894

WELKER, John Reed, 1936-
THE EFFECT OF WIND ON UNCONTROLLED
BUOYANT DIFFUSION FLAMES FROM
BURNING LIQUIDS.

The University of Oklahoma, Ph.D., 1965
Engineering, chemical

THE UNIVERSITY OF OKLAHOMA

GRADUATE COLLEGE

# THE EFFECT OF WIND ON UNCONTROLLED BUOYANT DIFFUSION FLAMES FROM BURNING LIQUIDS

A DISSERTATION

SUBMITTED TO THE GRADUATE FACULTY

in partial fulfillment of the requirements for the

degree of

DOCTOR OF PHILOSOPHY

BY

JOHN REED WELKER

Norman, Oklahoma

1965

THE EFFECT OF WIND ON UNCONTROLLED BUOYANT

DIFFUSION FLAMES FROM BURNING LIQUIDS

APPROVED BY

C. M. Sliepcevich

[illegible]

Phillip [illegible]

Michael L. McGinnis

C. H. Cook

F. M. Townsend

DISSERTATION COMMITTEE

## ACKNOWLEDGMENTS

There are always a number of people who contribute to a graduate program, and to whom sincere appreciation is owed. Of these, some deserve special recognition and gratitude. Justifiably, I am especially indebted to my committee chairman, Dr. C. M. Sliepcevich, and to the other members of the committee, Dr. T. J. Love, Dr. M. L. McGuire, Dr. C. P. Colver, Dr. C. H. Cook, and Dr. F. M. Townsend.

Unless the cooperation of those associates who are in daily contact with the many problems is available, those problems can be more difficult to solve. Among those associates deserving special appreciation are Dr. O. A. Pipkin and Mr. Joe Rios of the Flame Dynamics Laboratory. Neither should the work of Capt. Richard A. Milburn, who designed the wind tunnel and expedited its construction go unmentioned. I also appreciate the efforts of Mr. Mehdi Ghaffarzadeh, who made many of the calculations, and Mr. George Droescher who prepared the illustrations. The work of Mr. Jim Morrison, who supervised construction of the equipment and turned ideas into hardware was also important.

A special note of appreciation goes to those organizations who provided financial assistance during my graduate

program: Monsanto Chemical Company, The National Bureau of Standards, the U.S. Army Chemical Research and Development Laboratories at Edgewood Arsenal, and the University of Oklahoma Research Institute.

John Reed Welker

## TABLE OF CONTENTS

Page

APPENDICES

## LIST OF TABLES

## LIST OF ILLUSTRATIONS

Figure | Page

# THE EFFECT OF WIND ON UNCONTROLLED BUOYANT DIFFUSION FLAMES FROM BURNING LIQUIDS

## CHAPTER I

## INTRODUCTION

It has been estimated (53) that the annual cost of direct physical damage from fires in the United States is about $1,500,000,000. The annual deaths due to fire number about 11,500. If the costs of fire prevention, fire suppression, and treating the injured are considered, the total cost is found to be more than three times the direct fire loss cost. Even though these high costs occur each year, relatively little monies are available for increasing our basic understanding of fire. To be sure, much work has been done to determine the effects of fires in dwellings, particularly in Japan and Europe, but the information from this research is frequently difficult to analyze, and in many cases its usefulness is limited. Much of the fundamental work which has been carried out has been for small laminar flames; emphasis has been on spectroscopic studies, the measurement of temperature profiles in the flame and kinetic studies of the chemical reactions. Most of this fundamental work on small fires up to the present has been carried out using gaseous fuels. More recently, interest has been turned to larger fires, particularly those involving liquid and solid fuels. The incentive for studying fires from solids is the high loss due to fires in forests and buildings. Increased use of liquid and liquified gas fuels in commerce and industry has made necessary the study of fires from liquids.

In recent years an effort has been made to determine some fundamental properties of fires and to correlate those properties in such a fashion that it is possible to predict behavior of fires from design information based on model studies. It has been found possible to correlate fire data from gross flame and fuel properties in most cases, at least within the limits of experimental accuracy. Fundamental studies of flames from solid fuels were the first to be made, chiefly in Japan and Britain. These studies involved fires burning in wood cribs under calm conditions, both within inclosures and in the open. Both steady and unsteady state techniques have been devised to study fires from solids. Gaseous fuels have been used to study flame size as a function of burning rate and to aid in evaluating the interaction effects of fires. The study of fires from burning liquids has so far included the measurement of fire size and shape, flame temperature and radiation, and the fuel burning rate. The above work will be considered in more detail later.

Even though it has long been known that one of the most important factors to be considered in the study of fire problems is the influence of wind, most fires have been studied under calm conditions. A few of the effects of wind have been noted during fire studies, mostly because of their interference in attempts to burn fires under calm conditions. The few studies made on wind-blown fires have used gas or solid fuels almost exclusively. The information gained has been used to attempt to answer some of the questions concerning fire behavior under windy conditions. Unfortunately, enough information is not available in the literature to answer the many questions concerning the effect of wind on flames. Some of the questions which need to be answered are: What is the effect of wind on the rate of fuel consumption? How can the angle of tilt of a wind-blown flame be predicted? How does this bending influence the radiative and convective heat transfer downstream from flames? Since the temperature of the wake gases downstream from a flame are important in convective heat transfer, how can these temperatures be predicted? What is the effect of wind on the shape and size of a flame from a given source? All of this information should be correlated in such a way that it could be used for predicting wind effects on large-scale flames and estimating heat transfer rates. Ideally, the results of such studies should be correlated on readily available physical parameters.

As a first step toward answering some of these questions, this study was initiated to obtain experimental data on wind-blown fires. A large, low-speed wind tunnel for studying fires from burning liquids was constructed. The most important design requirement was to achieve a flat velocity profile for velocities in the range of 0.5 to 20 ft/sec and to have a suitable method for controlling the velocity. A special fuel delivery system was needed to maintain a constant fuel level in the burners. Both circular and channel burners were to be used, with circular burners ranging up to two feet in diameter and channel burners up to eight inches wide and five feet long.

Before proceeding with the discussion, some of the terminology requires definition. A flame is described as "buoyant" when the momentum forces causing it to rise from its source are largely due to the buoyancy of the hot flame gases. Such flames are the result of natural liquid and solid fires. "Jet" flames result when the fuel is fed to the fire at a rate such that the initial momentum of the fuel is large compared to the buoyancy forces of the hot flame gases. Gas fires frequently produce jet flames and are "controlled". Liquid and solid fires usually burn at a rate dependent only on the fuel and environmental conditions and are therefore called "uncontrolled". "Premixed" flames have fuel and oxidizer combined before the combustion zone is reached, and "diffusion" flames depend on molecular or eddy diffusion to mix the fuel and oxidizer at and within the combustion zone. The fires considered in the present study are uncontrolled, buoyant, diffusion flames.

## CHAPTER II

## REVIEW OF PREVIOUS WORK

### General Information

Historically, the investigation of fires from solid fuels was the first to be made. The incentive for studying solid-fueled fires was the damage to property resulting from fires in cities and forests. In fact, the first investigations were generally started following a particularly large fire in a city. These first studies were basically made to develop methods for preventing or slowing fire spread. The results were eventually translated into fire prevention and suppression techniques, fire codes, and later into methods for treating structural materials and clothing to limit flammability.

There are hundreds of papers in the literature which give results on fire research. They cover nearly all aspects of research into fire behavior, some in great detail and others with only a few bits of information. Kinbara (30) gives a summary of the historical background of fire research work in Japan and a bibliography of recent papers on fundamental fire research, fire detection, fire prevention, and fire suppression. Lawson (31, 32) summarizes the history of fire research in Britain and the work presently being done. He also gives a bibliography covering work by the Joint Fire Research Organization in several areas. Robertson (47) lists the work being done by the National Bureau of Standards in the United States, and Brown (7) summarizes current forest fire research work in the United States.

In addition to the large-scale fire tests there have been numerous investigations of small laminar flames. Temperature profiles through laminar flames from Bunsen burners and the compositions of these flames have been measured. Large numbers of spectrographic analyses have been reported in the literature. Reaction rates in small flames have been determined. The changes in flame size, reaction rate, temperature, and radiation have been measured for flames burning above and below atmospheric pressure. Since most of the information which has been gained does not directly concern the present problem, it will not be covered in greater detail. Most of the information presently available is covered by Gaydon and Wolfhard (22), Lewis and von Elbe (33), the _International Symposium on Combustion_ series (29), _Fire Research Abstracts and Reviews_ (17), and _Combustion and Flame_ (13). A new publication called _Pyrodynamics_ (43) has published an extensive bibliography covering many areas of fire research. Research into fire suppression and prevention activities is generally covered by the bulletins of various fire prevention societies in the countries where the work is being done. In addition, fire codes can often serve as a starting point for research in the fire prevention area.

## Fires From Burning Solids

Most of the early burning studies made on solid fuels were for the purpose of establishing enough information to allow for better design of buildings for fire prevention and suppression. Although much of the information gained is of limited value to the researcher who is considering basic fire behavior, the standards for testing materials and the codes controlling building practices constitute useful background information.

Obtaining and correlating data from large fires present two major difficulties: First, the number of variables involved is often so large as to preclude good measurement and environmental control. Second, by the very nature of larger fires, the turbulence generated by the fire causes fluctuation of the flame so as to complicate measurement of even the gross properties. Nevertheless, the best attempts to date in correlating large flame behavior have been presented as a function of the gross flame properties.

There are two general methods for testing fires from solids. Both utilize either a crib of wood sticks or a pile of randomly distributed fuel such as pine needles or excelsior. In one method all the fuel is ignited as simultaneously as possible, and the fire is allowed to burn in an unsteady fashion until the fuel is consumed. There is a period during which the fuel burning rate increases to a maximum, holds constant at this maximum for a period and then begins to decrease, until the fuel is finally consumed and the fire dies out. Data are generally taken during the constant burning rate period. In another method, a long crib or fuel bed is ignited at one end and the fire is allowed to burn through the fuel. In the first tests of this kind made by Fons, Bruce and Pong (19), the fuel crib was located on a movable belt. As the fire burned, the fuel was slowly moved into the fire, thereby keeping the location of the flame in the same position. After a few minutes, the fire could be studied at steady state conditions without the necessity for moving the instrumentation. Although many different sizes and configurations have been used, in most cases the dimensions of the cribs were of the order of 2 to 3 feet. The fuel depths generally averaged from a few inches to a foot, but there again there has been some variance. Differences in the sizes of the sticks used in the cribs and their spacing have also been investigated.

During the first studies on burning cribs an attempt was made to correlate the data on the physical size of flames. A number of studies has been made (20, 23, 57), using wood cribs. Thomas (57) has correlated some of these data by plotting the ratio of flame length to width or diameter as a function of $m''/\rho_a\sqrt{gD}$. He showed that the L/D ratios measured photographically could be correlated as

$$L/D = 42 \left(\frac{m''}{\rho_a \sqrt{gD}}\right)^{0.61} \tag{1}$$

where $L$ = flame height

$D$ = flame width or diameter

$m''$ = fuel burning rate, weight per unit time per unit area

$\rho_a$ = density of ambient air

$g$ = gravitational acceleration

Equation (1) is for fires burning under calm conditions from approximately radially symmetrical fuel beds. Thomas also correlated L/D data using the same dimensionless group for flames from large-scale wood fires, liquid fires, and gas fires, using the data of Blinov and Khudiakov (4), Broido and McMasters (6), Étienne (15), Faure (16) and Putnam and Speich (40). His correlation covers a range of L/D from about 0.01 to 100 and a range of $m''/\rho_a\sqrt{gD}$ of $10^{-5}$ to 100. The group $m''/\rho_a\sqrt{gD}$ is essentially a Froude number based on the burning rate, and L/D is of course the dimensionless flame height. In this same paper Thomas correlated data for the length of flames issuing from an enclosure through a window. The data were taken from fires burning within a cubical enclosure having one side completely removed. Flames burning from effectively infinite strips of wood were also studied and the L/D data correlated.

From the standpoint of the present work the L/D ratios for fires burning under windy conditions are more interesting. In this study Thomas photographed flames from burning cribs of white pine sticks in winds ranging from 5 to 15 ft/sec. From the photographs he was able to measure the lengths of the flames and correlate the L/D ratios. The resulting correlation showed

$$L/D = 70\left[\frac{(m'')^2}{\rho_a^2 gD}\right]^{0.43}\left(\frac{u^2}{gD}\right)^{-0.11} \tag{2}$$

where u is the wind velocity. As seen from Equation (2) the wind velocity affected the length of the flame much less than the burning rate did. The factor $u^2/gD$ is the Froude number in the form most frequently seen. The length of the flame may have also shown some slight dependence on the Reynolds number, but the effect was statistically insignificant. The results showed the L/D values for wind-blown flames to be about 0.82 times the L/D ratio for fires burning under calm conditions.

In a later paper (58), Thomas, Pickard, and Wraight reported on the height reached by the same wind-blown flames as discussed above. They also measured values of the inclination angle from the vertical, but they did not report them. The data used in this correlation show

$$\frac{\rho_a Hu}{m''D} = 56\left(\frac{u^2}{gD}\right)^{0.13} \tag{3}$$

where H is the height of the flame tip above horizontal. These data will be discussed later in connection with data from channel burners using liquid fuels.

All of the data reported by Thomas were from fires under the unsteady state. Fons (19) first developed the steady-state technique in which the object was to permit study of the parameters that govern combustion over an extended period. This technique was to be used to study solid-fueled fires under experimental conditions such that as many of the parameters as possible could be controlled and the quantitative effect of each on the fire could be determined. In order to study steady state systems, Fons designed a chain-belt mechanism to move the wood crib. The crib rests on its base on the chain belt; it is moved manually in such a manner as to keep the position of the fire constant with respect to a set measuring point. The mechanism also pulled two heavy asbestos sheets, one on each side of the fire, in synchronous movement with the flame to simulate the relative movement of the ground and the fire front. The base for the cribs consisted of several separate concrete slabs which were used as an aid in making heat balances by estimating the amount of heat conducted into them. Since the relative position of the fire was invariant, it was possible to fix thermocouples to a grid above the fire and to make measurements of the temperatures in the convection column. Samples of the combustion gas were collected in glass bottles for later analyses. Provisions were made for photography using time-lapse movies. The cribs were made relatively long, and after a period of buildup the fires reached steady-state conditions. The steady-state conditions were maintained until nearly all the crib had been burned. Through the use of this technique, steady-state fires lasting up to 30 minutes were possible. Fons used the above technique to measure the burning rates for cribs of white fir as a function of the wood density. He showed that burning rate and heat release rates decreased with increasing wood density. He also showed that the charcoal residue remaining after burning increased as the fuel loading ($lb/ft^2$) increased. Fons, Bruce, Pong, and Richards also used the steady state technique to measure flame size (20); these data were included by Thomas in his correlations.

Waterman, et al. (59) present some fairly extensive information on large fires in buildings, wood cribs, and liquid pools. The purpose of their work was not to treat exhaustively any single area, but rather to extend the available data to a higher level. Some of their wood cribs were larger than had been burned previously. They found a lower flame height than had previously been reported. They attributed this difference to the variation in wood spacing, which was not included as a factor in the correlations. In trying to model fire behavior in rooms, they found that it was necessary to use ½-scale models in order to obtain satisfactory results. Both liquid and solid fires were used to measure the parameters influencing the coalescence of fires from fuel sources in close proximity. The fires involved single and multiple cribs covering areas up to 150 square feet. The individual cribs ranged from two feet to six feet square. The results from these flame merging tests indicated that the fuel burning rates provide a more suitable description of flame coalescence than visual observations and that coalescence is a function not only of the proximity of the fires, but also of the total number of fires.

In a continuation of the work of Fons, Byram, et al. (12) burned cribs of wood sticks of different sizes and spacings to investigate further the work reported by Fons et al. (20, 21), in which it was found that burning rates decreased as fuel spacing decreased and smaller sticks were used. Byram et al. showed a decreasing burning rate with increasing stick size when the stick spacing was held constant. As the stick spacing increased for constant stick sizes, the burning rate increased. In order to measure some of the effects of wind on crib fires they constructed a wind tunnel with an 8-foot square cross section and facilities for controlling the air temperature and humidity entering the test section. A series of test runs was made in this tunnel during which they measured burning rates, flame angles of tilt and flame lengths. Their burning rate data show an increase with both wind speed and stick spacing for the ranges considered (0 - 13 ft/sec, 0.5 - 4.5 in, respectively). They noted that at higher wind speeds small secondary fires would ignite ahead of the flame front, making identification of the flame front and measurement of the rate of spread difficult. Although they report the flame angles of tilt and the flame length, they unfortunately did not include the width of the burning zone. It is therefore not possible to compare their data with that of other authors.

Although the primary fuels for studying solid-fueled fires in the laboratory have been wood sticks of various varieties, some work has been done using other fuels. Anderson (1) reports burning rate data for beds of ponderosa pine and white pine needles. He found that although fire spread rates were sensitive to fuel loading and the compactness of the fuel, he was able to make reproducible fuel beds. He also found that the width and depth of fuel bed influenced the fire spread rates unless the fuel bed was wider than 12 inches and more than 3 inches deep. Anderson used a variation of the moving fuel bed technique. He made one of the few systematic investigations into the effect of fuel moisture content on the rate of fire spread. He found that over a fuel moisture content range of 5 - 15 per cent the rate of fire spread decreased linearly with increasing moisture content. Fons, Clements, and George (21) had found a similar result for cribs of white fir sticks. Although Anderson found the rates of fire spread approximately the same for the two fuels he studied, he found a wide difference in fire intensity. This difference in fire intensity affected the results in several ways. The residue remaining following a fire in ponderosa pine needles was about 5 to 20 per cent; for white pine needles the residue was 60 to 90 per cent of the total fuel loading. The radiant heat flux was about three or four times as large for the ponderosa pine needle fires, but it decreased more rapidly with moisture content than did that from the white pine needle fires. The physical size of the flames was much larger for ponderosa pine needles according to photographs of the two types of fires.

Following the work by Anderson on fires burning under calm conditions, Anderson and Rothermel (2) conducted tests on the effect of wind on free-burning fires in pine needles. They used a wind tunnel which utilized virtually complete control over the air blown across the fires. They found that the L/D data could be correlated in the same manner as Thomas (57) had done with wood cribs, that the data formed a reasonable extension of the wood crib data, and that they lie just below Thomas' L/D values based on two large fires. The Anderson-Rothermel data include both calm and wind-blown fires since the effect of wind on the L/D ratios was not readily detectable. The factor most strongly influencing fire spread rates was the wind velocity. Winds having a velocity of 700 ft/min increased the fire spread rates from less than 1.0 ft/min to more than 20 ft/min.

For the higher wind rates low energy release rates were obtained under rapid flame spread rates. This behavior is characteristic of runaway fires. For slower wind rates, however, the energy release rates were much higher and resulted in the behavior characteristic of fire storms. Anderson and Rothermel also investigated the effect of air humidity on fire spread rates. They found that air humidity was not a factor except in cases where the fuel moisture content was changed by changes in humidity. Of special interest in the wind studies was a correlation of the flame bending angle. Anderson and Rothermel considered that the angle of the convection column was related to the momenta of the wind and the convection gases, as follows:

$$\tan\theta = \frac{\text{momentum of air stream}}{\text{momentum of convection column}} \tag{4}$$

where $\theta$ is the flame angle of tilt measured from the vertical. Since they hadn't enough data to evaluate the momentum of the convection column, they turned to the energy rates of the fire and the airstream. They assumed $\tan\theta$ to be proportional to the ratio of the energy rate per unit area of the airstream to the equivalent unit energy release rate of the fire. Their data showed good correlation with no evidence of dependence on moisture content or fuel species for the fires they burned. Their data were for fires having angles of tilt from about 25 degrees to about 60 degrees.

In 1952 Hamada (25) published the result of some work done in Japan to correlate the bending angles of flames. Apparently, no one in this country was aware of his work until very recently since it hasn't been referenced in any of the regular literature. Based on a momentum balance on the flame, Hamada derived the relationship

$$\tan \alpha = \frac{g(\rho_a - \rho_f)D}{K\rho_a u^2} \tag{5}$$

where

$\rho_f$ = flame density

K = a constant

$\alpha$ = angle of flame above the horizontal

In his work, $\alpha$ is the complement of the vertical angle of tilt $\theta$. After assuming that the ratio of flame density to air density could be replaced by the ratio of the absolute temperature of the airstream to the absolute flame temperature, and that the flame temperature was about 1000°C, Hamada obtained data in a wind tunnel to evaluate K in Equation (5). From the data on nearly a hundred runs he finally arrived at the relationship

$$\tan \alpha = \frac{4D}{u^2} \tag{6}$$

which was his practical equation for estimating the angle of inclination of a wind-blown flame. Equation (6) is a dimensional equation in which u must be expressed in meters/ sec and D in meters. The density ratio $(\rho_a - \rho_f)/\rho_a$ is assumed constant and equal to 0.772; the value of $\bar{K}$ was found by burning solid fuels. Hamada then obtained data for several burning houses and found reasonable agreement between the predicted angle and the actual angle.

McCarter and Broido (34) have recently measured radiative and convective heat transfer from burning wood cribs. They concluded that the radiation from burning cribs of western hemlock amounts to about 43 per cent of the total heat released during combustion. Of this radiative loss, they found that about one-half of the radiant energy came from the glowing combustion of the embers. They also indicated that the rate of spread of the fire depended very little on the amount of radiation from the flame itself.

The above data are largely from solid-fuel fires. As such, they may not be directly applicable to liquid fires, but nevertheless, are valuable from the standpoint of general design. If it proves possible to correlate flame behavior as a function of gross flame and fuel properties, the data from solid-fuel fires will prove invaluable.

## Fires From Burning Liquids

Even though liquid fuels have been used for some time, it has only been within the past ten years that any detailed studies have been made into their burning characteristics. In 1957 Blinov and Khudiakov (4) published the results of their extensive work on burning pools of liquid fuels ranging from 3.7 mm to 22.9 meters in diameter. An immediate interest was created in liquid fires since their data showed three burning regimes to be present. For burners having diameters less than 3 cm all the flames were laminar and the fuel burning rate decreased as the burner diameter increased. The flame L/D ratio also decreased as the burner diameter increased. (The burning rate reported in this work and most other literature sources is given as a liquid level regression velocity in units of length per unit time). For burners having diameters from 3 cm to 130 cm, flame turbulence started and gradually increased. As the pan diameters were increased from 3 cm to 10 cm the burning rate gradually leveled off, becoming a minimum at about 10 cm. A further increase in pan diameter increased the fuel burning rate until at about 130 cm a fully turbulent flame was obtained. For burners larger than 130 cm the burning rate was constant with changes in pan diameter. The flame L/D ratios continued to decrease until the turbulent regime was reached, after which they became constant at a value of about 1.7.

In a review of Blinov and Khudiakov's paper, Hottel (28) showed that by considering the heat transfer mechanisms in the laminar, transition and turbulent burning regimes it was possible to explain qualitatively the behavior of the liquid pool fires. The burning rate depends on the rate of fuel vaporization, which is in turn dependent on the rate of heat feedback from the flame to the fuel. Hottel showed that the vaporization rate per unit of surface area would be proportional to q, and that q could be given by

$$\frac{q}{\pi D^2/4} = \frac{4k(T_f - T_b)}{D} + U(T_f - T_b) + \sigma F(T_f^4 - T_b^4)(1 - e^{-\varkappa D}) \quad (7)$$

where

- $q$ = the heat transfer rate to the fuel
- $k$ = conduction coefficient
- $U$ = convection coefficient
- $\sigma$ = Stefan-Boltzmann constant
- $F$ = view factor
- $\varkappa$ = Beer's law extinction coefficient to allow for increasing opacity with thickness
- $T_f$ = absolute flame temperature
- $T_b$ = absolute temperature of fuel

It is apparent from Equation (7) that as the diameter increases the conduction term becomes smaller in comparison to the convective and radiative terms. Blinov and Khudiakov were aware of this fact and commented on the decrease of heat conduction relative to the other terms as a cause of reduced burning rates in the laminar region. As intermediate sizes are reached the influence of the convective term increases, but because of the flame thinness the radiative term will still be relatively small. For large diameters the convective term will become approximately constant and the radiative term will dominate due to the thickness of the flame. The radiative term will also become constant since $\varkappa D$ is so large. The burning rate will therefore become constant at large diameters. The fuels used by Blinov and Khudiakov were gasoline, tractor kerosene, diesel oil, and solar oil, all of which are mixtures of hydrocarbons.

Emmons (14) later designed some rimless brass dishes to study further the effect of pan diameter on burning rate. He burned methanol and acetone in dishes ranging from one-quarter to ten inches in diameter. The edges of his pans were very thin and well insulated. He found that the burning rate continued to drop as the size of the pans decreased; although his data agreed with that of Blinov and Khudiakov for pans having diameters from 4 inches to 10 inches, the data did not agree for the smaller pan sizes. When Emmons placed his pans on top of the table and exposed the rims, his data more nearly matched that of Blinov and Khudiakov. He therefore postulated a four-step mechanism by which heat was transferred in the conduction term proposed by Hottel. In this mechanism heat was first transferred from the flame to the table top by radiation. Convective heat transfer was then responsible for heat transfer to the inducted air; this inducted air then transferred heat to the pan rim by convection. Finally, the heat was transferred through the pan rim by conduction to the fuel. There were also the direct convection and radiation from the flame to the fuel. Emmons also measured the difference in burning rates before and after blackening the bottoms of his pans with lampblack. He found about 7 per cent increase in burning rates for acetone, but no change for methanol. As he pointed out, this observation does not imply that the radiation transfer to the liquid is small. More likely methanol tends to absorb its own radiation better than does acetone, and methanol burns with a nearly non-luminous flame. It might also be pointed out that Emmons used pans containing fuel only 3/16 inches deep. He measured the rate by igniting the fuel and noting the time elapsed until the fire burned out. His burning tests were therefore at unsteady-state conditions. In addition, it is probable that all the flame radiation back to the fuel was not absorbed by the fuel. In one test he measured the pan temperature with a single thermocouple and found the pan temperature to be higher than the boiling temperature of the fuel.

In 1956 Rasbash, Rogowski, and Stark (46) published the results of burning tests made using a circular pan 30 cm in diameter. They measured flame shape and size, flame temperature and emissivity, the rate of burning and composition changes for alcohol and hydrocarbon fuels. In their work the liquid level was maintained constant and steady-state burning measurements were made. They found that most of the flames had diameters near the base which were slightly less than the burner diameter, and that with the exception of the alcohol flames, all were nearly cylindrical in shape. They found that for alcohol heat transfer to the fuel could be assumed to be convection controlled, while for petrol, benzole, and kerosene radiation appeared to be the dominant factor.

The Bureau of Mines has carried out extensive work to measure and correlate the burning rates of liquid fuels, and the results are published in various places (9, 10, 11, 60). Burgess, Strasser, and Grumer (10) report much of this work. A number of fuels of widely different chemical species and burning rates were studied; their burning rates under calm conditions were measured as a function of the burner diameter. It was shown that the burning rates could be represented by the empirical expression

$$v = v_{\infty} \ (1 - e^{-kD}) \tag{8}$$

where

$v$ = liquid level regression rate

$v_{\infty}$ = liquid level regression rate for large pan diameters

$k$ = a constant

$D$ = pan diameter

They also found that the burning rate for tests made under windy conditions were approximately equal to $v_{\infty}$ as shown by data taken in various natural and artificial winds varying up to about 4 meters/second. They correlated the values of $v_{\infty}$ for nine fuels of widely varying burning rates ($v_{\infty}$ from about 0.2 cm/min to about 1.3 cm/min) as a function of the fuel properties, obtaining

$$v_{\infty} = 0.0076 \frac{\Delta H_c}{\Delta H_v} \tag{9}$$

where $\Delta H_c$ and $\Delta H_v$ are the net heat of combustion and the heat of vaporization, respectively. Measurements were made of the radiant heat flux to the surroundings, and it was found to be in the range of 20 per cent to 40 per cent of the heat of combustion.

Magnus (35) investigated the behavior of ethanol and gasoline fires with emphasis on applying the results to fire problems involving liquid storage tanks. He used for his burners tanks ranging from 12 cm to 120 cm in diameter and from 16 cm to about 160 cm in height. Investigations were made on the burning rate of the fuel and the temperature profile in the flame and convection column under calm conditions. He found, as have others, that the burning rate increased with increasing pan diameters. Furthermore, he investigated the effect of freeboard height (height of burner rim above fuel surface) on the burning rate. It was found that the effect of freeboard height on burning rate was a complex function, dependent not only on the freeboard height but also on the test tank height to diameter ratio and the fuel composition. It was found that an increase in freeboard height caused the burning rate to decrease. The rate of decrease was higher for gasoline than for ethanol. After the freeboard height became more than half the tank height, the ethanol burning rates were greater than the gasoline burning rates. The temperatures were found to have maxima from 600 to 800°C, with the gasoline temperature ranging about 10 to 15 per cent higher than the ethanol temperatures.

The maximum temperature would decrease as the freeboard height increased although for the test configurations studied, the maximum temperature for each run was found to be located at about the same height above the liquid surface.

Fons (18) reported data for liquid burning tests in which the pan diameters varied from 0.22 inches to 11.94 inches. His results showed the same sort of behavior as did those of Blinov and Khudiakov, even though his burners had a water jacket surrounding them to cool the rim. His tests must be regarded as unsteady state because he did not allow the fuel temperature to become constant. Further, for fires from burners 6 inches and larger in diameter, the burning rates were still increasing slightly when the runs were stopped.

There has been a controversy raised in the literature concerning whether the dominant factor in heat feedback to a liquid pool (or any freeburning fire in general) is convection or radiation controlled. Spalding (50) took issue with those who felt that radiation was the dominant mechanism of heat feedback for large fires and presented arguments showing that calculations based on his earlier convection theory (51) would predict the burning rate constant in Equation (9) to be 0.003. He inferred that an extension of his earlier theory predicted the constancy of burning rate at large pan diameter and that the predicted rates would be of the same order of magnitude as experimental data. Burgess and Grumer (8), however, pointed out that the flames above a large liquid pool do not conform to the shapes assumed by Spalding. Further, they showed that the fuel vapors above a burning liquid pool might be much cooler than the flame temperature and that a sharp discontinuity at the liquid surface was not found in some cases. They also pointed out that the sides of the flame near the fuel (for calm flames) are remarkably steady, thus making convection transfer less important. It seems that in order to resolve this question some specific measurements of radiation back to liquid pools should be made. Nevertheless, it must be admitted that both convection and radiation are important, both are present in pool burning, and as yet no completely satisfactory method has been found to separate them.

There have been few studies showing the effect of wind on liquid pool fires. Hirst and Sutton (26) studied the effect of wind on kerosene and isododecane fires to determine the velocity at which the flame would blow off the pool. Their work was prompted by the need for information concerning the nature of aircraft fires at high altitude. They used a 5-inch square tray 0.8 inches deep mounted in a variable-density wind tunnel and measured the extinction velocity as a function of pressure. The extinction velocity varied from about 2 ft/sec at 0.2 atm to about 15 ft/sec at 1.0 atm for a fuel burning at the same level as the top of the test airfoil. They also found that the presence of a small plate in front of the flame increased the extinction velocity sharply until a maximum was reached; the extinction velocity then decreased for larger plates.

Byram et al. (12) burned ethanol in a pan 12.7 inches square to aid in the determination of the mechanisms of fire spread. They observed that the burning rate was approximately constant with wind speeds up to 13 ft/sec. They do not give data for the angle of tilt of their flames, but they state that it was about 55 degrees for a wind speed of 3.7 ft/sec and nearly 80 degrees at 13.3 ft/sec. Perhaps the most interesting aspect of the information they give is that relating to the shape of the flames from a wind-blown pool fire. Figure 1 is essentially a reproduction of one of their figures showing that the vapors from the liquid fires do not immediately rise as they evaporate from the liquid fuel surface. These vertical cross sections of the flames were drawn from photographs of the flames with the exception of Diagram A. Diagram A shows the usual concept of the shape and deflection of a wind-blown flame in which there is a slight indentation of the flame on the downwind side due to air induction. Diagrams B, C, and D are the observed cross sections of flames burning under wind speeds of 3.7, 13.3, and 0.0 ft/sec. The dashed lines represent the estimated extent of the convection column. This trailing effect has not been noted in previous literature although several authors, Emmons (14) and Burgess, et al. (9), have

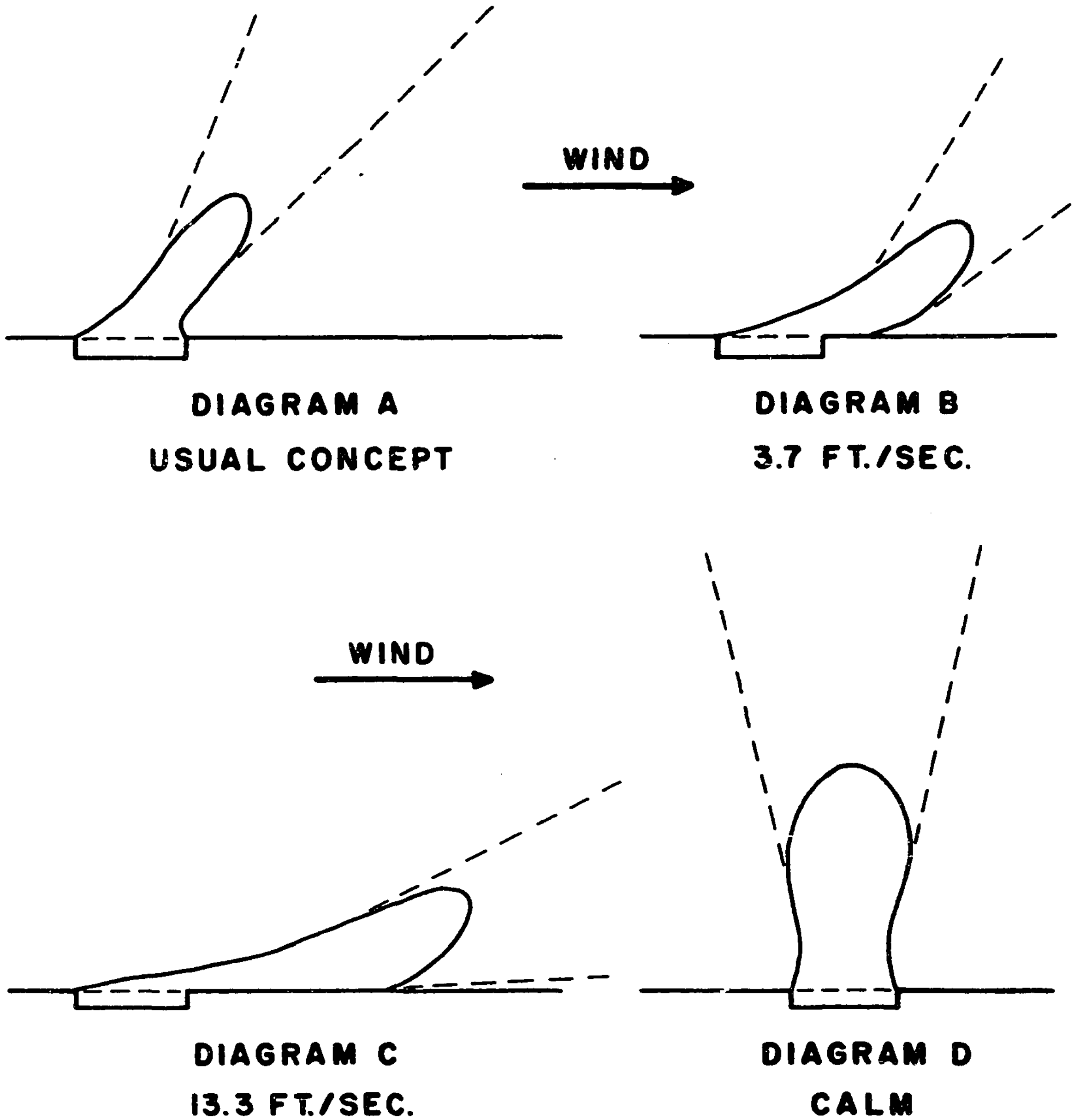


Figure 1. Shape and Bending of Wind-Blown Ethanol Flames

noticed that flames from burning liquid pools would slip off the burner edges due to slight wind movements. The reason for the trailing effect seems to be that the density of the fuel vapor at the fuel boiling point is higher than that of the surrounding air and thus tends to descend until it has been heated. In the case where the fuel is in a wind tunnel the vapors trail and burn along the floor. This sort of behavior has not been reported for fires from solids or for gas fires. The reason is probably because in the case of fires from solids pyrolysis must occur in order for vapors to be present and support a flame. This pyrolysis occurs at temperatures which are sufficiently high that the densities of the vapors are less than that of the surrounding air. In gas fires, of course, the usual fuel consists largely of methane, and the fuel density is less than the surrounding air. In such cases the vapor which supports the flame is of low enough density that it would rise even though it did not burn.

Waterman, et al. (59) performed a number of large-scale fire tests using liquid fuels in order to be better able to control various sizes and geometries of fires in their studies aimed at predicting fire damage from nuclear blasts. Although they conducted numerous liquid fires, they met with little success because of sideward movement of the flame. In many cases fuel vapors moved horizontally across the floor for some distance before igniting, resulting in a disturbance to the main flame. Since they felt that part of the difficulty was due to uneven heating of the fuel, they designed special fuel beds containing ceramic beads which protruded above the liquid surface to help even out the heating. Although the burning rate and flame height were reduced and the flame was a little more stable, even this technique did not produce the desired flame, so larger-scale tests were conducted outdoors. In their outdoor tests they burned single fires 16 feet square and groups of fires ranging up to 36 pans, 5 feet square and separated by 2.5 feet. They found the rate of burning to be constant at 0.14 in/min for No. 2 fuel oil, which indicated that wind velocities were not large enough to have a significant effect, although the wind was blowing at 5-15 mph for most of the tests. They noted a flame tilt of about 30 degrees at 5 mph and a flame tilt of 45 degrees or larger in winds of 10-15 mph. They were primarily interested in the coalescence of flames. They found that coalescence is not only a function of fire size and spacing but also the total number of fires. They also noticed that the wind did not penetrate the fires but rather tended to distort the flames. Although they produced some general information on the coalescence of fires, they stated that the uncontrolled wind and the large number of fires necessary for such a study made it difficult to analyze the many interacting effects.

## Gas Fires

Although it is probable that more laboratory investigations have been made using various gases as the fuel than any other kind, few of these studies have investigated any effect of wind on flame properties. Many very precise studies have been made of the behavior of gas fires under low pressures and high pressures, different atmospheres, different fuel rates, different fuels and a variety of other conditions. Flame temperature profiles and the composition of the gases in the flame have been measured. Many spectrographic analyses have given firm support to kinetic theories and have shown some of the intermediate products of combustion reactions. Much of this work is covered in the general references given previously. Since it is not directly connected with the present work further discussion of it is unnecessary.

Gas fires have one property which can be both an asset and a liability: their rate of fuel consumption is always fixed by the experimenter. This of course allows the use of widely varying fuel rates and fires ranging from small pilot flames to large jet flames. There is, however, no natural burning rate for a gas fire because it is not possible to have an open and yet contained vessel of a gaseous fuel for burning studies. Gaseous fuels do permit the use of premixed fuel-oxidizer combinations and have been extremely useful in studying kinetics of flame reactions.

Putnam and Speich (40, 42) have used gaseous fuel jets singly and in array to study the merging of individual fires into mass fires. In order for the study to satisfy the requirement of turbulent, buoyancy controlled flames, it was necessary to have a Reynolds number exceeding a critical value and a Froude number less than a critical value. They kept the orifice Reynolds number above 5000 to insure turbulent behavior and the Froude number below 8000 to insure buoyancy controlled flames. They found critical spacing distances below which the flame from a multiple point source behaved as a single-source flame and above which the behavior was that of a number of single flames. Putnam and Speich (41) and later Putnam (39) also reported on wind-blown gas fires from single sources, hexagonal patterns and single and multiple line sources. They were able to correlate the length of the flame and the horizontal and vertical projections of the flame as a function of a modified Froude number $u^2/gL^*$ where $L^*$ is the height of a flame from the same source under calm conditions. For point sources they found (for $u^2/gL^* > 0.2$)

$$L_{SV}/L^* = 0.45 \ (u^2/gL^*)^{-1/4} \tag{10a}$$

$$L_{SH}/L^* = 0.60 \ (u^2/gL^*)^{1/6} \tag{10b}$$

and for line fires they found the ratio of lengths to be

$$L_{SH}/L_{SV} = 1.4 \ (u^2/gL^*)^{1/2} \tag{11}$$

where $L_{SH}$ and $L_{SV}$ are the horizontal and vertical projections of the flame lengths, respectively. They also considered the data of Thomas, Pickard, and Wraight (58) and found for high

Froude numbers the $L_{SH}/L_{SV}$ ratio seemed to become constant for wood crib flames although the data scatter was bad. The data for flame lengths reported by Putnam and Speich (41) for single flames all have flame L/D values greater than 100. This value would seem to suggest that their single burner flames were affected at least to some extent by jet forces; they at least must have had a larger percentage of their momentum from the fuel than would a natural, uncontrolled flame or have had much larger fuel rates. Their single-flame data would therefore be difficult to compare with that from uncontrolled flames.

Perhaps the information available in the literature which has the greatest interest from the standpoint of flame bending is that of Pipkin and Sliepcevich (37). In their work they postulated a simple model for flame tilt based on the momenta due to flame buoyancy, fuel velocity and wind velocity. They assumed that a flame could be considered cylindrical in shape and that it retained its cylindrical shape when it was tilted by the force of the wind. They found that the angle of tilt of a wind-blown flame from a circular burner could be given by

$$\theta = \tan^{-1} \left\{ \frac{2C_f u^2/\pi}{(1 - \frac{\rho_f}{\rho_a})\ gD} \right\} \qquad (12)$$

where $C_f$ is a flame drag coefficient which must be evaluated experimentally. Pipkin and Sliepcevich measured the drag coefficients for flames from gas burners having an orifice velocity of about 0.5 ft/sec; this value is about the same velocity as that of the fuel vapors rising above a burning pool of liquid methane. After applying suitable corrections based on the difference in projected shape due to flame angle of tilt and on the differences in flame roughness factor, they were able to correlate their data as a function of the Reynolds number based on wind velocity, burner diameter, air density and viscosity. As they pointed out, their data could not be extrapolated to large-scale fires. Their success in correlating the flame drag coefficient certainly appears to validate their choice of model, and their model represents a simple and reasonable approach to the practical problem of fire modeling. They also propose an extension of their data based on casual observation of large flames which gives

$$\tan \theta = \frac{0.24\ \beta u^2}{D} \tag{13}$$

where $\beta$ is the correction for angle of tilt, and the extension is valid for large diameter flames. In Equation (13) u is in ft/sec and D is in feet. The extrapolation represented by Equation (13) is based on an approach to unity by the drag coefficient at high Reynolds numbers.

## Modeling and Dimensional Analysis

In an area such as the investigation of flame behavior it is generally difficult, if not impossible, to control all the variables in an experimental analysis and to explain mathematically the behavior of the system under consideration. Because of these difficulties modeling and dimensional analysis have been used as tools in analyzing the behavior of flames. In addition a large amount of work has been done in the area of modeling plumes, particularly plumes under calm conditions. While the methods proposed for modeling plumes are probably of little value in the area ne . a fire, it may be possible to modify them to aid in explaining the behavior of the convective columns farther away from the fire.

As yet, the theories proposed to explain the behavior of plumes under windy conditions are not applicable for studying fire problems because of the usual practice of attempting to predict the height of plumes above the ground and of assuming constant density of the plume. Bosenquet, et al. (5), Sutton (54), and Priestley (38) have presented theories which have been reasonably successful in predicting plume heights. The three methods are compared in the paper by Priestley for experimental data taken by Bosenquet, et al. Priestley's theory seems to give better results for these data than does either of the other two. Ball (3) obtained data for the height of the smoke plume rising from four orchard burners and used it to compare the three theories. He found that Priestley's theory represented his data best. It is important to realize that these theories and data are appropriate for measuring the height of a plume at some distance from the source. Temperature measurements were not made, and for most of the theories temperature differences between plume and surroundings must be very small.

Since it is impractical to make full-scale fires studies, it has been the usual practice to use models and attempt to correlate the data from model tests. Spalding (49) discusses the art of partial modeling; here he considers the fact that in cases where modeling is used it is frequently impossible to control (indeed, sometimes to specify) all the variables. For this reason many model experiments have deliberately ignored some of the similarity rules which should ordinarily be followed. He presents a table of dimensionless groups which are relevant to combustion modeling and then goes on to explain some of the simplifications which can be made. Although in all but a few rare cases complete combustion modeling is impossible, experience has shown that in many cases flouting certain of the rules does not cause too large an inaccuracy in the result. If the interest in an experiment is limited to fluid-mechanical processes, certain dimensionless groups may be neglected. For example, at high Reynolds numbers the effect of changing the Reynolds number may be neglected. The same may be said of high Froude numbers or low Mach numbers. In some cases exact geometrical similarity may be neglected, especially when only minor departures are used.

Hottel (27) reviews three methods for establishing dimensionless groups. The pi theorem, which has been used widely, defines a procedure which is largely mechanical in nature. It often yields dimensionless groups which are valid but in an unfamiliar form. Consequently it tends to mask the physical significance. A second approach is to formulate the equations applicable to the problem and to manipulate them until dimensionless groups appear. This procedure is bound to work, but it requires enough knowledge of the systems to write the equations, which is not necessary in using other methods. The third method is to take ratios of forces, mass rates, and energy rates expected to enter the problem at hand. Hottel has shown the method of applying these ratios by giving examples.

Taylor (55) has discussed the experimental results of Rankine (44, 45) on the temperature field downwind of a line of butane burners. Two sets of tests were made. One of these tests was outdoors in a large, new, unfilled reservoir and the other was in a series of wind tunnel experiments. It was realized that scaling in this case was possible only if both density and temperature distribution at similar points were the same. These requirements can be attained if

$$\left(\frac{u_0}{u_1}\right) = R^{-1/2} \quad \text{and} \quad \left(\frac{Q_0}{Q_1}\right) = R^{-3/2} \qquad (14)$$

where subscripts 0 and 1 refer to model and prototype, Q is the heat output of the fire per unit time and R is the ratio of linear size to full-scale size. The model tests were set up in accordance with Equation (14) and were found to correlate very well with the full-scale tests. Temperature rises were on the order of 10-15°F maximum.

Thomas (56) later used Rankine's data to prepare a dimensionless plot of the temperature rise downstream from the line of butane burners. He plotted the dimensionless temperature rise $\Phi_L$ versus the dimensionless velocity $\Omega_L$ for a number of values of z/x. Here

$$\Phi_L = \frac{(T - T_a)\,gx}{T_a\,(gQ'/\rho_a C_p T_a)^{2/3}} \tag{15}$$

and

$$\Omega_L = \frac{u}{(gQ'/\rho_a C_p T_a)^{1/3}} \tag{16}$$

where

- $T$ = the temperature at a point in the plume
- $C_p$ = specific heat of air
- $Q'$ = convective heat output per unit length per time
- $z$ = vertical distance above the ground

This form of the correlation can be obtained either from the differential equations governing the heat and momentum balance or from a direct dimensional analysis. The data used had been smoothed and interpolated and did not represent any temperature rises greater than 30°C. Wind speeds varied from 1.5 to 5 ft/sec and heating rates were up to 16,000 Btu per hr-ft. The convective flux was assumed to be 80 per cent of the total heat output. The correlation showed a surprisingly good relationship.

The foregoing are only a few examples of the use of modeling and dimensional analysis. Most of the correlations of flame length and interaction effects are based on modeling whereas dimensional analysis has been used to correlate most of the data presently available in its general forms. Use of dimensional analysis will be illustrated as it applies to the present problems in the next chapter.

# CHAPTER III

## THEORETICAL CONSIDERATIONS

### Flame Bending

The angle of tilt of a wind-blown flame does not seem to have been considered in most of the literature on flame behavior. Hamada (25) presented the results of his investigations in the form of an equation relating flame angle, flame size and wind velocity. Pipkin and Sliepcevich (37) correlated their data on flame bending in the form of a drag coefficient. Although Byram, et al. (12) measured and reported flame angles for burning solids, they did not report the size of the flames; neither did they correlate the flame bending data. In their work on burning wood cribs, Thomas, Pickard, and Wraight (58) measured flame angles. Although they did not report the bending data, they did list the lengths of the vertical and horizontal projections of the flame; these data can be used to calculate the bending angles. The following analysis follows the pattern of Pipkin and Sliepcevich (37), although it deviates slightly as will be explained.

Consider a flame from a pool of burning liquid such as shown in the photographs of Figure 2 and schematic diagram

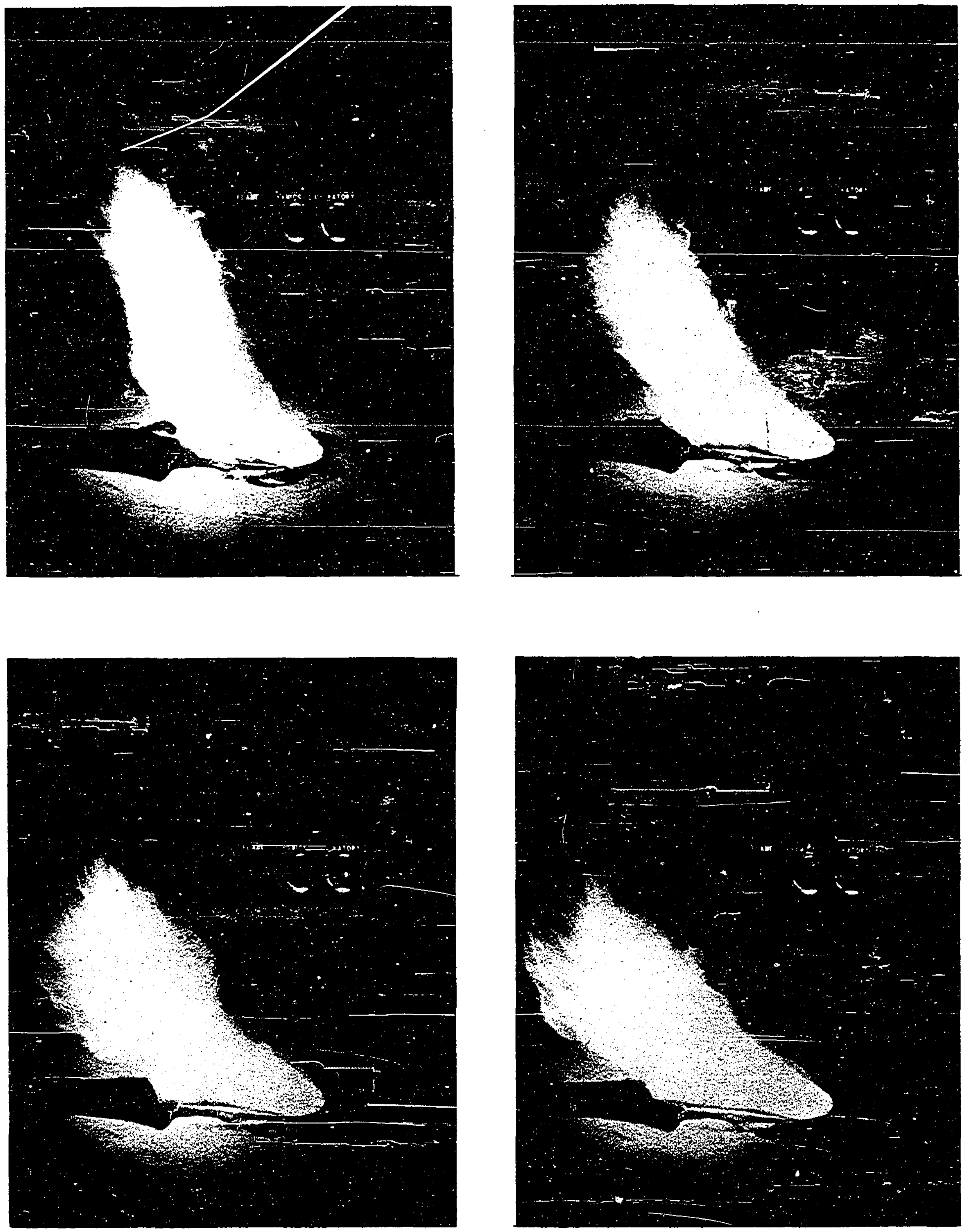

Figure 2. Effect of Wind on Fires From Circular Burners

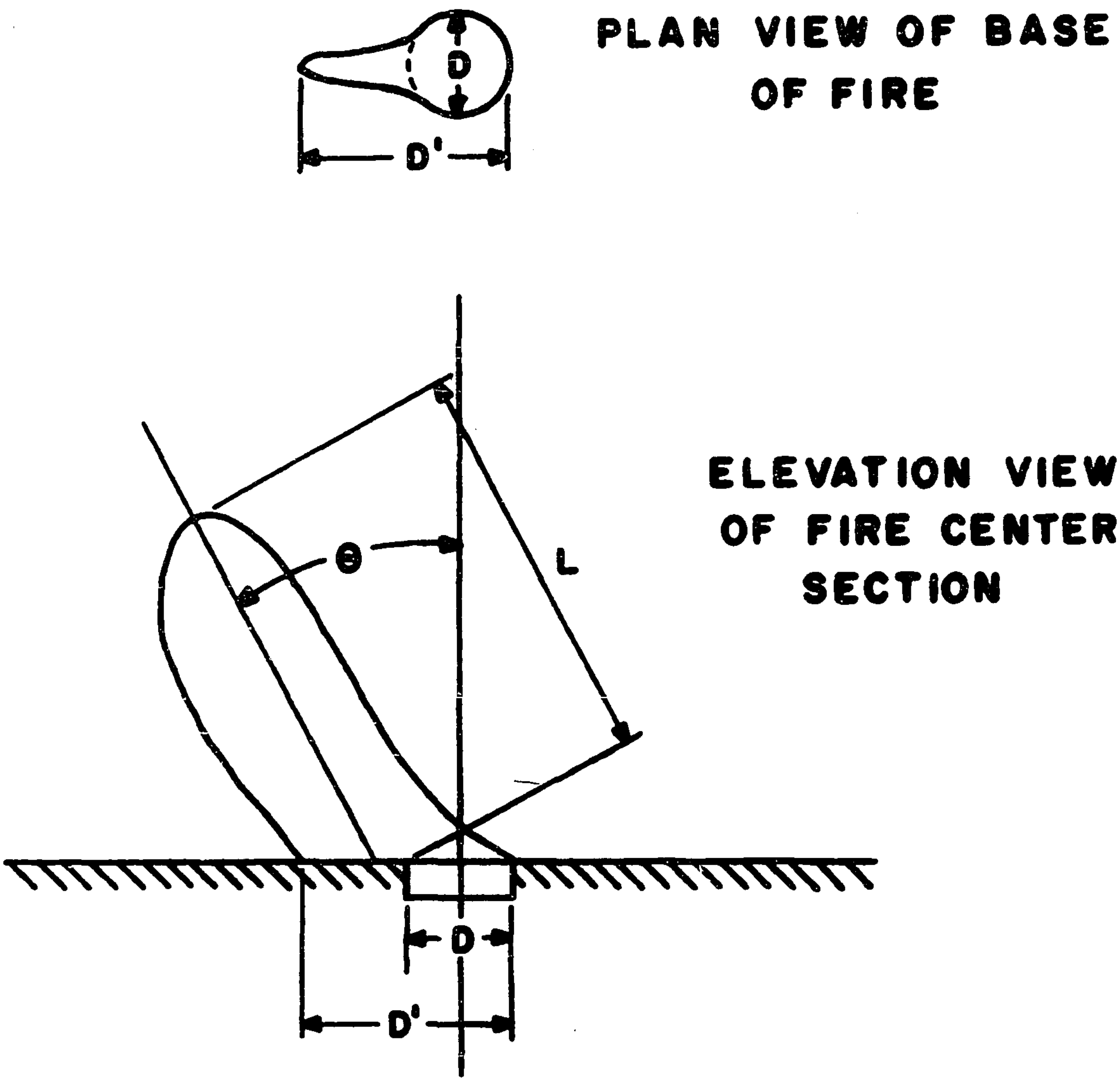


Figure 3. Plan and Elevation Views of a Wind-Blown Fire from a Circular Burner

of Figure 3. The photographs are of cyclohexane fires above a burner 8 inches in diameter, with wind speeds from about 1 ft/sec to 2 ft/sec, and the flame shape is seen to be similar to those shown by Byram, et al. for ethanol fires at similar velocities, Figure 1. Although it is not readily apparent from views such as those shown, the flame trailing along the floor follows a somewhat streamlined shape such as is also shown in Figure 3. Because of this streamlined shape and the fact that the flame near the upwind edge of the burner does not rise rapidly from the burner rim, the volume of the flame is approximately that of a cylinder of diameter D and length L.

The flame bending angle can be related to the other variables involved through a momentum balance. For an accounting period $\Delta t$, the momentum balance may be written in difference form as

$$\Delta_t(MV) = \Sigma(MV)_I - \Sigma(MV)_O + g_c \, \Sigma\int_t^{t+\Delta t}(F_f + F_b)dt \qquad (17)$$

where $MV$ = momentum

$F_f$ = field forces

$F_b$ = body forces

$g_c$ = gravitational constant

$t$ = time

Since only steady-state flames are being considered, the momentum change with respect to time is zero, and Equation (17) becomes

$$\Sigma(MV)_I - \Sigma(MV)_O + g_c \, \Sigma(F_f + F_b)\Delta t = 0 \qquad (18)$$

It is now assumed that air entrainment on diametrically opposed sides of the flame is approximately equal in magnitude; there is therefore no net momentum transfer into the flame due to the influx of air. Inasmuch as observations of the flame show that it becomes more nearly cylindrical as it rises from the source, the assumption of uniform air entrainment is probably not too unreasonable. The trailing of the flame along the floor is caused primarily by the negative buoyancy of the fuel vapors and not by uneven air entrainment for two reasons: first, the fuels having higher vapor densities trail along the floor farther, and second, the flame rises sharply from the floor as soon as the vapors are sufficiently heated.

With the assumption of uniform air entrainment, the horizontal component of the momentum balance can be written as

$$-(MV)_f \sin\theta + g_c F_b \Delta t = 0 \tag{19}$$

where $(MV)_f$ is the momentum of the flame gases and particles in the direction of the angle of tilt, and the downstream direction is considered positive. In this case the only body force acting on the flame is the drag due to the wind. It is given by

$$F_b = C_f LD \cos\theta \, \rho_a \frac{u^2}{2g_c} \tag{20}$$

where $C_f$ is the flame drag coefficient. Substituting Equation 20 into Equation (19) results in

$$(MV)_f \sin\theta = C_f\ LD \cos\theta \rho_a \frac{u^2}{2}\ \Delta t \tag{21}$$

The vertical component in the flame momentum balance is

$$-(MV)_f \cos\theta + (MV)_g + g_c\ F_f\ \Delta t = 0 \tag{22}$$

where $(MV)_g$ is the momentum contribution of the fuel gases rising from the liquid surface. The fuel momentum can be calculated by

$$(MV)_g = \frac{\pi D^2}{4} \frac{(m'')^2}{\rho_g}\ \Delta t \tag{23}$$

in which $\rho_g$ is the density of the fuel vapor. The only field force is that due to flame buoyancy,

$$F_f = \frac{\pi D^2}{4}\ L\ (\rho_a - \rho_f)\frac{g}{g_c} \tag{24}$$

where the assumption of constant flame volume equal to that of a cylindrical flame of diameter D has been used. Combining Equations (22), (23), and (24) gives the vertical component of momentum of the flame as

$$(MV)_f \cos\theta = \frac{\pi D^2}{4} \frac{(m'')^2}{\rho_g}\ \Delta t + \frac{\pi D^2}{4}\ L(\rho_a - \rho_f)g\Delta t \tag{25}$$

The flame momentum term is now eliminated by dividing Equation (21) by Equation (25). The result gives

$$\frac{\sin\theta}{\cos\theta} = \frac{C_f\ DL\ \rho_a \frac{u^2}{2} \cos\theta}{\frac{\pi D^2}{4} \frac{(m'')^2}{\rho_g} + \frac{\pi D^2}{4}\ L(\rho_g - \rho_f)g} \tag{26}$$

After rearranging Equation (26) becomes

$$\frac{\tan\theta}{\cos\theta} = \frac{\frac{2}{\pi}(C_f\ u^2)}{\left(\frac{\rho_a - \rho_f}{\rho_a}\right) Dg + \frac{D}{L}\frac{(m'')^2}{\rho_g\ \rho_a}} \tag{27}$$

A further simplification can be made in Equation (27) if the relative magnitude of the buoyancy and fuel momentum terms is considered. For a burner one inch in diameter, a conservative estimate shows that the fuel momentum term is less than one per cent of the buoyancy term. Further, for larger burners the fuel momentum term tends to remain constant or at the least only increases slowly, while the flame buoyancy term is approximately proportional to the burner diameter. With this difference in relative magnitude prevailing, the effect of the fuel momentum can be neglected and Equation (27) becomes

$$\frac{\tan\theta}{\cos\theta} = \frac{2C_f\ u^2}{\pi\left(\frac{\rho_a - \rho_f}{\rho_a}\right) Dg} \tag{28}$$

Equation (28) differs from the equation proposed by Pipkin and Sliepcevich by the factor cos $\theta$ appearing in the denominator of the left side of the equation. Although they do not state it, the derivation proposed by Pipkin and Sliepcevich assumes that the flame volume decreases as the angle of tilt increases. The decrease in flame volume would be proportional to cos $\theta$ and would vary up to about 75 per cent for larger angles. The model presented here is considered more realistic for the following reasons. The fuel consumption rate, although known to be influenced by the wind, probably does not change greatly until the flame is bent nearly horizontally. The reaction rate in the flame probably increases somewhat with increasing wind velocity due to greater air entrainment, but again the attendant decrease in flame volume is probably small. Since the reaction rate and fuel consumption rate are approximately the same, the flame volume should be approximately the same even though it is tilted at a greater angle. Published photographs of wind-blown flames support the assumption of constancy of flame volume since they generally do not show a strong decrease in size as the flame is tilted by the wind. It might also be pointed out that the correction factor $\beta$ applied by Pipkin and Sliepcevich to their data has the same qualitative effect as does the $\cos\theta$ term in Equation (28). In fact, the quantitative difference between $\beta$ and $\cos\theta$ is less than 20 per cent in the worst case.

The analysis followed above can readily be extended to other flame shapes. Although it will not be derived here, the result for a flame from a channel (or rectangular) burner is

$$\frac{\tan\theta}{\cos\theta} = \frac{c_f\ u^2}{2\left(\dfrac{\rho_a - \rho_f}{\rho_a}\right) g\ D} \qquad (29)$$

where the flame cross section is assumed to have the shape of a parallelogram. Since the flame tip fluctuates for turbulent flames, the average flame shape from a channel burner can probably be well represented by the parallelogram configuration. In any case the difference in shape would be absorbed into the drag coefficient.

The use of either Equation (28) or (29) to predict the angle of tilt of a wind-blown flame requires the knowledge of the flame drag coefficient. It is therefore necessary to make a number of measurements on the bending angles of wind-blown flames, to calculate the flame drag coefficients, and to correlate them in such a manner that they can be used to predict behavior of large-scale fires. In order to make tests with the greatest possible amount of control, small tests should be made in a controlled wind and their angles used for extrapolation to larger fire sizes. For this reason, among others, the above analysis was simplified as much as possible. The choice of the burner diameter and the assumption of cylindrical flame shape for the circular burners were based partially on the availability of design information. For example, in an industrial accident a spilled liquid fuel would generally be confined to an area known in advance, such as within a dike or a storage tank. This information, along with the fuel properties and the prevailing wind velocity, could be used to calculate the extent of flame bending if the flame drag coefficient was known.

Since the correlation of drag coefficient versus Reynolds number used by Pipkin and Sliepcevich requires corrections for flame angle and flame roughness, the latter correction being made empirically, it seems wise to investigate further methods of correlation. Dimensional analysis was used as an aid in predicting the appropriate parameters for a correlation. Remembering that fuel momentum is negligible, the drag coefficient is assumed to be a function of the burner diameter, the flame length, air viscosity, wind velocity, the densities of air, fuel vapor, and flame and the gravitational acceleration. It is now supposed that the drag coefficient is proportional to some product (as yet unspecified) of the variables involved. Thus,

$$C_f \propto D^a L^b \mu_a^c u^d \rho_a^e \rho_f^h \rho_g^j g^k \tag{30}$$

For the relationship stated in Equation (30) to be true, it must be dimensionally homogeneous; that is, both sides of the proportionality must have the same dimensions. Therefore, the expression

$$(\ell)^a (\ell)^b \left(\frac{m}{\ell t}\right)^c \left(\frac{\ell}{t}\right)^d \left(\frac{m}{\ell^3}\right)^{e+h+j} \left(\frac{\ell}{t^2}\right)^k \tag{31}$$

must be dimensionless, as is $C_f$. In expression (31) m signifies units of mass, $\ell$ units of length, and t units of time. In order that the expression will be dimensionless, the following equations must be satisfied:

for mass

$$c + e + h + j = 0 \tag{32}$$

for length

$$a + b - c + d - 3e - 3h - 3j + k = 0 \tag{33}$$

for time

$$c + d + 2k = 0 \tag{34}$$

From Equation (32),

$$e = -c - j - h \tag{35}$$

and from Equation (34)

$$d = -c - 2k \tag{36}$$

Solving Equation (33) in terms of k results in

$$k = -a - b + c - d + 3e + 3h + 3j \tag{37}$$

If Equations (35) and (36) are substituted in Equation (37) and the resulting equation is simplified,

$$k = a + b + c \tag{38}$$

Since d is expressed in terms of k in Equation (36) it can be further simplified by the substitution of Equation (38),

$$d = -2a - 2b - 3c \tag{39}$$

Equation (30) can now be rewritten substituting the values for e, k and d given by Equations (35), (38), and (39) respectively, such that

$$C_f \propto D^a L^b \mu_a^c u^{-2a-2b-3c} \rho_a^{-c-j-h} \rho_f^h \rho_g^j g^{a+b+c} \tag{40}$$

Collecting the factors having like exponents together gives

$$C \propto \left(\frac{Dg}{u^2}\right)^a \left(\frac{Lg}{u^2}\right)^b \left(\frac{\mu_a g}{u^3 \rho_a}\right)^c \left(\frac{\rho_f}{\rho_a}\right)^h \left(\frac{\rho_g}{\rho_a}\right)^j \tag{41}$$

Proportionality (41) suggests several dimensionless groups which might be used to correlate $C_f$ although there is no a priori way of determining whether such a correlation will work. It is immediately noticeable that the dimensionless groups $Dg/u^2$ and $Lg/u^2$ are forms of the Froude number. Two of the other groups are density ratios. The final group, $\mu_a g/u^3 \rho_a$ is not immediately recognizable. However, if it is multiplied and divided by D and inverted it is seen to be the product of the Reynolds and Froude numbers,

$$ReFr = \frac{Du\rho_a}{\mu_a} \frac{u^2}{Dg} \tag{42}$$

If the problem of correlating flame drag coefficients is considered further, the result of Equation (42) is not really too surprising. It is well known that drag coefficients for a body submerged in a flowing fluid can be correlated as a function of the Reynolds number. In the present case the body is the flame and the flowing fluid is the air stream. It is also known that the behavior of bodies subjected to gravitational forces in flowing fluids often can be correlated as a function of a Froude number. Furthermore, the Reynolds number is

$$Re = \frac{\text{Inertia forces}}{\text{Viscous forces}} \tag{43}$$

and the Froude number is

$$Fr = \frac{\text{Inertia forces}}{\text{Gravity forces}} \tag{44}$$

The product of Reynolds and Froude number is therefore

$$ReFr = \frac{(\text{Inertia forces})^2}{(\text{Viscous forces})(\text{Gravity forces})} \tag{45}$$

and is a function of the three forces acting in the flame problem. A quotient of Reynolds and Froude numbers, however, is a function of only viscous and gravity forces. The important contribution of inertia forces, which is a major factor for high wind velocities, is completely neglected. These arguments tend to support the use of the ReFr product as a function to correlate flame drag coefficients. As has been previously pointed out, variables dependent on Reynolds and Froude numbers tend to become independent of those numbers when the dimensionless groups are large. This behavior should carry over to the present case, and a constant flame drag coefficient should be obtained for large enough ReFr products. Such a behavior would substantiate the observation of Pipkin and Sliepcevich that flame drag coefficients become constant at large diameters where wind velocities are high.

In order to try the ReFr correlation suggested by dimensional analysis, the data given by Pipkin and Sliepcevich were used. A plot of the uncorrected drag coefficient as calculated by Pipkin and Sliepcevich versus the ReFr product is shown in Figure 4. A reasonably satisfactory correlation is obtained without recourse to empirical corrections for the effect of flame angle or flame roughness. The plot suggests that the drag coefficient is not strongly dependent on the properties of the fuel or the flame, but is rather dependent on the wind properties, chiefly the wind velocity. The flame drag coefficient is apparently not even dependent on the flame size. This conclusion is not to say that the

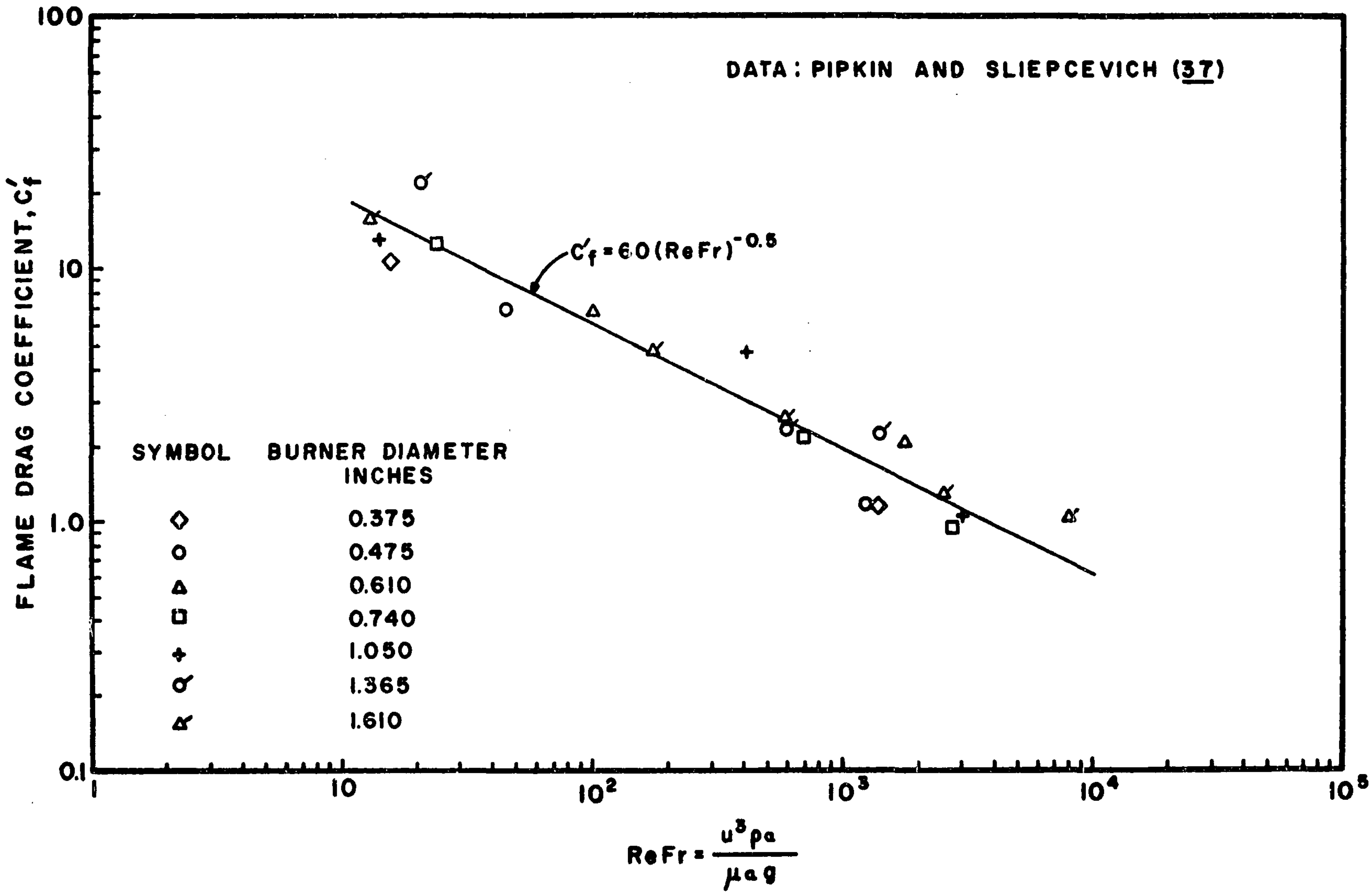


Figure 4. Correlation of Flame Drag Coefficients as a Function of ReFr

angle of tilt is independent of size. The data of Figure 4 can be represented by the equation

$$C_f' = 60(\mathrm{ReFr})^{-0.5} \tag{46}$$

where $C_f'$ is the uncorrected drag coefficient and equals $C_f \cos\theta$. A word of caution is necessary in using these results: the data of Figure 4 and Equation (46) are based on relatively limited data for small-size, natural gas fires. They should therefore not be used to estimate data for other cases outside the limits of the experimental conditions they represent. Perhaps the most significant aspect of the success of the correlation is that it suggests a method of correlating flame bending data.

## Downwind Temperatures

The prediction of the temperatures of the gases in the wake of a wind-blown flame is of interest in the study of fire spread. The following simple derivation is aimed at finding dimensionless groups which can be used to correlate such temperatures. To start, consider the convective column rising from a fire burning above a long burner of finite width. The energy output from the fire can be considered to be uniformly distributed in the amount of Q' Btu/ft-sec. The length of the column at some height z above the ground is X, and since the problem is two-dimensional, an arbitrary width Y of the fire and convection column will be studied. A momentum balance written for steady state conditions for a section of thickness $\Delta z$ of the column gives

$$\rho\Delta_z(w^z) = \Delta z(\rho_a - \rho)g \qquad (47)$$

where w is the vertical component of the velocity of the gases in the column. Dividing by $\Delta z$ and taking the limit as $\Delta z$ approaches zero yields

$$\frac{d(w^2)}{dz} = \left(\frac{\rho_a - \rho}{\rho}\right)g \qquad (48)$$

If it is assumed that the molecular weight of the gases in the column is about that of the surrounding air and that the gases behave ideally, Equation (48) can be written as

$$\frac{d(w^2)}{dz} = \left(\frac{T - T_a}{T_a}\right)g \qquad (49)$$

where T and $\rho$ refer to the gases in the column and $T_a$ and $\rho_a$ are for the surrounding air. Integration of Equation (49) yields

$$w^2 = \left(\frac{T - T_a}{T_a}\right)gzf_a(z) + \text{constant} \qquad (50)$$

where $f_a(z)$ is included because T is dependent on z. For the case of a fire burning above a liquid pool, the initial velocity at z = 0 is small compared with the velocity a few feet up in the column, and the constant can be neglected. In addition, z can be considered as

$$z = x\ f_b(\frac{z}{x}) \qquad (51)$$

After substituting Equation (51) in Equation (50) and solving the upward velocity of the gases in the column becomes

$$w = \sqrt{\frac{(T - T_a)}{T_a} gx} \quad f_c(\tfrac{z}{x}) \tag{52}$$

Now considering the energy balance for the same section of the column,

$$wX\rho \, c_p(T - T_a) = Q' \tag{53}$$

where $T_a$ is chosen as the reference temperature, and it is assumed that all the convective heat leaving the fire is retained in the convection column. Equation (53) is solved for w to give

$$w = \frac{Q'}{\rho_a c_p (T - T_a) x} f_d(\tfrac{z}{x}) \tag{54}$$

where X is taken to be a function of z/x multiplied by x, and $\rho$ is taken to be a function of z/x multiplied by $\rho_a$. Setting the values of w given in Equations (52) and (54) equal to each other gives

$$\sqrt{\frac{(T - T_a)}{T_a} gx} \; f_c(\tfrac{z}{x}) = \frac{Q' f_d(\tfrac{z}{x})}{\rho_a C_p (T - T_a) x} \tag{55}$$

Equation (55) can also be put in the form

$$\frac{(T - T_a)^{3/2}}{T_a^{\;3/2}} T_a \frac{g^{3/2}}{g} \frac{x^{3/2}\rho_a C_p}{Q'} = \frac{f_d(\tfrac{z}{x})}{f_c(\tfrac{z}{x})} \tag{56}$$

Taking the two-thirds power of Equation (56) results in

$$\frac{(T - T_a)}{T_a} \frac{gx}{\left(Q'g/\rho_a C_p T_a\right)^{2/3}} = f_e(\tfrac{z}{x}) \tag{57}$$

The term on the left of Equation (57) can be considered a dimensionless temperature rise and will be denoted as $\Phi_L$.

Equation (52) can also be solved for the temperature rise to give

$$(T - T_a) = \frac{w^2 \; T_a}{gx \; f_c^2(\frac{z}{x})} \tag{58}$$

and solution of Equation (54) for the temperature rise gives

$$(T - T_a) = \frac{Q'}{w\rho_a C_p x} \, f_d(\frac{z}{x}) \tag{59}$$

Setting Equations (58) and (59) equal, it is possible to solve for the vertical component of velocity in the plume

$$w = \left(\frac{gQ'}{\rho_a C_p T_a}\right)^{1/3} \; f_c^2(\frac{z}{x}) \;\; f_d(\frac{z}{x}) \tag{60}$$

Wind tunnel tests set up by Halitzkey, <u>et al</u>. (24) to measure the angles of buoyant smoke plumes were shown by Priestly (38) to have an angle from the vertical such that

$$\tan \theta = \frac{u}{w} \tag{61}$$

Since the temperature rise downstream from a plume obviously is dependent on the plume angle, it is logical to extend the argument to the present case and use the ratio of velocities as a parameter in correlating downwind temperature data. The velocity ratio is

$$\frac{u}{w} = \frac{u}{\left(gQ'/\rho_a C_p T_a\right)^{1/3}} \; f_e(\frac{z}{x}) \tag{62}$$

The function

$$\Omega L = \frac{u}{\left(gQ'/\rho_a C_p T_a\right)^{1/3}} \tag{63}$$

will be termed the dimensionless velocity and will be used in correlating the dimensionless temperature. The functions of z/x are not specified. Rather, the correlation of data will be made for different parameters of z/x in order to account for the position of the temperature measurement.

A similar analysis can be made for fires burning above a liquid pool of circular geometry. The resulting expressions for dimensionless temperature rise and dimensionless velocity are

$$\Phi_c = \frac{(T - T_a)}{T_a} \; \frac{gx}{\left(Q''/\rho_a c_p T_a\right)^2} \tag{64}$$

and

$$\Omega_c = \frac{u}{\left(Q''/\rho_a c_p T_a\right)} \tag{65}$$

where Q" is the convective heat output of the circular fires per unit area per unit time. The correlations suggested by the dimensionless temperature rise and dimensionless velocity parameters will be tested with the data obtained in this study in Chapter VI.

Thomas (56) has used with good success the dimensionless functions $\Phi_L$ and $\Omega_L$ to correlate the temperature data reported by Rankine (44, 45) for a line of burners set in such a way as to simulate a line fire. The use of a function analogous to $\Phi_L$ was suggested by Priestly (38) in his work for bent plumes, and Hottel (27) derived functions similar to $\Phi_L$ and w for convective plumes above calm fires. In addition, Byram, et al. (12) have suggested a dimensionless group which they term the convection number

$$N_c = \frac{gQ'}{\rho_a C_p T_a u^3} \tag{66}$$

to correlate convective heat transfer data downwind from a fire. $N_c$ is seen to be a rearrangement of $\Omega_L$. Although they calculated $N_c$ for a number of wind-blown fire tests, they gave no idea as to its effect on any of the parameters they investigated. They also propose a convection number for a point source,

$$N_c = \frac{gQ}{r\, C_p T_a \rho_a u^3} \tag{67}$$

where Q is the rate of convective heat output of the source and r is the radius of the convective column at height z.

## Flame Trailing

The flame trailing downwind of a fuel source seems to be unique to liquid-fuel fires. It would be of importance in heat transfer downstream of the fire, especially by direct flame impingement. For this reason a correlation of the flame trailing length, D', is desirable. Such a correlation might be found, as was the one for $C_f$, by direct dimensional analysis. Assume to start that

$$\frac{D'}{D} \propto D^a u^b \rho_a^c \rho_g^d \mu_a^e g^h \tag{68}$$

The expression

$$(\ell)^a \left(\frac{\ell}{t}\right)^b \left(\frac{m}{\ell^3}\right)^{c+d} \left(\frac{m}{\ell t}\right)^e \left(\frac{\ell}{t^2}\right)^h \tag{69}$$

must therefore be dimensionless. The resulting equations are:

for mass

$$c + d + e = 0 \tag{70}$$

for length

$$a + b - 3c - 3d - e + h = 0 \tag{71}$$

and for time

$$-b - e - 2h = 0 \tag{72}$$

Solving Equation (70) for d gives

$$d = -c - e \tag{73}$$

and from Equation (72) b is found to be

$$b = -e - 2h \tag{74}$$

Using the values thus found for d and b, Equation (71) can be solved for a to give

$$a = h - e \tag{75}$$

Proportionality of Equation (68) then becomes

$$\frac{D'}{D} \propto D^{h-e} u^{e-2h} \rho_a^c \rho_g^{-c-e} \mu_a^e g^h \tag{76}$$

or

$$\frac{D'}{D} \propto \left(\frac{\rho_a}{\rho_g}\right)^c \left(\frac{\mu_a}{Du\rho_g}\right)^e \left(\frac{Dg}{u^2}\right)^h \tag{77}$$

Thus D'/D is expected to be a function of the density ratio $\rho_g/\rho_a$ , a Reynolds number and a Froude number. Of these dimensionless groups, the density ratio and Froude number would intuitively seem most important. The correlation suggested by Equation (77) will be tested with the data obtained in this study in Chapter VI.

## Fuel Selection

The selection of fuels was made on the basis of chemical type, heat output, burning rate, the amount of expected flame radiation and the ease of obtaining sufficiently pure fuels at reasonable cost. The five fuels selected were methanol, acetone, normal hexane, cyclohexane and benzene. Methanol was selected as an alcohol fuel; it burns slowly with a low heat output and its flames are a pale blue, resulting in low radiative transfer. Acetone burns with a bright flame but with no smoke, a medium heat output and medium radiative output. Cyclohexane and normal hexane were chosen as two hydrocarbon types; both burn with a smoky flame and high heat output. Both also have high radiative output. Benzene burns with a sooty flame and has high heat output. The benzene flame is optically more dense and has high radiative heat output.

# CHAPTER IV

# FACILITIES AND EQUIPMENT

## Wind Tunnel Design

The problems encountered in designing a low-speed wind tunnel for flames research were compounded by a lack of information in the literature concerning such facilities. Only three wind tunnels in the United States had been designed for flames research, and they were primarily intended for solid fuels research. Personal communication with Rothermel (48) was helpful in the aerodynamic design of the tunnel, but several design estimates, particularly for tunnel size and wind speed, had to be made on the basis of data available from fires burning under calm conditions and data from small fires.

The first problem was to select the size of the tunnel test section. The cross section of the tunnel was to be set to allow burning of fires up to two feet in diameter. The data for flames given in the literature suggested that flame lengths would be about three times the pool diameter. In order to allow for fluctuations of the flames and for air flow above the flame the tunnel height was selected as 8 feet.

A tunnel width of 8 feet was selected in order that channel burners 5 feet long could be used and still maintain air flow past the ends. The length of the test section was set at 20 feet. This length would allow temperature and radiation readings to be made up to approximately ten burner diameters downstream from the flame.

The next problem was to select the range of wind velocities for the tunnel. The only relationship available for such estimates was Equation (13) proposed by Pipkin and Sliepcevich based on an extrapolation of their data from small gas burners. Equation (13) predicted that wind speeds of about 8 ft/sec would be required to tilt a 2-foot flame by 75 degrees. In order to allow for uncertainties in Equation (13), for the lack of low-speed wind tunnel design information, and for future use of the wind tunnel in other studies, it was decided to base the design on a wind velocity of 25 ft/sec. This wind velocity would require an air rate of approximately 100,000 cfm. The blower was mounted to provide for forced-draft air flow through the tunnel although it was known that forced-draft conditions would lead to greater turbulence and poorer velocity profiles than would an induced-draft system. The reasons for choosing forced-draft flow were to prevent possible explosion due to a buildup of fuel vapor in the tunnel and to eliminate the buildup of soot on the blower and motor during the burning of smoky and sooty fires. A single pass tunnel was specified for the reasons listed above, and, additionally, to keep the air coming into the test section at constant ambient conditions. Plan and elevation views of the tunnel facility are shown in Figure 5.

The floor of the test section was about 2 feet above ground level. It was made in removable sections about 2 feet wide. The space beneath the floor was needed to provide room for the lower part of the burners and for fuel delivery lines. The removable floor sections increased the versatility of the tunnel and allowed for future modification for other uses, particularly the burning of solid fuels. Two access doors were provided for the crawl space, which was provided with an exhaust fan to clear any fumes that might tend to collect beneath the floor. The bottom of the crawl space was divided into two sections sunk about 3 inches beneath ground level to prevent fuel spread in the case of accidental spillage.

Four observation windows were placed in the wall of the tunnel between the test section and the observation room. They were made of 3/8-inch thick tempered plate glass for strength and heat resistance and were located as shown in Figure 6. A fifth window was located directly across from the window farthest upstream. In it were installed a clock, a stop clock, and a counting device, all of which could be controlled from the observation room. An access door to the test section, 4 feet long and 4 inches high, was provided below the upstream window. Its purpose was to allow access for igniting and extinguishing the test fires.

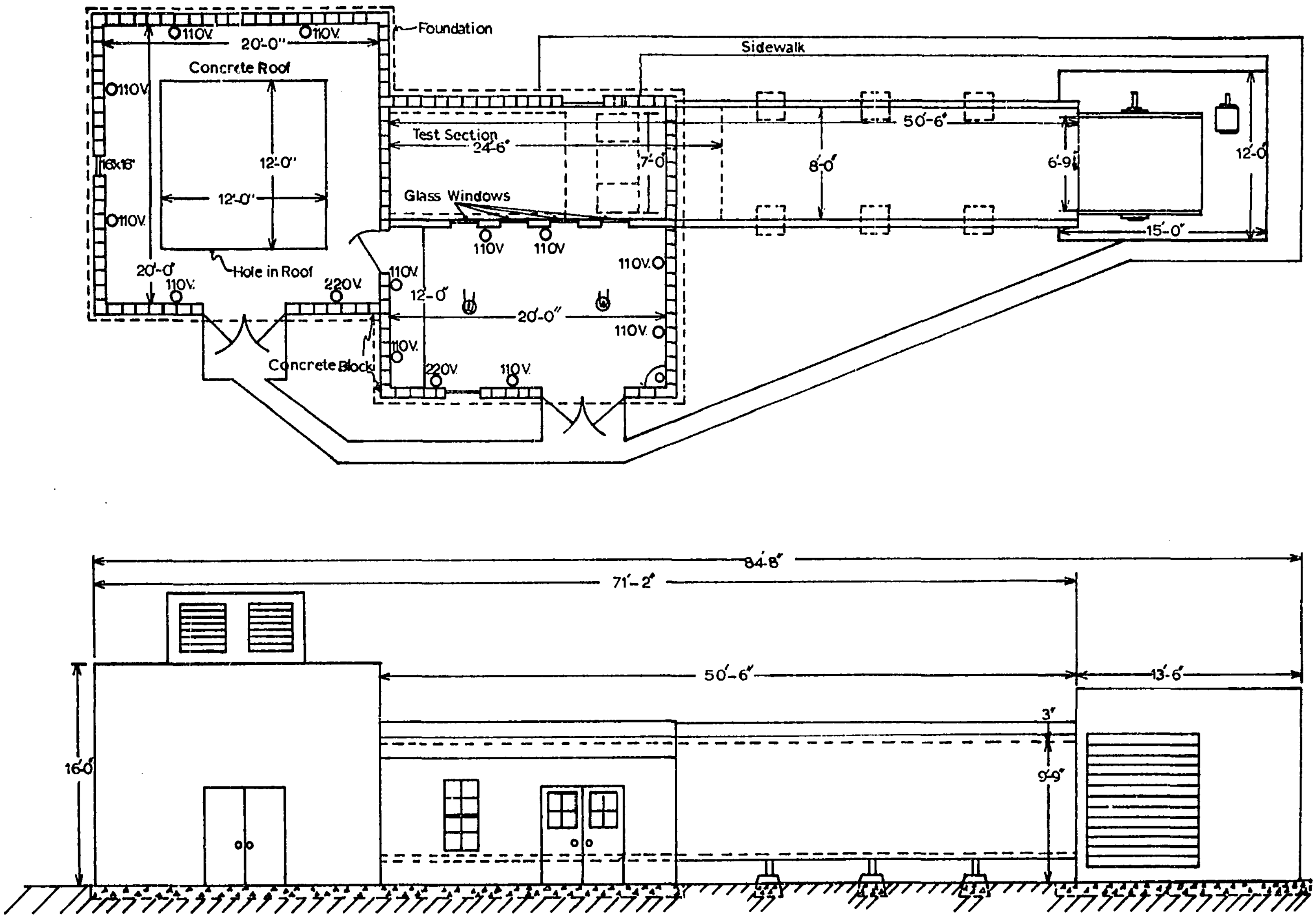


**Figure 5. Layout of Flame Wind Tunnel**

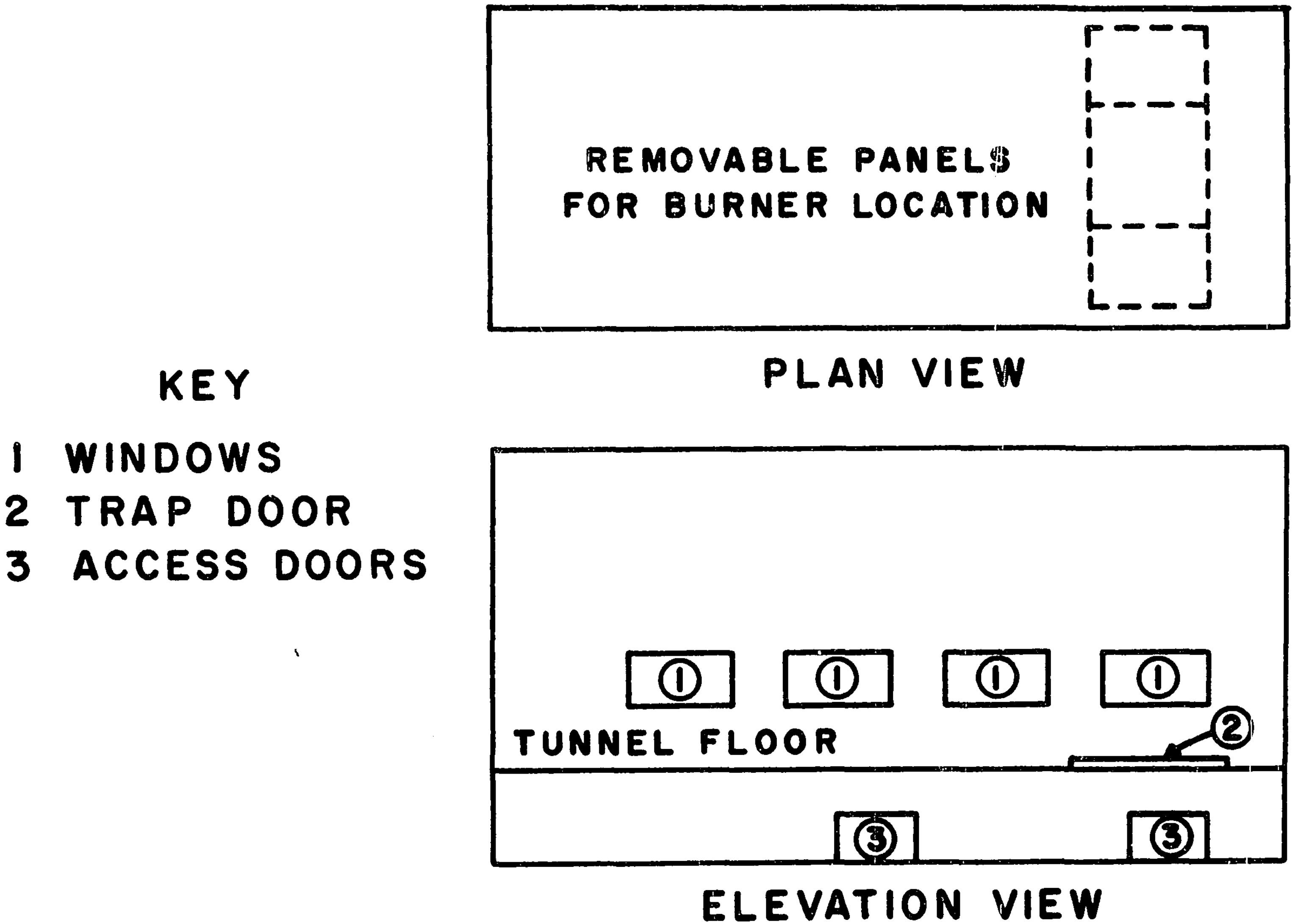


Figure 6. Schematic Drawing of Test Section

Two of the most important design considerations were that a flat velocity profile be obtained and that the scale of turbulence be small. Wind tunnel literature indicated that the one way to provide for smooth flow was to use a large settling chamber upstream of the test section. The settling chamber should be of diverging-converging shape and its cross section should be several times larger than that of the test section. Budgetary limitations dictated the use of a straight-through design, however. Such a straight-through design required the development of new techniques to deal with the variations in velocity and turbulence. Since Milburn (36) gives all the aerodynamic design information in his thesis, the only points considered here will be those pertinent to the flame studies. Basically, the flow through the tunnel was smoothed using screens and honeycomb. The honeycomb attenuated and damped out most of the turbulence, but it still left an unacceptable velocity profile. The screens, 14 x 18 mesh size, were positioned in such a way as to result in a flat velocity profile; they also broke down the remaining turbulence. Figure 7 shows a plot of the percentage variation in velocity along the vertical and horizontal centers of the tunnel with the screens and honeycomb sections in their final configurations. The velocity profiles were obtained using equipment to be described later. The amount of turbulence present in the air stream was judged by using fine strings suspended from nylon thread stretched

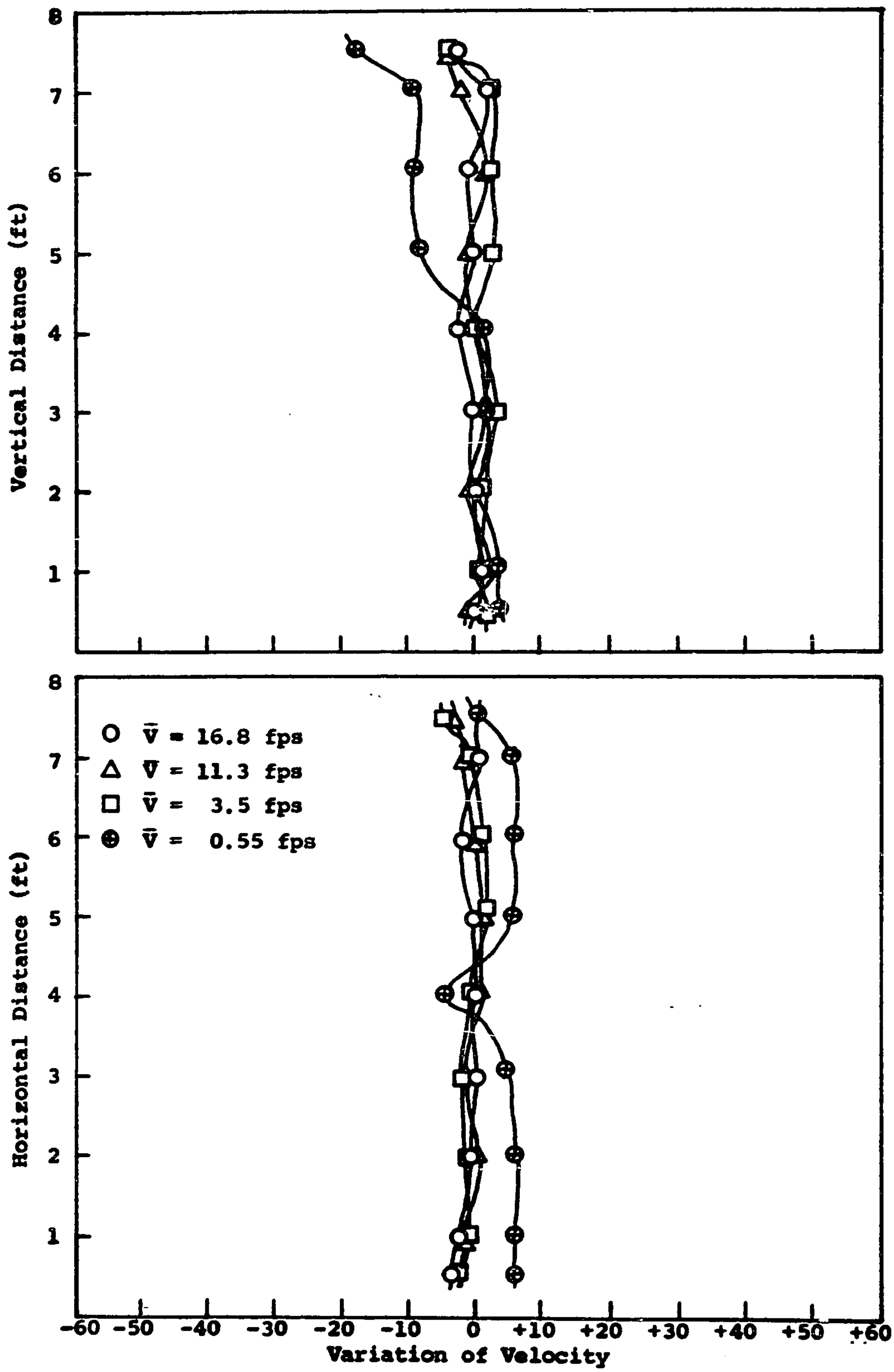


Figure 7. Final Wind Tunnel Velocity Profiles

across the tunnel. Prior to installation of the honeycombs and screens, tests using a cloth banner had shown some reverse flow and gross turbulence in the tunnel. After all the dampening devices had been installed no turbulence or velocity fluctuations were noticed over long periods. Figure 8 is a time exposure of thirty seconds duration showing the strings. As can be easily seen, the positions of the strings did not change significantly during the time of exposure. Although it is not evident from the photograph because of the camera angle, the angle of each of the strings was approximately the same, giving further indication that the velocity profile was essentially flat.

At the exit of the test section was a large room constructed for two purposes. One purpose of this room was to provide space for testing fires under calm conditions. For this purpose a large hood was suspended from the ceiling down to a level about 8 feet from the floor. This hood served to collect smoke and soot, and a fan installed above the hood exhausted the smoke and fumes from the room. The second purpose of the static test room was to serve as a surge chamber. Since the outside wind conditions were subject to considerable fluctuations, the surge chamber helped to prevent low-frequency velocity fluctuations caused by outdoor wind gustiness.

The air entered the tunnel facility through variable inlet vanes in the sides of the blower. The position of the

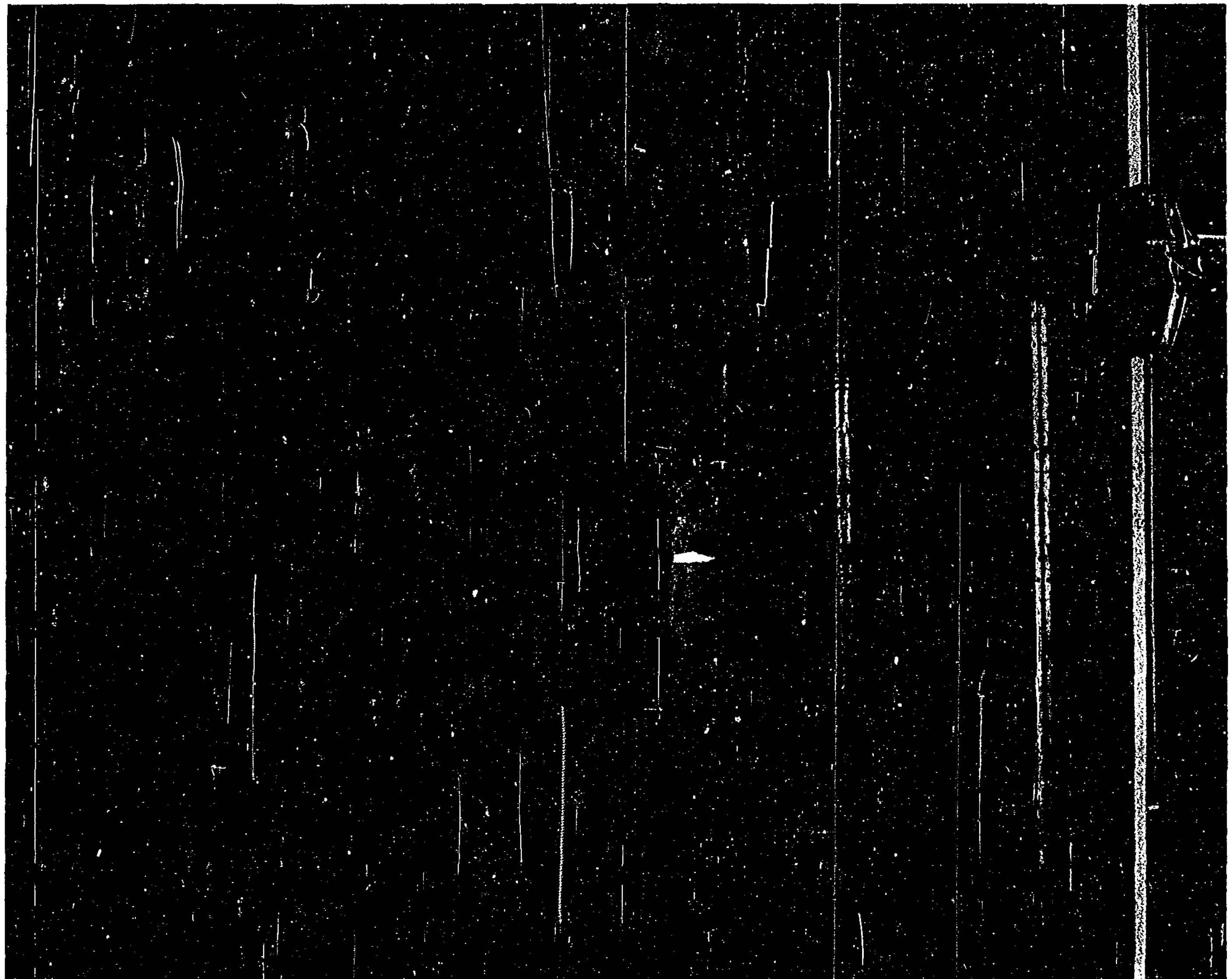

Figure 8. Thirty-Second Time Exposure Showing Strings in Steady Flow

vanes could be controlled remotely from the observation room, and the variable vane control was used to control wind velocity within the test section. The air left the tunnel through spring-loaded shutters in the roof of the static test section. Although these shutters allowed air to pass out, they were closed by prevailing outdoor winds. In this way much of the problem of velocity variation due to outdoor wind gustiness was resolved.

The test section, static test room and observation room were constructed of concrete block with concrete floors. The entrance section containing the honeycombs and screens was of sheet metal, and the blower housing was of wood covered with asbestos shingles. No combustible materials of construction were used in areas near the test section or the fuel storage area. Figure 9 is a photograph of the wind tunnel facility after construction was complete. The velocity range runs from about 1 ft/sec to 20 ft/sec, but it may go slightly higher or lower depending on outdoor weather conditions.

## Burners and Fuel Delivery System

The tests to measure flame bending angles were made using circular and channel burners. The burners were made to fit into removable panels which could be placed in the test section as shown in the plan view in Figure 6. Brass was used as the construction material for the burners; Figures 10 and 11 show the details of construction of the circular and

**Figure 9. Flame Wind Tunnel**

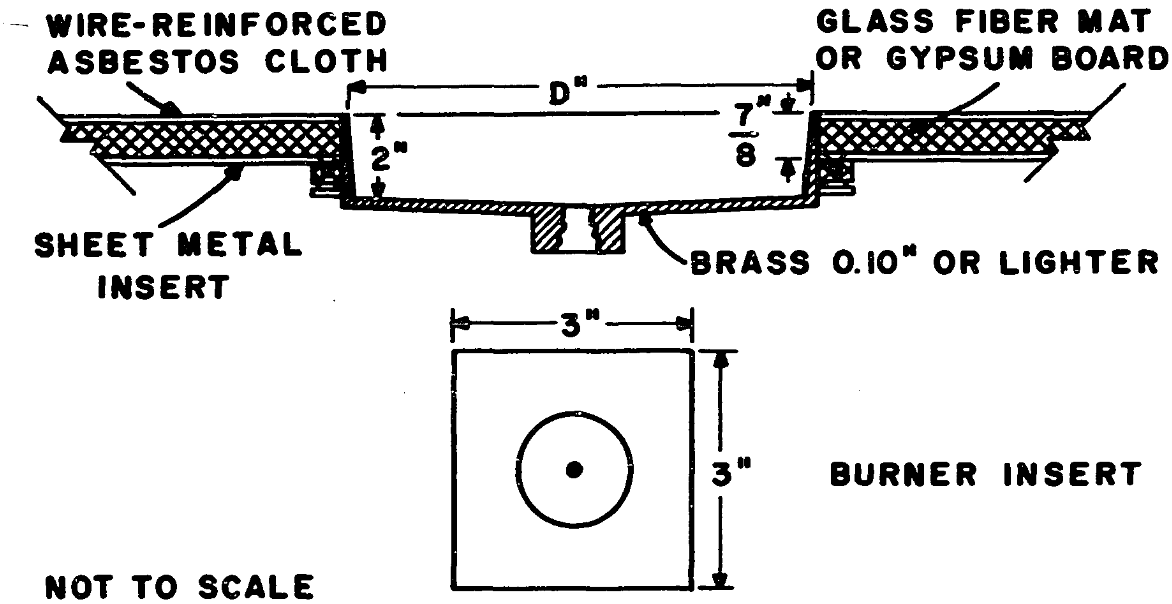


| NOMINAL DIAMER INCHES | ACTUAL DIAMETER FEET |
|---|---|
| 1 | 0.083 |
| 2 | 0.167 |
| 4 | 0.349 |
| 8 | 0.677 |
| 12 | 1.015 |
| 18 | 1.526 |
| 24 | 1.969 |

Figure 10. Detail of Circular Burner

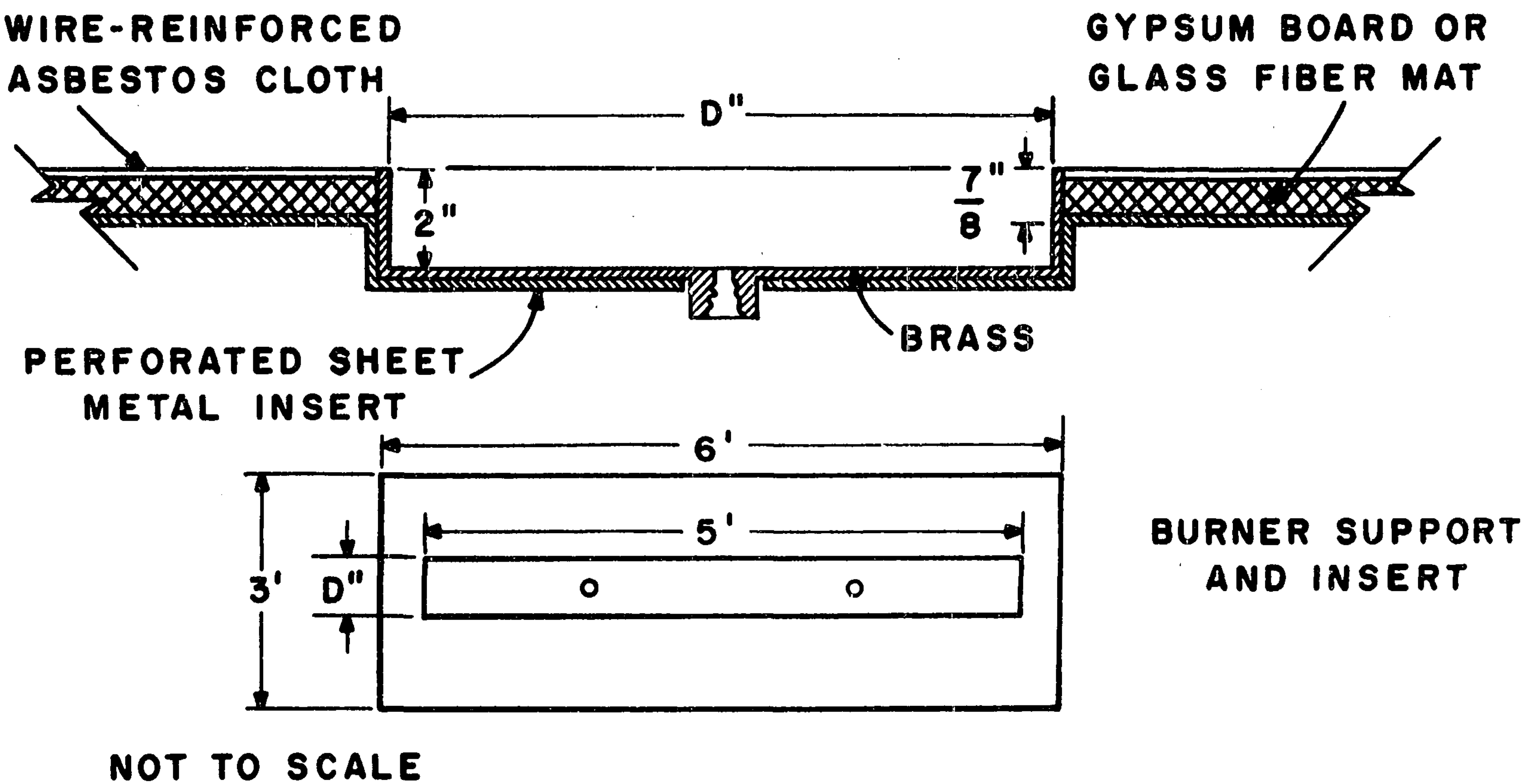


Figure 11. Detail of Channel Burner

channel burners, respectively. Since the circular burners were supported around the rims, their rims were made of heavier material and tapered at the top to keep the exposed edge of the rim as thin as possible consistent with structural requirements. The reason for the thin rims was to keep heat conduction from the floor to the fuel at a minimum. The floor was also insulated with glass fiber mats or gypsum boards, either being covered with a layer of reinforced asbestos cloth. Neither the glass fiber mats nor the gypsum boards was entirely satisfactory from the viewpoint of durability, but they did provide reliable insulating qualities and were easily obtained. The burners were made 2 inches deep to allow for enough fuel thickness to absorb most of the radiative energy incident on the fuel surface. Tests at the Bureau of Mines (10) gave information indicating the 2-inch depth would be more than sufficient. The burners were installed so that they were flush with the insulation on the floor of the tunnel. This flush mounting helped to prevent perturbations in the flow downstream and the "bluff body" effect at the burners themselves. The effect of a bluff body has not been fully studied, but it is known that it changes the burning behavior.

Circular burners having nominal diameters of 1, 2, 4, 8, 12, 18, and 24 inches were constructed and used in the tunnel. No useful data were collected for the 1- and 2-inch burners; except for special outdoor wind conditions the velocity obtained in the tunnel was greater than about 1 ft/sec, which was too high to use for the smallest burners. The flames from these burners were nearly horizontal at all wind velocities obtainable in the tunnel. Channel burners having widths of 1, 2, 4, and 8 inches were constructed. Again, wind velocities prevented taking data with the 1-inch channel burner because the flames were so nearly horizontal as to make accurate reading of them impossible.

It was desired to make the burning tests under steady state conditions with the fuel level constant and so near the top of the burner as possible. Estimations based on data given by Rasbash et al. (46) indicated that approximately twenty minutes would be required to reach steady state conditions; at least 10 minutes would probably be required for each run after steady state was reached. Fuel consumption rates based on the data of Burgess et al. (10) were calculated and plotted as shown in Figure 12, which shows the amount of fuel consumed for a fires of 20-minute duration. The data were plotted as a function of the linear regression rates over the range expected in the tests. It was readily apparent that regardless of the fuel delivery system chosen several fuel reservoirs would be necessary to insure accurate measurement of the fuel consumption.

So far as could be determined from the literature, all of the burning tests using liquid fuels and controlled liquid levels had used a delivery system that had exposed

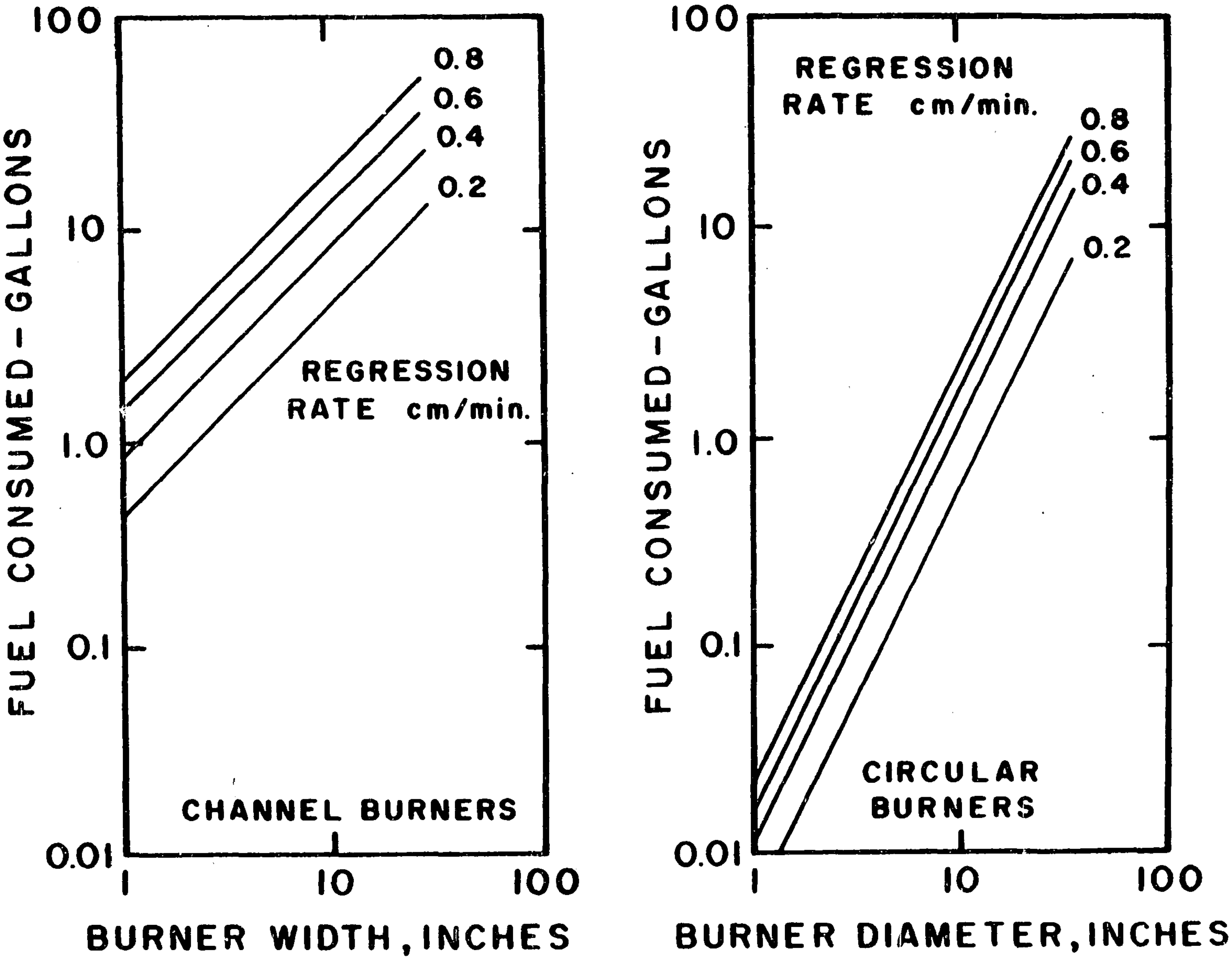


**Figure 12. Fuel Consumption for Fires of Twenty-Minute Duration**

the fuel to the atmosphere at some point. In the case of the wind tunnel tests it was desired to have so little air contact with the fuel supply as possible. Particularly to be avoided was any delivery system that used a weir and overflow system. The danger from fuel spillage and the troublesome fuel measurement necessary in overflow systems was felt to be unnecessary. The fuel reservoir and delivery system which were designed specifically for this work are shown schematically in Figure 13. The system is basically a constant head siphon which uses the liquid fuel in the delivery lines as a liquid seal between the burner and the fuel reservoir. The end of the breather tube is positioned at a level the same as the desired fuel level in the burner. As the burner fuel level rises, the liquid head at the burner and the end of the breather tube balance and flow stops. The liquid level inside the reservoir is under a slight vacuum induced by the removal of fuel. As fuel is burned and the level in the burner starts to drop, air is sucked in through the breather tube allowing the pressure to rise slightly and more fuel flows out. When the fuel use rate is constant accurate control can be easily established, and the fuel level is accurately maintained without much attention. The breather tube should be inserted through the tunnel wall since there is a slight pressure difference between the observation room and the wind stream in the test section. Even this requirement is unnecessary if care is used. Since air is being

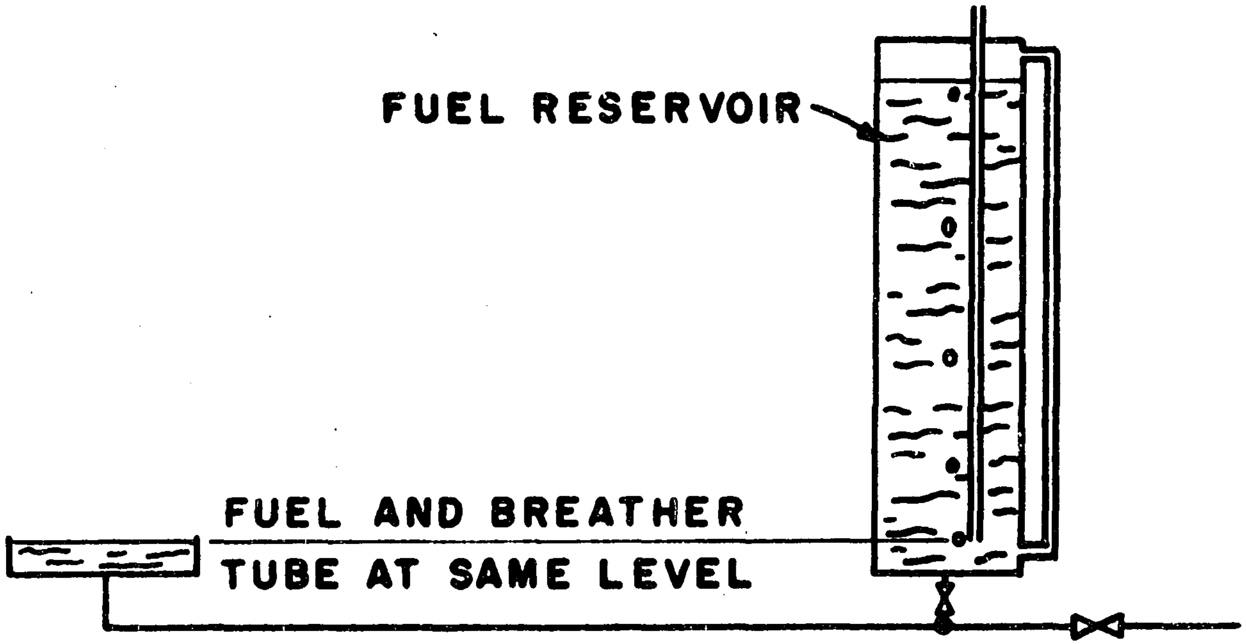


**Figure 13. Schematic Diagram of Fuel Level Control System**

continuously sucked into the reservoir, no fumes escape into the observation room where the reservoirs are kept, which is desirable from the safety viewpoint.

Figure 14 shows the details of construction of the fuel reservoirs. Four reservoirs were constructed from thin-walled aluminum tubing. They were 2, 4, 6, and 10 inches in diameter and allowed fuel measurements to within less than one per cent of the total used in most of the runs. Fuel measurement was made by noting the drop in liquid level in the fuel reservoirs through the sight glasses. The sight glasses were thick-walled and covered by a clear acrylic shield to prevent accidental breakage. Each fuel tank was calibrated volumetrically using water, and each was found to give a linear relationship between fuel content and fuel level. A least-squares analysis of the data was used to calculate the proportionality constant from which fuel use rates were calculated.

The fuel reservoirs were connected through the wall between the observation room and the test section to the underneath side of the burners with copper tubing. The valves used were all brass ball valves with teflon seals and packing. The draining of fuel from the reservoir and the burners was done through an outside wall to an outdoor location as a safety measure. Screens were installed over the fuel inlet holes in the burners to prevent flash-back to the reservoirs.

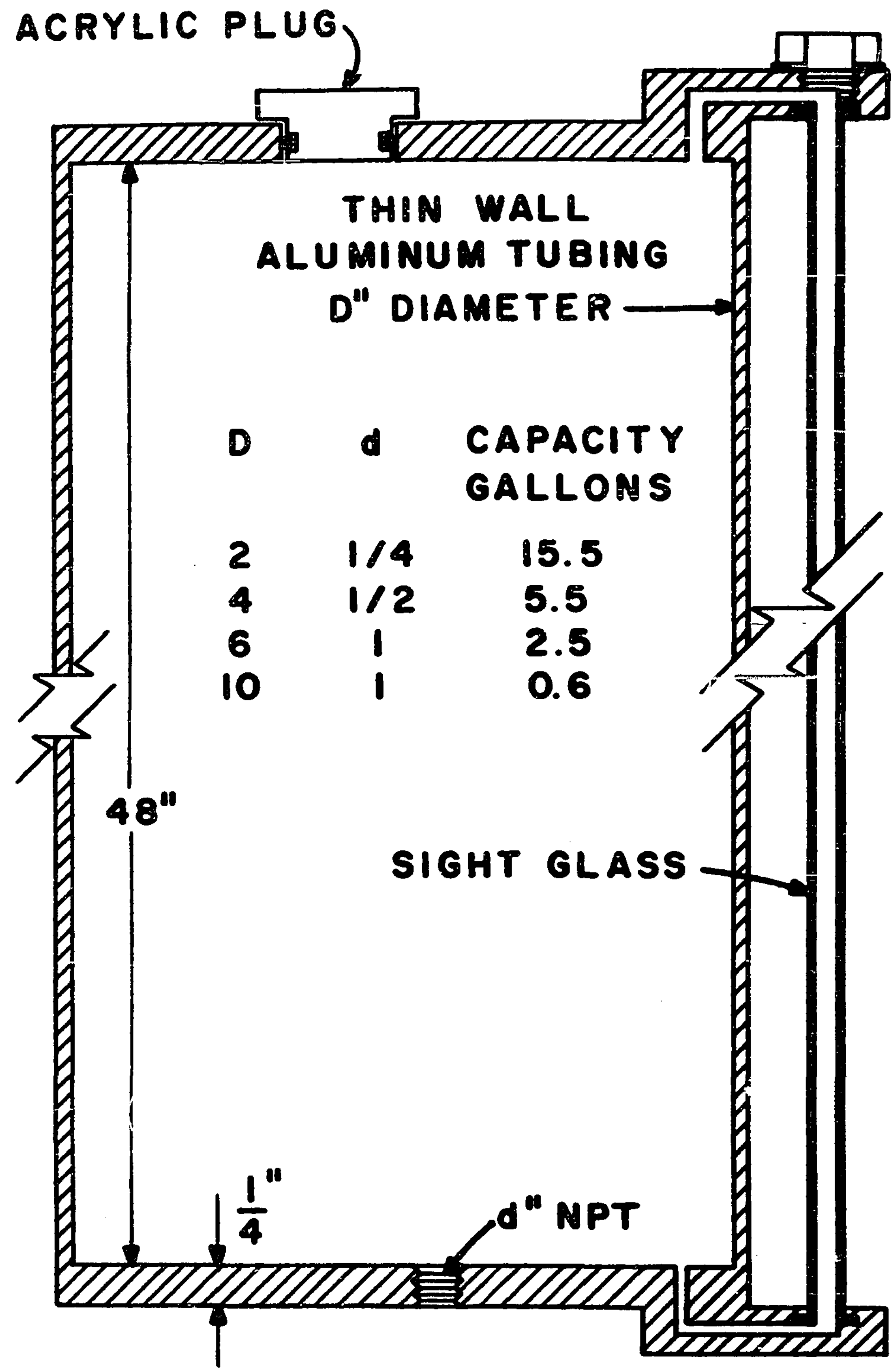


Figure 14. Detail of Fuel Reservoir

## Instrumentation

An attempt was made to use, so far as possible, standard pieces of equipment which could be readily obtained and for which service was reasonably available. It was also desired to have instruments with direct readout or with continuous recording of test variables.

A survey of possible instruments for measuring wind velocity was made. Two basic types of anemometers were available: the vane type, which measures the air velocity by counting the number of revolutions of the vane per unit time, and the hot-wire type, which measures wind velocities through the cooling effect of the air stream on a fine wire. Since the hot-wire type instrument provides rapid and continuous readout it was selected for use in the tunnel. After considering several models, the Alnor Type 8500 Thermoanemometer was selected as most suitable. It differs from the usual hot-wire anemometer in the use of a thermocouple-type readout instead of using a constant current probe. It basically consists of a piece of fine wire connected to two supports. The supports supply electrical current to the fine wire, which is heated to about 350°F in calm surroundings. As the air flow across the wire increases, its temperature decreases. A fine thermocouple junction at the center of the wire measures the wire's temperature, and the resultant reading is shown on a scale calibrated to read the air velocity in feet per minute. The fine cross wire and the thermocouple wires are 0.002

inches in diameter and provide rapid response. In addition, the thermocouple has a built-in reference junction which is also exposed to the air stream and compensates for differences in readings due to varying air temperatures. The accuracy is stated to be ± 2 ft/min or ± 3 per cent of indicated value, whichever is larger. The range is 10 to 2000 ft/min with two range scales. Since it is a hot-wire device, it is calibrated under conditions of known mass flow; a correction must therefore be applied for air densities other than 0.075 $lb/ft^3$. As obtained, the instrument had a probe which provided for a two-foot insertion and a power cord 25 feet long so that air velocity could be monitored at any point across the test section without entering the tunnel. In use, the probe was mounted on a positioning device in the test section about two feet upstream of the flame test area. A photograph of the positioning device is shown in Figure 15. A small reversible DC electric motor is built into the rear of the housing, and provides for vertical positioning of the probe assembly. Horizontal positioning is accomplished by a system of cables and pulleys which can be used to move the vertical rail across the tunnel. The combination of vertical and horizontal movement permits positioning of the thermo-anemometer probe at any point in the tunnel except within 6 inches of the floor and ceiling. A pitot-static probe can also be seen extending forward from the housing. It was used in the early stages of calibration and in determining at

Figure 15. Anemometer Positioning Device and Pitot-Static Tube

which positions the damping screens should be located. Since the pitot-static system could not be read accurately at low velocities, it was not used in any of the flame tests in the tunnel.

Making visual observations of flames is a somewhat capricious method of obtaining data; what the eye sees is frequently not the event that is actually occurring. Since the flame length fluctuates irregularly, most observers have turned to photography to measure it. Generally, a short duration time exposure has proved best, since an instantaneous snap may well catch the flame at an unusual position. Movies have also been used to study flame behavior. In these studies two special cameras were constructed for still shots. One of these was a simple pinhole camera; it consisted of a sheet metal box which had a piece of foil cemented across a hole in front. The foil was pierced with a small pinhole located approximately in the center of the camera face. The back of the box was built to receive a Polaroid film holder which used 4 by 5 film packs. The camera was built to have an extremely wide angle, approximately 100 degrees. Since the focusing is done through the pinhole, objects farther than a few inches from the front of the camera are always in focus. The shutter was placed just behind the pinhole and was remotely controlled using a solenoid switch. The second special camera was of wood construction and used a fixed-focus lens. The lens aperature could be opened or closed from the front of the camera, and the shutter was operated manually from a shutter release attached to the lens. This camera was made to take a narrower angle photograph on 4 x 5 Polaroid film. It also was used for taking pictures of the dim methanol flames. Polaroid film was selected so that the photograph could be seen shortly after its exposure, thereby avoiding loss of a photograph because of camera failure or the necessity of having to take extra shots. Three different types of films were used: a very fast film (ASA 3000), a medium speed film (ASA 400), and a film permitting both a positive and a negative copy to be taken. The fast film was used in the pinhole camera for exposures of 1/2 to 5 seconds and in the lens camera for photographing methanol flames. The medium speed film was used in the lens camera for photographing luminous flames of smaller size where the wide angle was not necessary. The positive-negative film was used to photograph a grid in the tunnel which could be used for measurements of flame size. The grid was constructed as a reference datum. It was 8 feet square, and was painted black with white lines running vertically and horizontally every inch. The grid was positioned vertically in the center of the tunnel and a time exposure taken with each camera for a period long enough to overexpose the negative slightly. After processing the negative was used as a template for measuring the flame length at the center of the tunnel. There was, of course, some distortion in depth, especially for the pictures taken with the pinhole camera. However, there was little distortion in any vertical plane, and flame heights and angles could be easily measured from the photographs. Flame angles were measured directly from the photographs using a protractor.

In addition to the still photographs, about 200 feet of 16-mm movies were taken. The purpose of the movies was to allow a careful scrutiny of fires for qualitatively analyzing their behavior. Actually, only the slow-motion (taken at 64 frames/sec and viewed at 16 frames/sec) pictures proved to be worthwhile for this purpose, and even they were not as valuable as had been hoped. This inadequacy was due partially to the lack of a wide-angle lens for the movie camera, which prevented taking full-length movies of the fires through the windows. The film used was Kodachrome II, and exposure was at f 1.9. Normal speed movies were slightly overexposed at this setting, but it was about right for slow motion.

Several methods were considered for measuring flame temperatures: thermocouples, resistance wires, optical pyrometers and total radiation pyrometers. Each had its advantages and drawbacks. Thermocouples are usually reliable, but in a flame they have three problems: they must be coated with a suitable material to prevent catalytic burning on the wire surface, they require a correction for radiation, and they are subject to much fluctuation in the turbulent flame. The wires also tend to deteriorate in the hot flame gases.

Resistance wires suffer much the same disadvantages; they can be used to measure average temperature more easily, however. The optical pyrometer has the advantage of remote measurement, but again requires a radiation correction to get the flame temperature. The total radiation pyrometer suffers from the corrections necessary for radiation effects, and it also must have a very narrow viewing angle in order to be of value for small flames or at more distant observation points. Both pyrometers suffer a loss of usefulness because of the difficulty of sighting them on a turbulent flame. No point in the flame is stable and the temperature varies from point to point and as a function of time. A further difficulty in all cases is that when radiation corrections must be made, they are usually made assuming graybody radiation. In the case of flames the assumption of graybody radiation is not completely valid since the energy of reaction may be given off at discrete bands of wavelength. After considering the possible methods of temperature measurement, the optical pyrometer was chosen. It allowed estimation of the temperatures for all but the methanol flames. In the present work on flame bending it was found that the effect of flame temperature was not so strong as to require more sophisticated temperature measurements. Such would probably not be the case if more detailed analysis of flame kinetics or thermodynamics were involved.

It was desired to make some measurements of the flame radiation at points downstream from the flame. In order to make these measurements it was necessary to use a radiometer with a window which would protect the receiver from convective effects of the wind. Such a radiometer is discussed briefly by Stempel and Rall (52). This radiometer is referred to as an asymptotic radiometer. It basically consists of a copper body with a thin, blackened constantan foil suspended across a cavity. A fine copper wire is attached to the center of the foil, and a differential thermocouple is formed with the hot and cold junctions at the center and periphery of the foil, respectively. Such a radiometer has a fairly rapid response time (0.25 seconds or less), and gives a signal proportional to the incident flux. It is small, rugged, and is insensitive to ambient temperature variations within design limitations of the specific instrument. An asymptotic radiometer was obtained which had a range up to 3 solar constants (about 0.36 Btu/ft$^2$-sec) with an output of 0 to 5 millivolts.

In order to check for potentially dangerous buildups of vapors in the tunnel, beneath the tunnel floor, and in the adjoining rooms prior to ignition an explosion meter was purchased. It was calibrated for use with natural gas, but it indicated the presence of any combustible in the air by catalytic action on a platinum wire. It was found to be reliable for checking purposes, even though most of the fuels used had enough unpleasant odor that they could be smelled before a dangerous concentration built up. The great utility of the

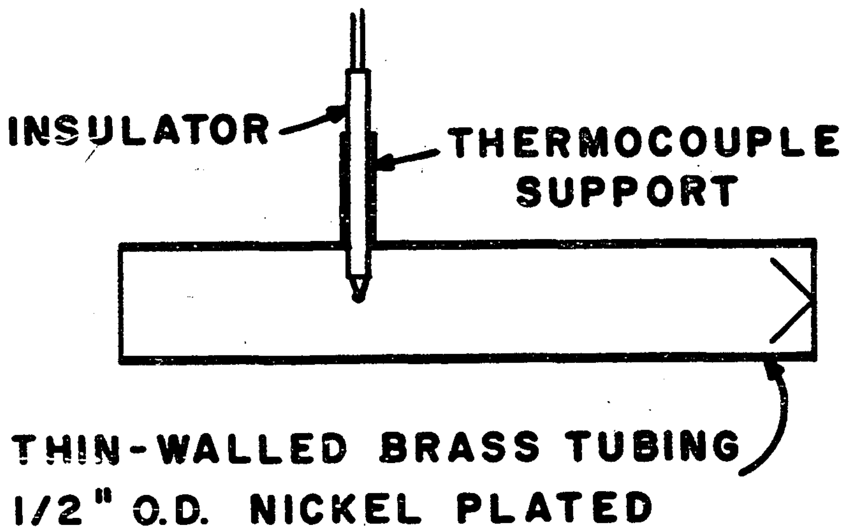


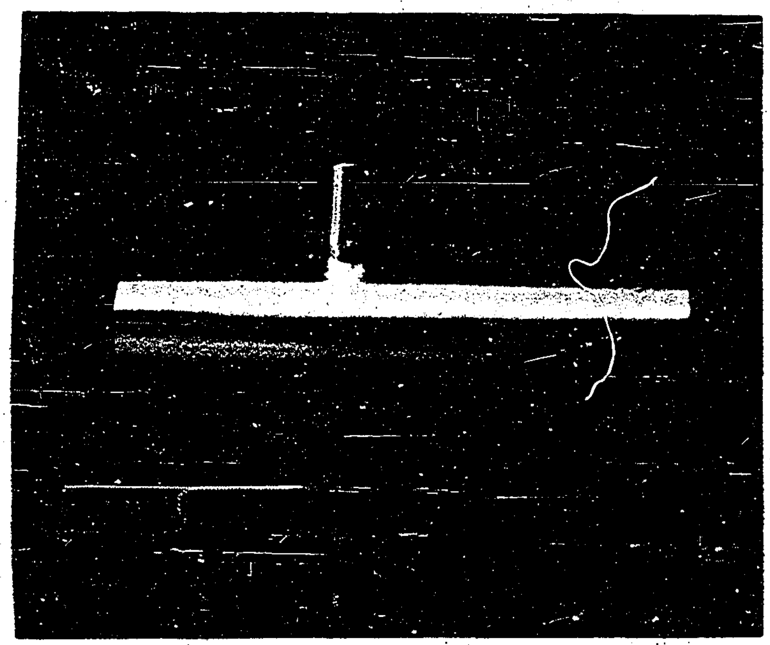

Figure 16. Thermocouple Shield

explosion meter was in checking beneath the floor and in inaccessible areas where a stagnant layer of vapor might form.

It was desired to make a number of readings of the air and wake gas temperatures downstream of the fires. A grid network of thermocouples was set up for this purpose. The network was constructed by attaching a movable support to railings running along both sides of the tunnel. The supports could be moved up and down the tunnel simultaneously through the use of a reversible AC motor and a system of pulleys and cables. Attached to each support was a series of hooks from which fine nichrome wires were strung across the tunnel. These wires were spring-loaded at each end to support the thermocouples and shields. Two types of thermocouples were used. Iron-constantan thermocouples were used for reading temperatures up to 400°F and Chromel-Alumel thermocouples were available for temperatures up to 1500°F. The hot junctions were made by twisting the wires together and then welding them electrically. The temperatures were recorded on two 12-point multipoint recorders, one of which was calibrated for use with iron-constantan thermocouples and the other for Chromel-Alumel thermocouples. It was recognized that shielding of the thermocouples from the flame radiation would be necessary if reliable temperature measurements were to be made. Several shield designs were considered; a sketch of the final selection is shown in Figure 16. The shield was fabricated from thin-walled brass tubing which had a cone-shaped copper shield placed in the nose near the entrance. The thermocouple was positioned perpendicularly to the direction of air flow through the access tube in the side of the shield. It was located so that the hot junction was shielded from direct flame radiation by the cone in the nose. Before final assembly the shields were plated with a bright nickel coating so they would reflect as much radiation as possible and would have low emissivity.

The thermocouple shields were checked for efficiency during one of the regular runs by mounting two of them side-by-side in the tunnel. One of these was aspirated, and the other was not. Both thermocouples read the same temperature, approximately 150°F. The temperature of the brightly polished shield was approximately 35°F higher than the thermocouples. This test showed that the shields were effective in blocking flame radiation from the thermocouples which would interfere with the temperature readings. The positions of the thermocouples in the test section during the runs are shown in Figure 17.

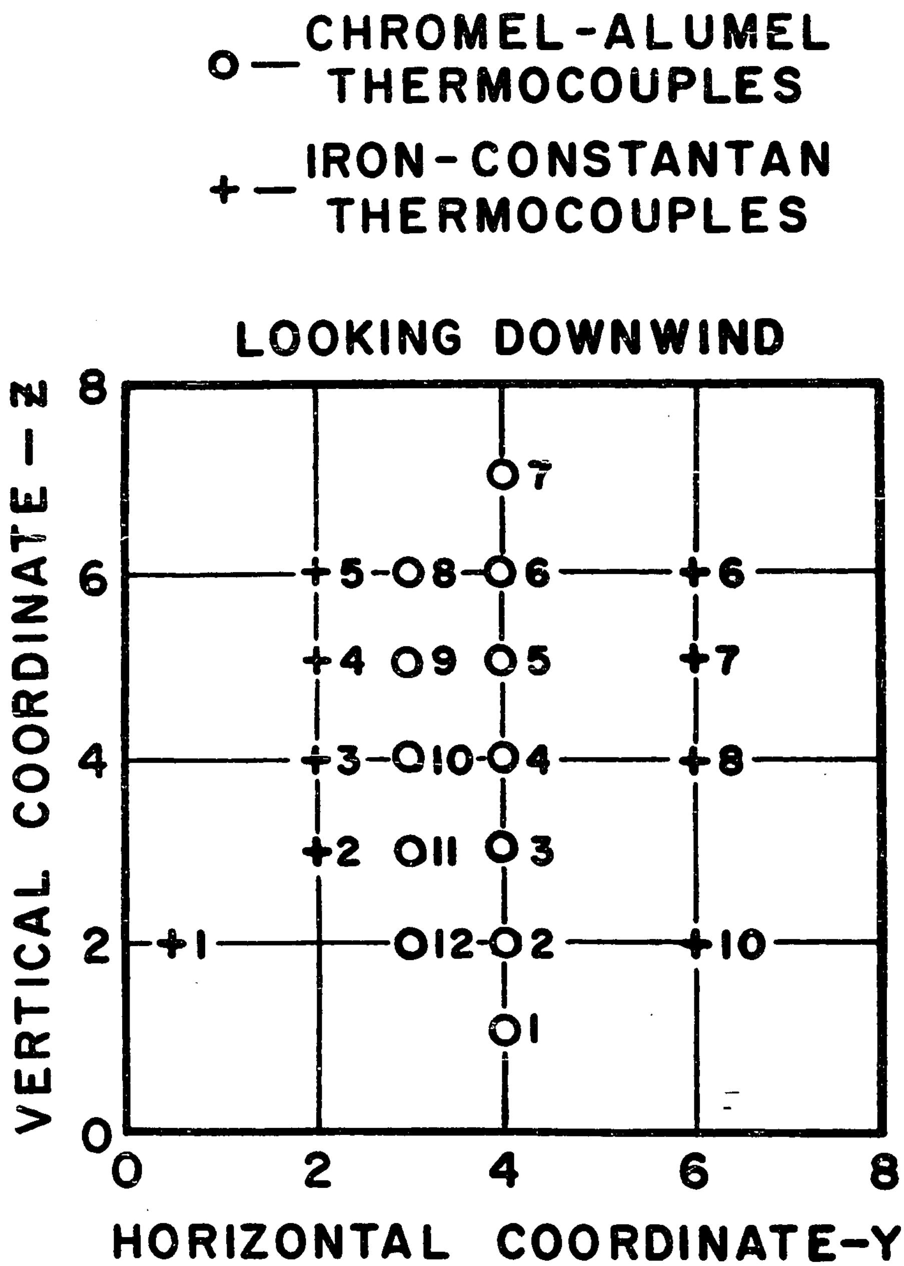


Figure 17. Location of Thermocouples in Wind Tunnel

# CHAPTER V

## EXPERIMENTAL PROCEDURE

This chapter will present a short explanation of experimental procedure and some of the problems involved. Since this study is apparently one of the first on liquid fires in a wind tunnel, the problems encountered may be of interest to others who desire to do work in this area.

A typical experimental run started with the installation of the burner. The burner was set into the floor space provided and was connected by copper tubing to the fuel reservoir. The tubing was sloped downward towards the reservoir to prevent air bubbles from forming in the line and to permit drainage at the finish of a run. A piece of glass fiber mat or gypsum board with a cut out hole was fitted over the burner rim; the rim protruded about 7/8 inches above the sheet metal floor insert. After the insulating mat or board had been tightly fit around the rim, a piece of reinforced asbestos cloth was cut and also fitted around the rim. The asbestos cloth was stapled to the insulation to hold it in place. In addition, the cloth was tucked in around the burner rim whenever possible to provide extra insulation. Following installation of the burner, all the instruments were switched on except the thermo-anemometer, and the thermocouple grid was placed in position. The anemometer was generally left off until after ignition since it was possible that one of the wires might break and arc, causing a fire if enough vapors were present. During the instrument warmup period the appropriate fuel reservoir was filled with fuel. A reservoir was chosen which would contain about the proper amount of fuel for the series of runs to be made. Before the burner was filled the blower was turned on and air was blown through the tunnel at maximum rate for a few minutes as a purge, and the exhaust fan under the floor was started. The burner itself was then allowed to fill from the reservoir. The breather tube in the reservoir was kept low enough to prevent overflow. The fuel level was gradually brought up to as near the top as possible consistant with the amount of boiling expected from the fuel. During the time the burner was being filled the fuel delivery tubing was closely monitored for leaks. After filling was completed the explosion meter was used to check beneath the floor for possible buildup of fuel vapors. None was ever detected.

The blower speed was then decreased and the pool ignited with an electrical spark igniter which could be used from the observation room. The anemometer was switched on and the wind speed adjusted until the flame was bent at about the desired angle. The fire was allowed to burn for a time until boiling started or (especially in the case of methanol) enough time had elapsed for steady burning to be neared. During this unsteady period the pool of liquid was watched closely for possible boilover, and frequent checks were made under the floor for leaks. At the time when fuel boiling appeared to be reaching its maximum, recording of data was begun. This initial period required about 15 to 30 minutes, depending on the fuel. Data taking was continued until the burning rate and downwind temperatures were established. A photograph was then taken and processed. It was marked immediately with the run number to avoid later confusion. If movies were to be taken, they were shot after this period of steady burning had been established. During this data-taking period visual observation of the fire and fuel system was continued. When the necessary amount of data had been taken, the wind velocity was changed until the flame angle was different and a new run was started. Four runs were usually made in a series although in some cases more or fewer runs would be made due to special circumstances.

At the end of a series of runs the fuel was turned off and the fuel level allowed to burn down a little. The fire was then extinguished in one of two ways. For smaller burners a sheet-metal slide was pushed through the narrow access door and the fire was smothered. For larger fires the fuel was drained from the burner and the fire allowed to burn out. The blower vanes were opened fully to allow maximum air flow through the tunnel, which promoted faster cooling of the test section and cleared the last traces of smoke and vapors from the tunnel. While the tunnel was cooling, the fuel reservoir was drained and the instruments were turned off. After the blower had been switched off, the tunnel test section and burner were inspected for possible damage before the next series of runs were started.

Several problems were encountered during the experimental runs. Two of these were due to the trailing of fuel vapors along the floor downstream of the burner. This burning along the floor caused deterioration of the insulation beneath the asbestos cloth. The glass fibers in the mats melted and therefore could not be used with larger fires. The gypsum board tended to crumble although it usually retained enough coverage to do a satisfactory job of insulating. Neither of the insulating materials used could ever be reused once they were removed from the tunnel. The second problem caused by the vapor trail was due partially to the tunnel conditions. The wind in the test section had a slight positive pressure due to the forced draft blower setup. The exhaust fan beneath the floor pulled a very slight vacuum. The combination of slight positive pressure above the floor and slight negative pressure beneath the floor caused some vapors to penetrate beneath the floor. This condition was noticed only for the larger burners, and in one case was the contributing factor in an accident. The fuel vapors burning beneath the floor heated the burner enough to weaken its supports and it fell through the floor. Since the burning beneath the floor had already been detected, the fuel had been shut off and draining started. This single case of an accidental fire was minor; it was extinguished before serious damage was done. The supports were reinforced and extra precautions were taken to seal the burner around the edges before the runs were continued.

One of the problems found with larger fires was the difficulty in establishing wind velocities. The larger fires could not be burned at low velocities because of the induced draft and the length of the flame. Smoke from larger fires tended to circulate in the test section if the wind velocity was too low. If care was not taken this circulation tended to make the angle of the flame less than otherwise. The fluctuations of the flame, particularly the buildup and collapse of flame sections that broke away from the main flame, caused a fluctuation in the anemometer readings. This effect was also noticed only for large flames and only near the top of the flames. The velocity profile below about 2/3 of the flame height was flat and smooth. For smaller flames, the flames tipped more than about 45 degrees, the velocity fluctuations were not noticed.

The problem of outdoor wind gustiness was generally not too severe. For velocities greater than about 2 ft/sec no rapid changes in tunnel air velocity were noticed. Some low frequency (15 to 30 seconds per cycle) changes of about ±5 ft/min were noticed on particularly windy days, but they seemed to be caused about as much by flame fluctuation as wind gusts. Even on calm days the large flames would create surges of ±5 ft/min in the test section velocities, and for velocities of 1 ft/sec or less, no large flame tests could be run. Winds from the north affected the test section wind to a slightly greater extent since the north side of the blower inlet was not as sheltered as the south side.

Two difficulties were encountered because of the radiant heat output of the fires. One of these was the overheating of the test section walls and windows near the flame. Wall temperatures often went higher than 300°F, and at one time the window temperature exceeded 375°F. These high wall and window temperatures were especially bad in the case of benzene fires, and they resulted in limiting benzene fires to circular burners under 1 foot in diameter and channel burners 4 inches in width or less. Cyclohexane and n-hexane fires were nearly as bad, and they were limited to 18-inch circular burners and 4-inch channel burners. Insulating the walls and cooling the windows would help this problem considerably. The second problem encountered due to radiant heating was that the cameras overheated. The cameras were permanently mounted within a few inches of the windows, and were painted with a flat black paint inside and out to minimize reflections. Because of the black paint they also were good absorbers of the radiant energy transmitted through the windows. The camera bodies therefore became very hot, probably about 300°F, melting the glue in the lens camera. In the case of the pinhole camera, the solenoid switch would not operate at the high temperature and the shutter mechanism had to be left open and exposure controlled from the outside. This problem was minor compared with the very slight radiant energy emission from the inside of the camera. The pinhole camera was designed to use a very fast film (ASA 3000), and even the slight infrared radiation from the hot camera was enough to cause the pictures to be mottled and appear overexposed. An attempt to prevent the camera from heating by placing a radiation shield in front of it was only partially successful because the camera rested on the metal window frame and heating by conduction through the frame was noticeable.

In general, no problems were encountered due to faulty fuel level control. In one instance one of the sight glass gaskets became loosened so that a vacuum could not be maintained above the fuel in the reservoir. This situation was noticed before the burner was filled since the fuel level in the burner could not be maintained; it was easily repaired.

# CHAPTER VI

## DISCUSSION OF RESULTS

The primary purpose of this investigation was to determine and correlate the flame bending angles for wind-blown flames from burning liquids. It was known from the start that other information, such as flame lengths, fuel burning rates and downwind temperatures, could be obtained at the same time with little additional effort. Of course, some of the additional information obtained would be far from enough to allow final correlations to be made, but it would permit an evaluation of experimental techniques and equipment and allow some preliminary attempts to be made at correlating the data.

A total of 7 circular burners and 4 channel burners were originally made for use in the wind tunnel. The circular burners had nominal diameters of 1, 2, 4, 8, 12, 18, and 24 inches, and the channel burners had widths of 1, 2, 4, and 8 inches. It was found that the 1- and 2-inch circular burners and 1-inch channel burner were too small to use in the wind tunnel. The flame from these burners was so small that the flames were forced nearly over to the floor. For this reason, data from these small burners are not included. Wind tunnel velocities ranged from less than 1 ft/sec to nearly 7 ft/sec, with most data being obtained in the 1 ft/sec to 5 ft/sec range. These velocities were sufficient to cause flame bending angles to range from less than 10 degrees to more than 60 degrees. Temperature rises downstream of the flame of over 250°F were measured using the shielded thermocouples.

The drag coefficients for fires burning above circular pools of liquids are shown in Figure 18. They were calculated as

$$C_f = \frac{\pi}{2u^2}\left(1 - \frac{T_a}{T_f}\right) gD\,\frac{\tan\theta}{\cos\theta} \tag{78}$$

Equation (78) is a rearrangement of Equation (28) in which it has been assumed that

$$\left(\frac{\rho_a - \rho_f}{\rho_a}\right) = \left(\frac{T_f - T_a}{T_f}\right) \tag{79}$$

In using Equation (78), the brightness temperatures of the flames were used since they were reproducible and readily obtained. Actually, the quantity $(1 - T_a/T_f)$ was essentially constant for all runs and had a value of approximately 0.8. The use of Equation (79) is not exact since it assumes the molecular weight of the flame to be the same as that of air. However, it does represent a reasonable assumption which has been used before (25, 37). In Figure 18, the drag coefficients are plotted versus the ReFr product, and

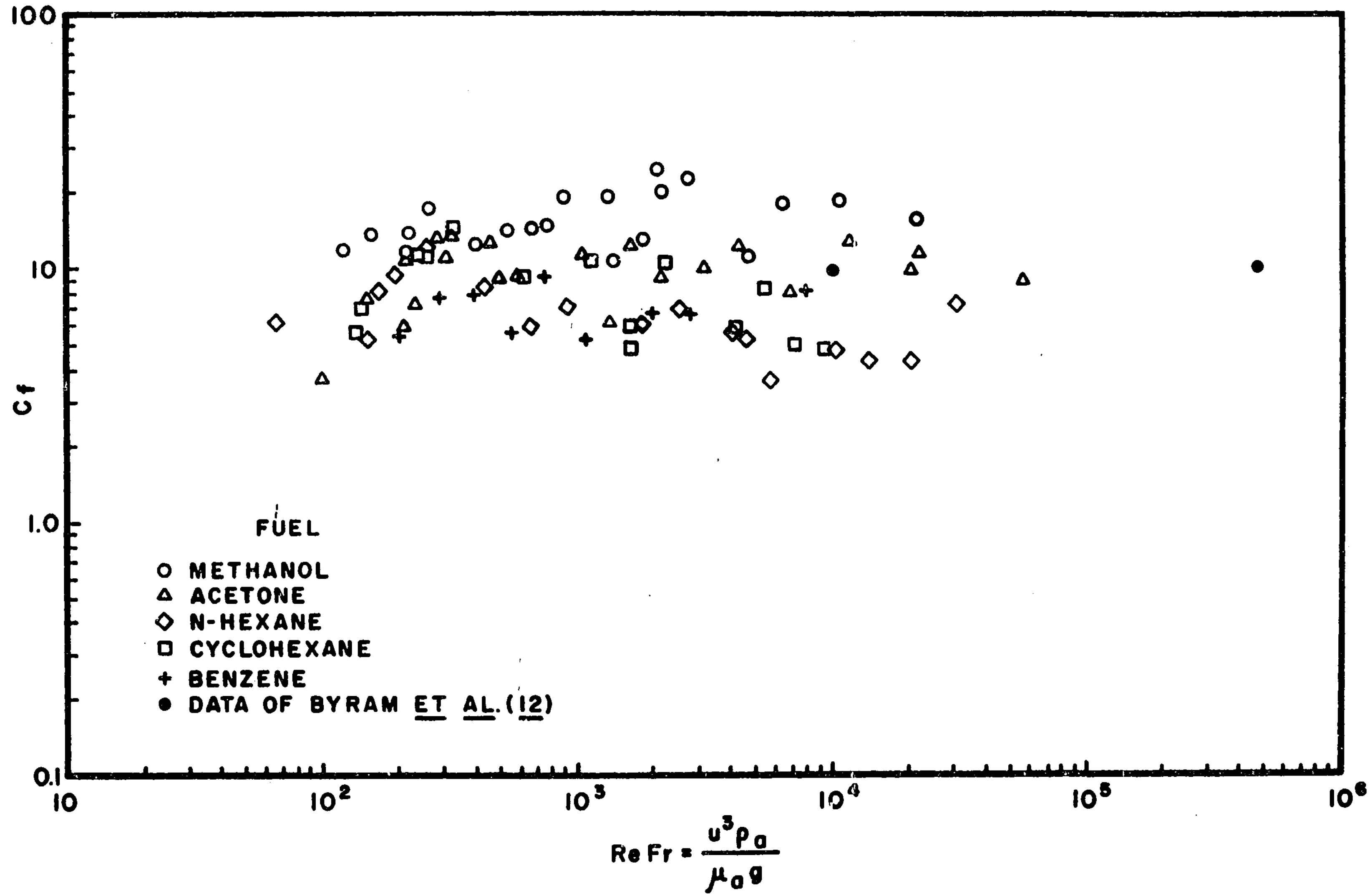


Figure 18. Drag Coefficients for Circular Burner Fires

the data are for five different fuels and five different burner diameters. Table 1 in Appendix A gives the original data as well as the calculated results for these tests. It can be seen from Figure 18 that even though there is considerable scattering of data, the calculated drag coefficients tend to fall into lines for each of the five fuels burned. Further, it is seen that the lines are apparently lower for fuels having greater vapor densities. This behavior, plus the increased amount of flame trailing, indicated that the vapor density of the fuel was important in determining the flame angle. The results of the dimensional analysis that showed the ReFr product to be important had also suggested the use of $\rho_g/\rho_a$ as a possible contributor to the drag coefficient. A linear analysis of the data was performed, assuming that log $C_f$ was a linear function of log (ReFr) and log $(\rho_g/\rho_a)$. In this analysis, $\rho_g$ was assumed to be the vapor density of the fuel at its normal boiling point. The analysis showed $C_f$ to be strongly influenced by the fuel vapor density, and a least-squares fit of the data was calculated as

$$C_f(\rho_g/\rho_a)^{0.88} = 16.4\ (\mathrm{ReFr})^{-0.015} \qquad (80)$$

Figure 19 is a plot of $C_f(\rho_g/\rho_a)^{0.88}$, and shows that a much better fit of the data results when fuel vapor densities are included. Attention is again drawn to the fact that five different burner sizes were used for the five different fuels indicated.

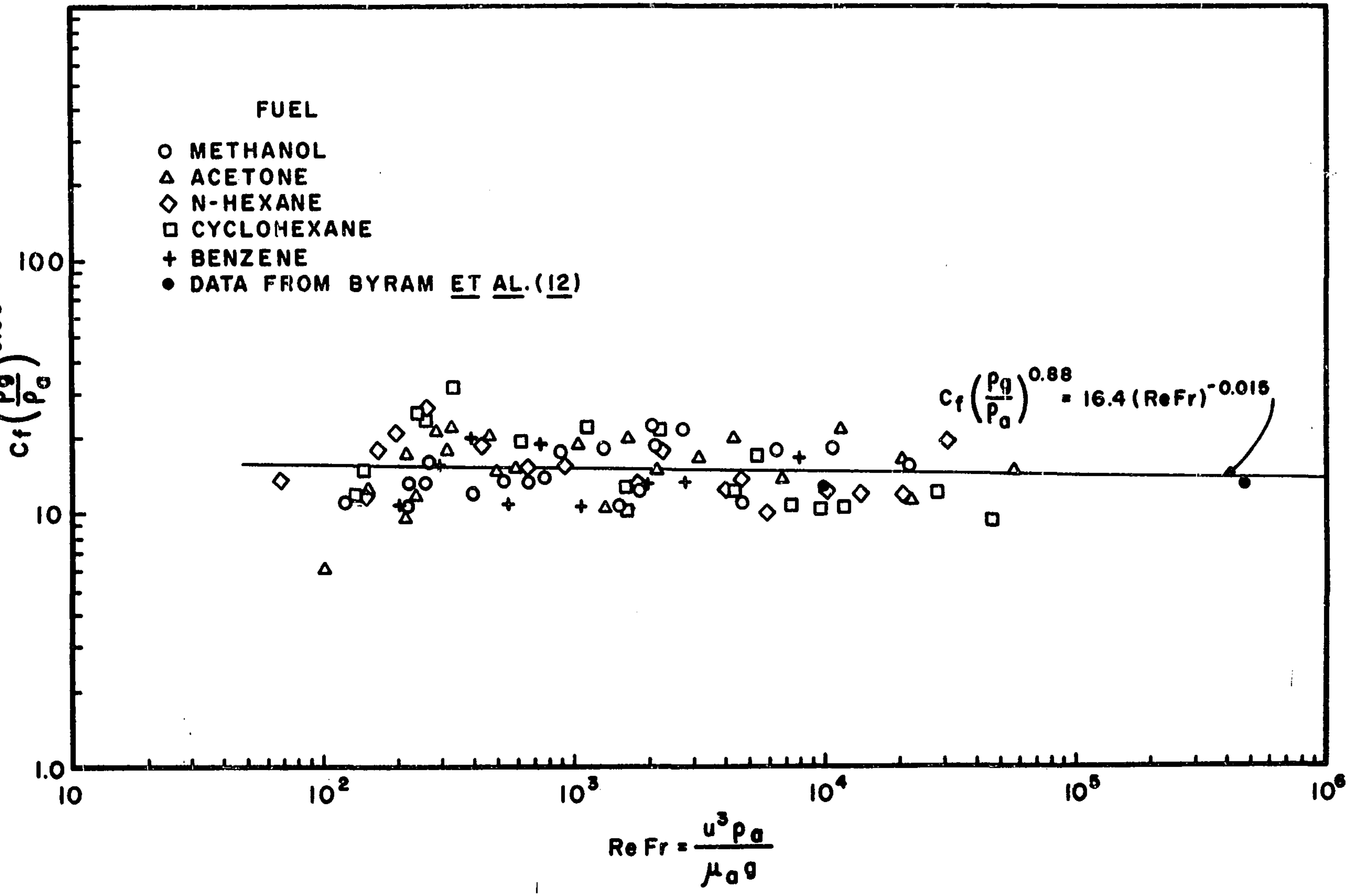


Figure 19. Corrected Drag Coefficients for Circular Burner Fires

Although Byram, et al. (12) do not report flame bending angles for their ethanol studies, they do state that at 3.7 ft/sec the angle was about 55 degrees and for the highest speed (about 13.3 ft/sec) the angle was about 80 degrees. Although their fires were from square burners, a comparison of the drag coefficient from their data and that of the present work is interesting. Using their data, the two points shown in Figures 18 and 19 were estimated. The two points agree well with the present circular burner data. They would not be expected to agree as well with the channel burner data because the end effects are proportionately larger for the square burner than for the channel burners. The edge effects would be expected to be approximately the same for circular and square burners since the ratios of area to perimeter are the same.

The drag coefficients for fires burning above liquid fuels contained in channel burners are shown plotted versus the ReFr product in Figure 20. They were calculated by rearranging Equation (29) to give

$$C_f = \frac{2}{u^2} \left(1 - \frac{T_a}{T_f}\right) gD \; \frac{\tan \theta}{\cos \theta} \tag{81}$$

where the ratio $\rho_f/\rho_a$ has again been replaced by $T_a/T_f$. It is again seen that the drag coefficients are a function of fuel vapor density, and the same method of analysis was used as was used for the circular burner data. This time the least-squares fit of the data resulted in

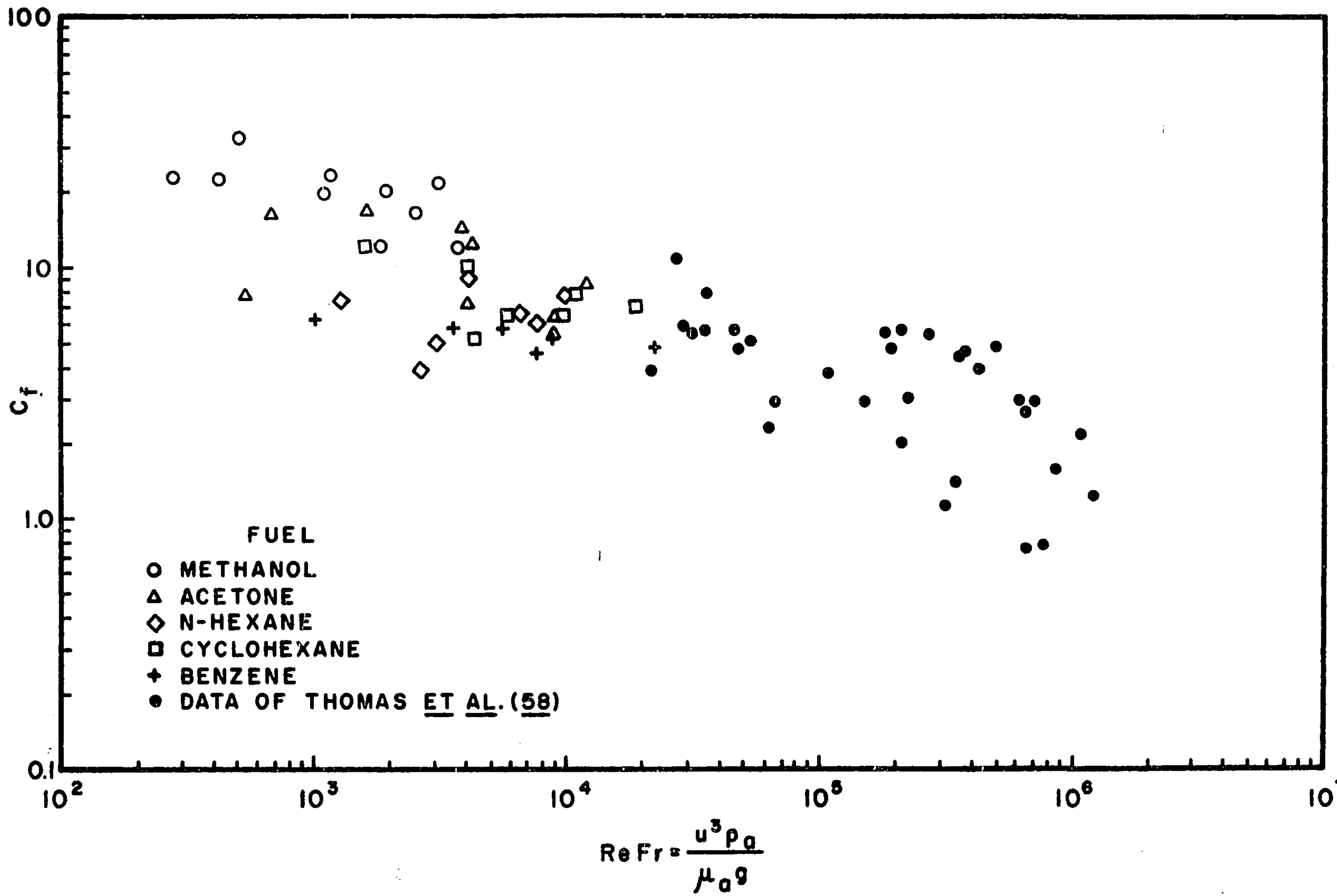


Figure 20. Drag Coefficients for Channel Burner Fires

$$C_f \; (\rho_g/\rho_a)^{0.88} = 55 \; (ReFr)^{-0.16} \qquad (82)$$

A plot of $C_f \; (\rho_g/\rho_a)^{0.88}$ versus ReFr is given in Figure 21, and shows that the correlation is again improved. In Figures 20 and 21, three burner widths were used for the five fuels indicated. Table 2 in Appendix A contains the data and results for the channel burner tests.

Turning attention back to Figure 20, the data reported by Thomas, Pickard, and Wraight (58) are plotted along with the channel burner data. These data are for rectangular-based wood cribs of various heights and various fuel loadings. The different fuel loadings were obtained by using different-sized white pine sticks. These drag coefficients were also calculated using Equation (81). Since the actual flame angles were not reported, they were calculated from the lengths of the horizontal and vertical projections of the flames. The drag coefficients calculated in this way are seen to give a not unreasonable extension of the data for liquids in channel burners considering the scatter in the data. It is not possible to extend the data to Figure 21, of course, since the vapor density cannot be estimated. The results of Figure 20 do show hope, however, that data from fuels other than the liquid fuels used may be used to extend the data presented here. If such is the case, the prediction of flame bending would be much simplified.

An interesting point in the correlation of the $C_f$ data is that the $\rho_g/\rho_a$ term has the same exponent for the

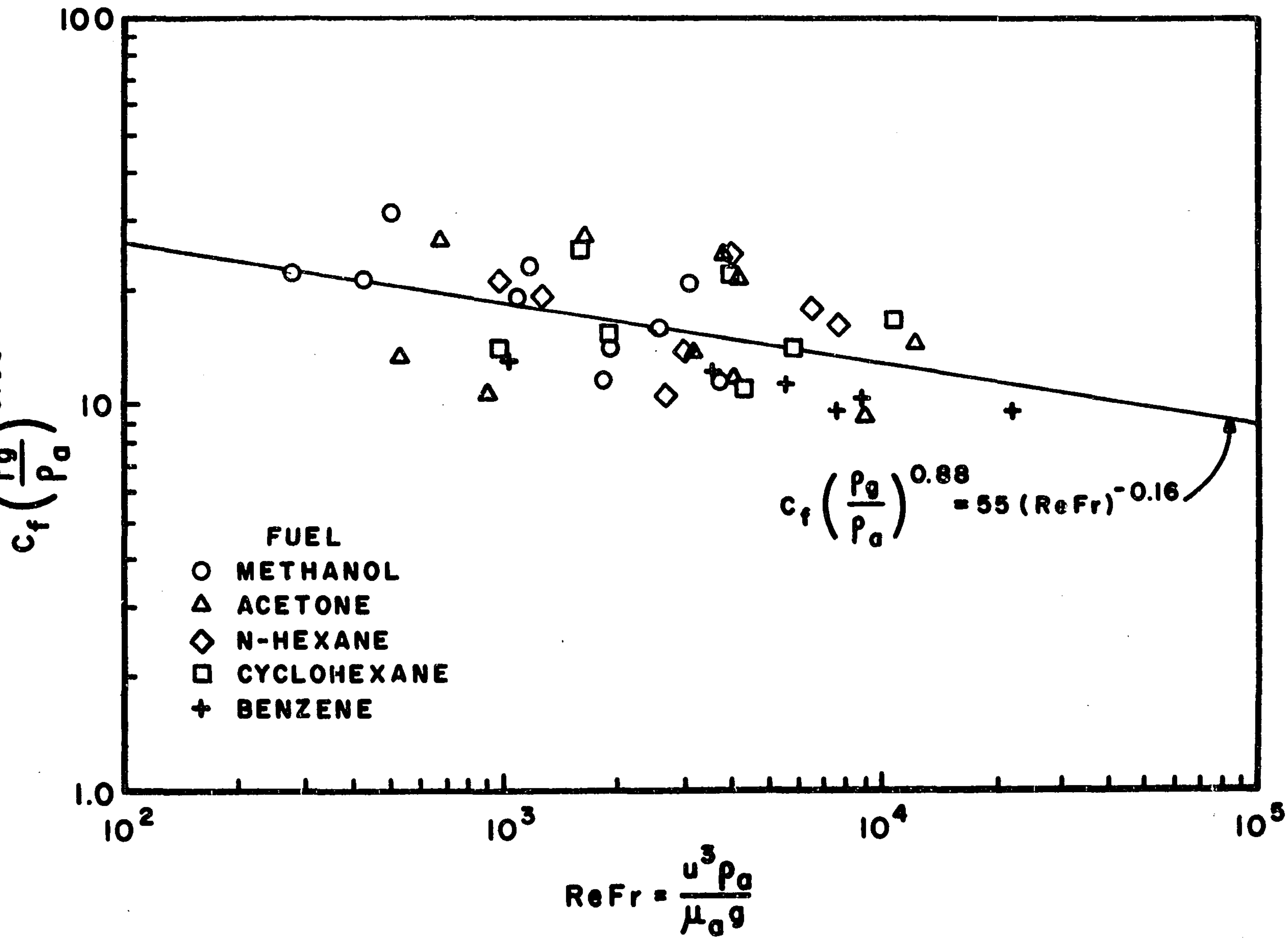


Figure 21. Corrected Drag Coefficients for Channel Burner Fires

circular and channel burner data. This result lends support to the supposition that flame bending from channel- and circular-burner fires is affected to about the same extent by differences in fuel vapor densities.

Actually, several different methods of correlating the flame bending data were tried. Figures 19 and 21 are those plots which gave the best results. It might be informative to mention a few of the other methods tried. First was a plot of $C_f$ versus the Reynolds number. It proved less satisfactory than did the ReFr correlation. A plot of tan $\theta$ versus the ratio of unit airstream energy to the unit energy release rate of the fire, as suggested by Anderson and Rothermel (2), was also tried. The data showed less success in correlating by this method, and the flame angles— were larger than those of Anderson and Rothermel for comparable energy ratios. One reason for this discrepancy may be the differences in burning characteristics of the fuels. The Anderson-Rothermel data could not be plotted using the drag coefficient method since enough data were not available on flame angles and flame widths.

The equations given by Pipkin and Sliepcevich (37) and Hamada (25) were used to calculate flame bending angles for comparison with the present data. Of course, all three must give the same angle at no-wind conditions and at conditions where the flame angle approaches 90 degrees. The poorest comparisons were obtained in the region of flame angles from 40 degrees to 50 degrees. In this range, the maximum deviation of the data of Pipkin and Sliepcevich was about 8 degrees--quite close considering the amount of extrapolation involved and the fact that their data were obtained on natural gas jets. Hamada's data showed a deviation of about 30 degrees in the 40- to 50-degree range. It must be remembered that Hamada used wood cribs, and his data may therefore not be readily comparable to that for liquid fires. Both of the previous methods gave flame angles smaller than those presently found in the range of poorest agreement.

An attempt was made to correlate the flame bending data using a slightly different model. In this model, the flame shape was taken as an elliptical cylinder with semi-major axis of D', which was taken as the length from the upwind edge of the burner to the point where the flame left the floor entirely, and semi-minor axis D, which was taken as the burner diameter. This model proved unsuitable for two reasons. First, the resulting correlation was no better than that obtained using the circular cylinder. Second, and more important, a second correlation was necessary to find the value of D' for estimating the drag coefficient to be used in extrapolating the bending data to large flames. This second correlation was undesirable since it increased the effort necessary to predict flame bending angles and at the same time decreased the accuracy of the result. The simplest correlation which represented the data was desired, so after considering the alternatives, the plots of Figures 19 and 21, and Equations (80) and (82) were chosen as best suited to represent the data.

The above discussion does not mean that D' is unimportant in flame behavior. Indeed, quite the opposite is true. The most important mode of heat transfer from a flame is direct flame impingement on a surface. Heat transfer to objects near a fire is thus strongly influenced by their proximity to the flame. If the flame trails far enough downwind of a fire to impinge directly on a surface, the surface is much more likely to be destroyed or damaged by the fire. This condition is particularly true of solid objects which will ignite more readily if a pilot flame is present.

The dimensional analysis previously presented suggested that D'/D could be correlated as a function of the Froude number and the $\rho_g/\rho_a$ ratio. Such a correlation was made, and the result is shown in Figure 22 for fires from circular burners. In Figure 22 the data are for five different pan sizes and five different fuels. The resulting equation is

$$\frac{D'}{D} (\rho_g/\rho_a)^{-0.48} = 21 \ (Fr)^{0.21} \qquad (83)$$

While the accuracy of Equation (73) is not particularly good, it is the only method presently available to estimate

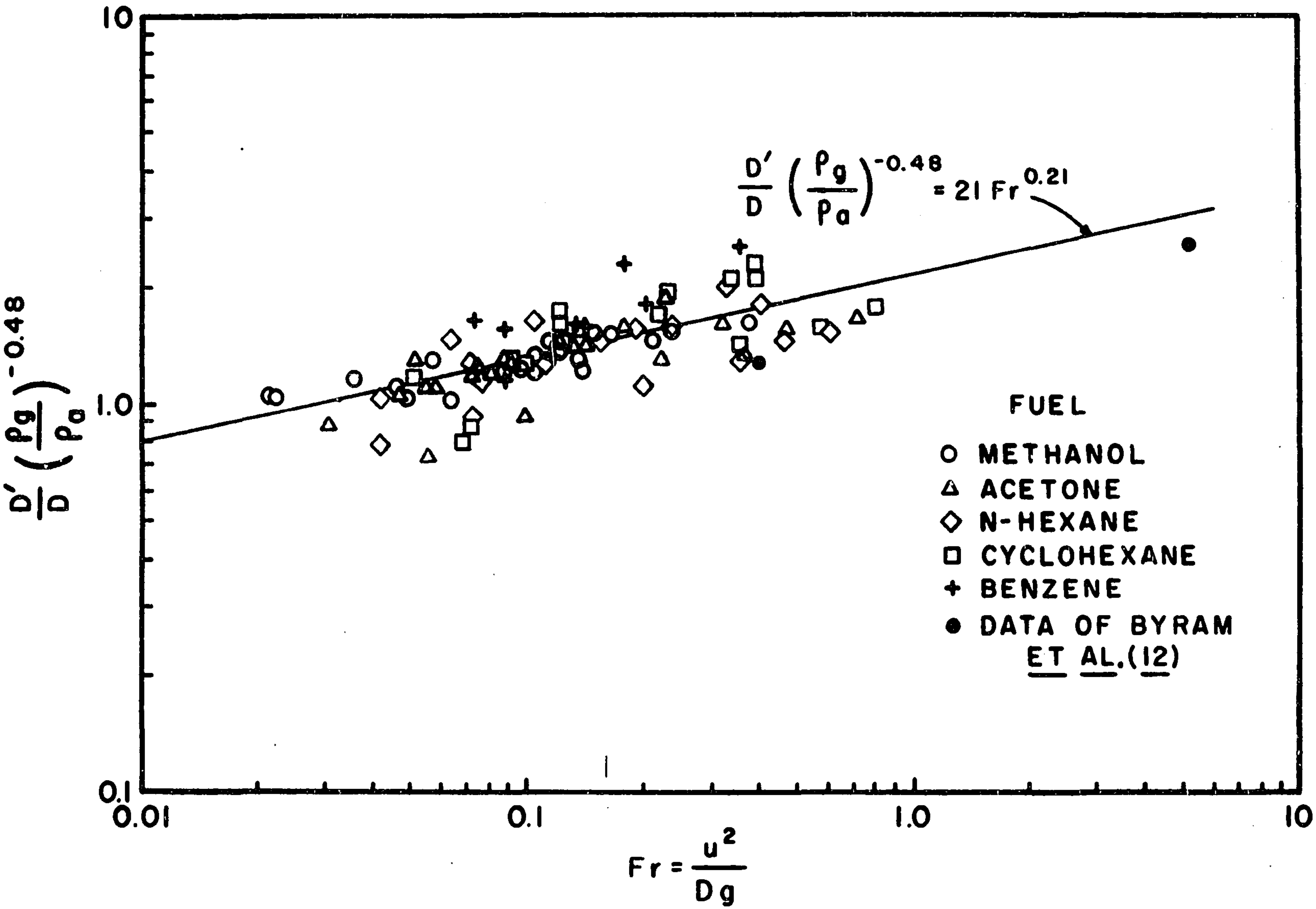


Figure 22. Flame Trailing from Circular Burner Fires

the amount of trailing of a flame downwind of a liquid fire. It was not possible to photograph the flame trailing from channel burners using the camera in the window mounts; in fact, except for methanol and acetone fires it was difficult or impossible to locate visually the trailing edge because of smoke. Visual observation of the trailing of acetone and methanol fires leads to the belief that flame trailing may be about the same as for circular fires. Certainly no great differences were noticed in the flame trailing behavior. An additional encouraging note is added by estimating the flame trailing for the ethanol fires of Byram, et al. (12). These two data points are plotted in Figure 22 along with the present data; the disagreement is not large. These flames were from 12.7-inch square burners, and the data were estimated from sketches similar to Figure 1.

The knowledge of air temperatures downstream of the flame are of importance in predicting convective heat transfer. Since it required little additional effort to obtain a small amount of these data during the flame bending tests, shielded thermocouples were used to measure the downwind temperatures for the larger circular fires and for the channel fires. These data were correlated as suggested by Equations (57) and (63) for channel burners and Equations (64) and (65) for circular burners. Plots of the dimensionless temperature rise versus dimensionless velocity for circular burners are shown in Figure 23 for z/x of 0.4 and in Figure 24 for z/x of 0.8. It is apparent that there is little

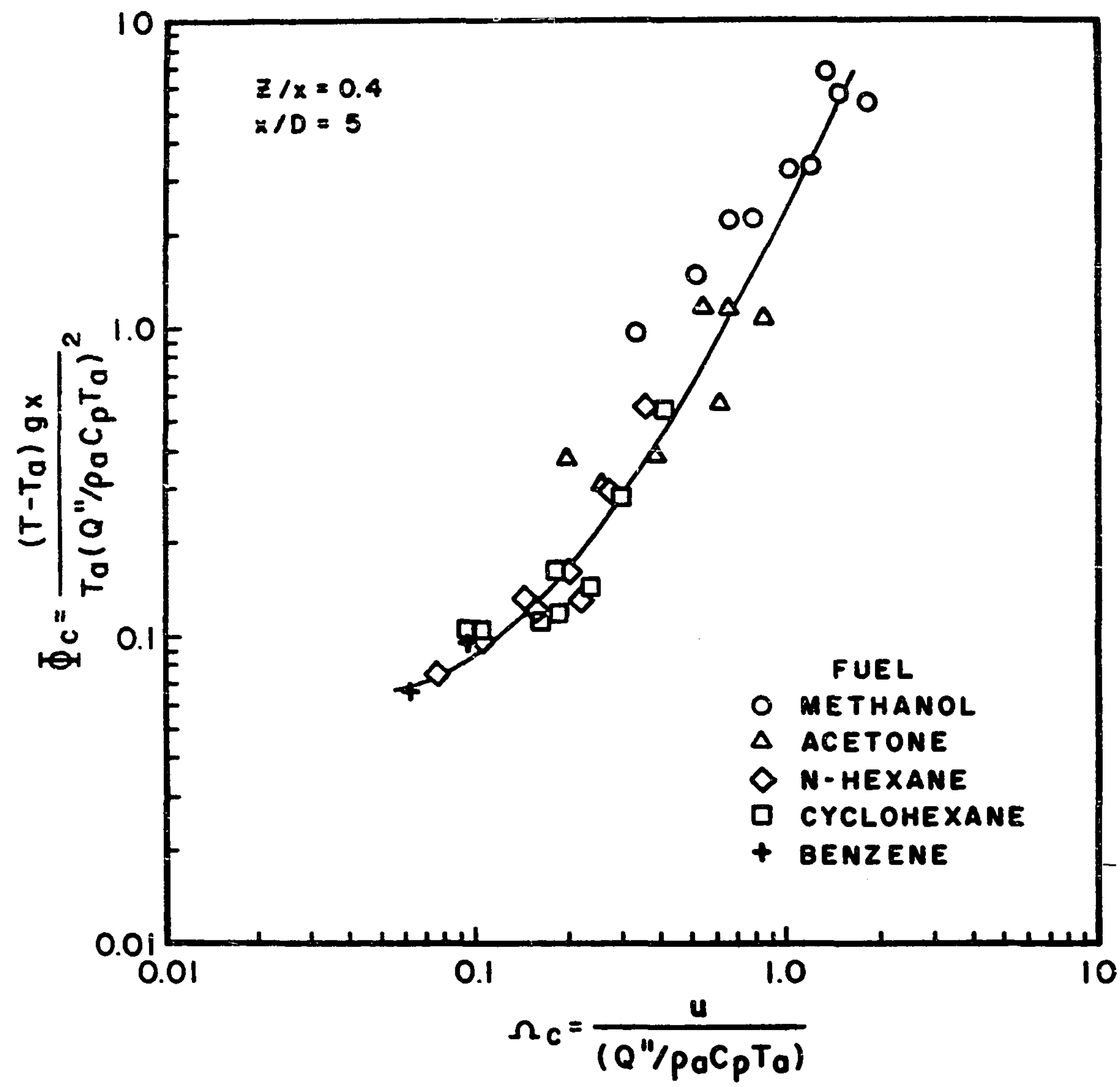


Figure 23. Temperature Rise Downstream from a Circular Burner

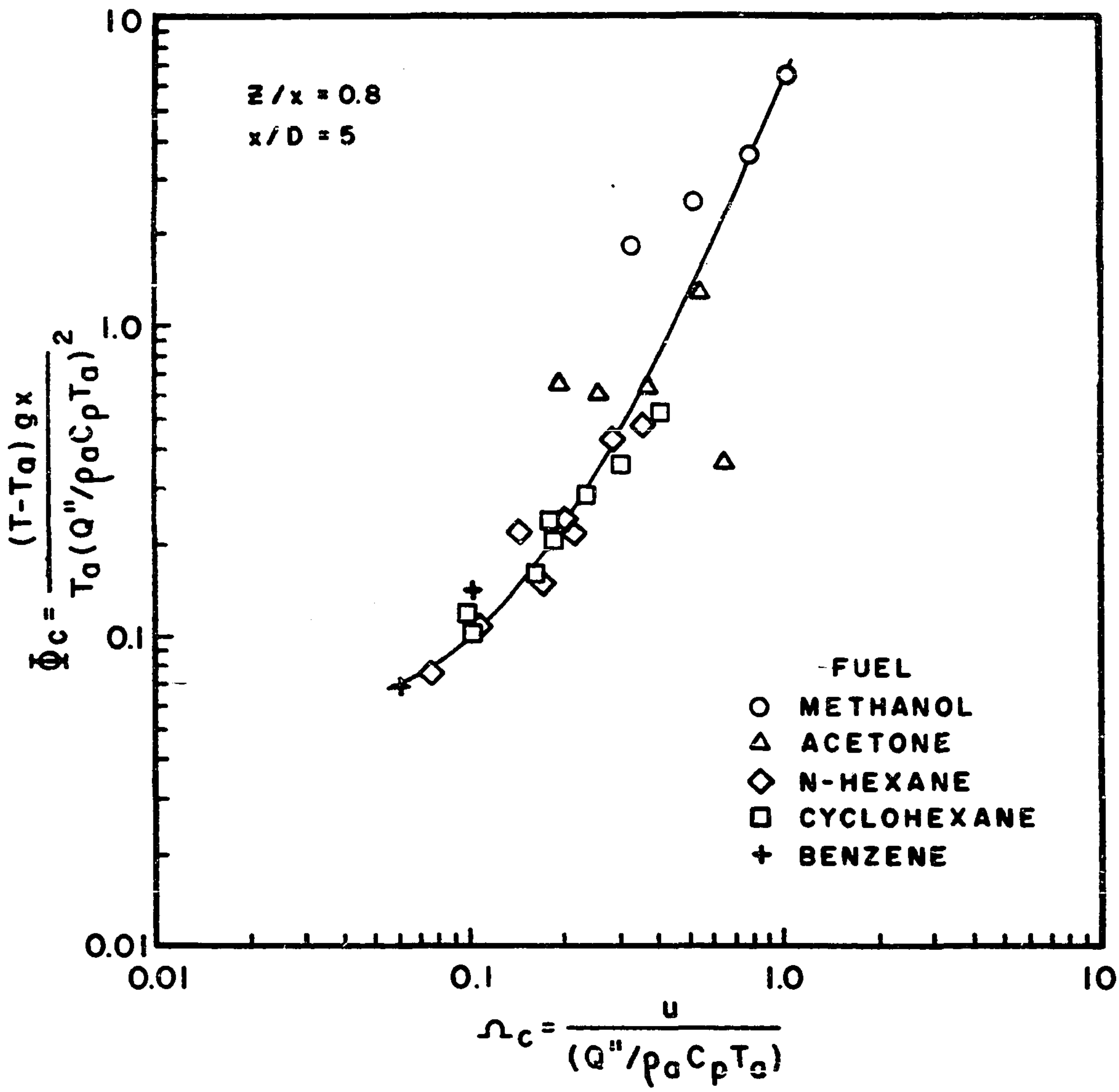


Figure 24. Temperature Rise Downstream from a Circular Burner

difference in the two curves. The data for temperature rises were read from the charts taken from the multi-point recorders. So far as could be established, the temperature readings were steady; they usually did not vary by more than a few degrees from point to point on the recorder plot. Although some scattering of data is noticed, Figures 23 and 24 reaffirm the choice of the dimensionless temperature rise and dimensionless velocity as parameters to use in data correlations. In Figure 23 the data are from three burner diameters, and in Figure 24 they are for two burner diameters. The choice of the distance downwind from the burner center, x/D = 5, was arbitrary, but it was held constant for all circular burner thermocouple readings.

Figures 25 and 26 show a correlation of $\Phi_L$ versus $\Omega_L$ for the data from three sizes of channel burners. Figure 25 is for z/x of 0.4 and Figure 26 is for z/x of 0.8. These data show a somewhat greater amount of scatter than do the data from the circular burners. This deviation is partly due to the flame angles, which were such that for a particular thermocouple position there was a change from low temperature through high temperature and back to low temperature as the hot gas plume was bent across and then below the thermocouple. These data therefore can be used to estimate the maximum temperature rise to be expected in a plume having x/D of 15. Here again, the choice of x/D was arbitrary and was chosen for convenience of use in the tunnel. In Figure 25 two

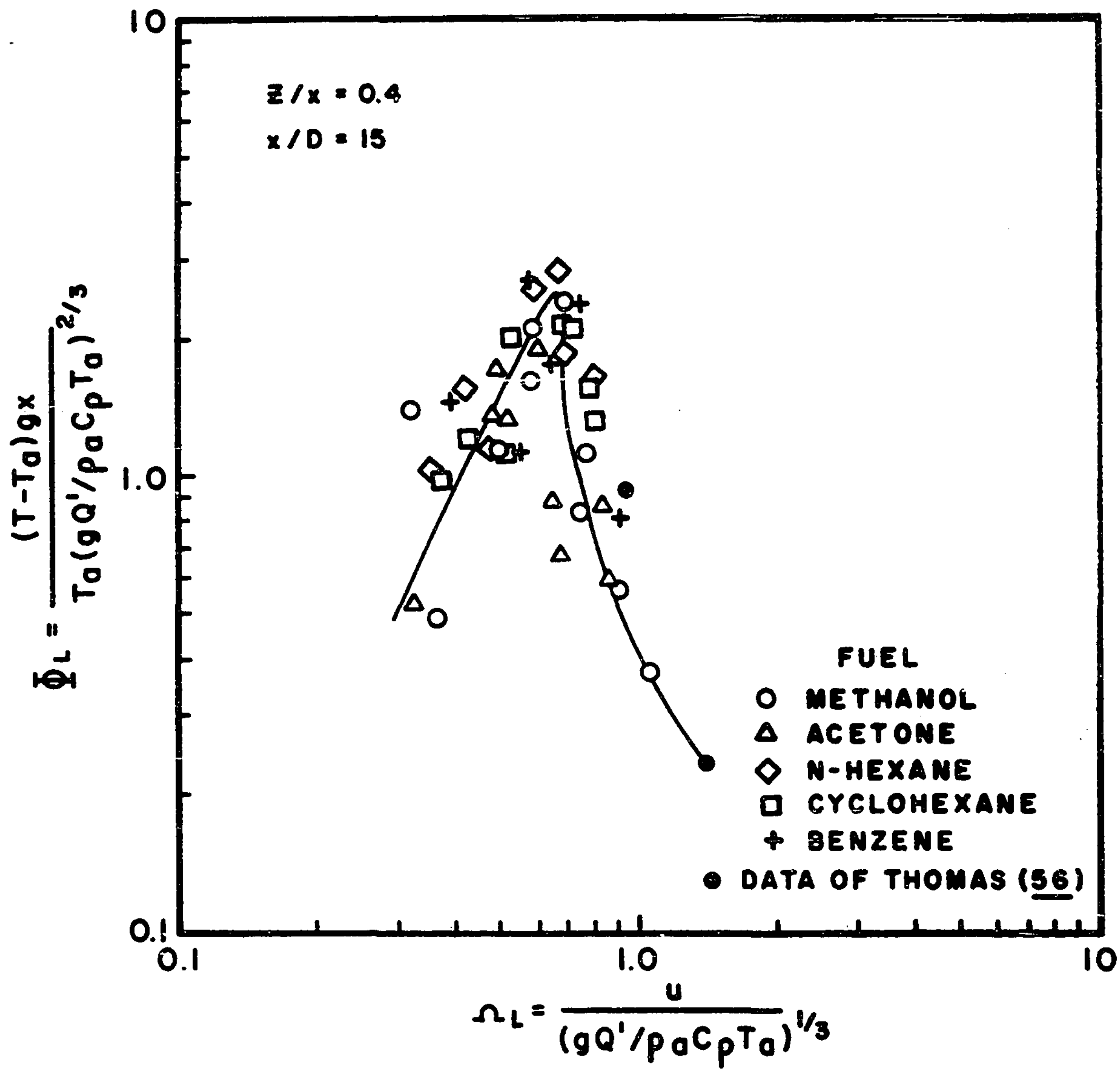


Figure 25. Temperature Rise Downstream from a Channel Burner

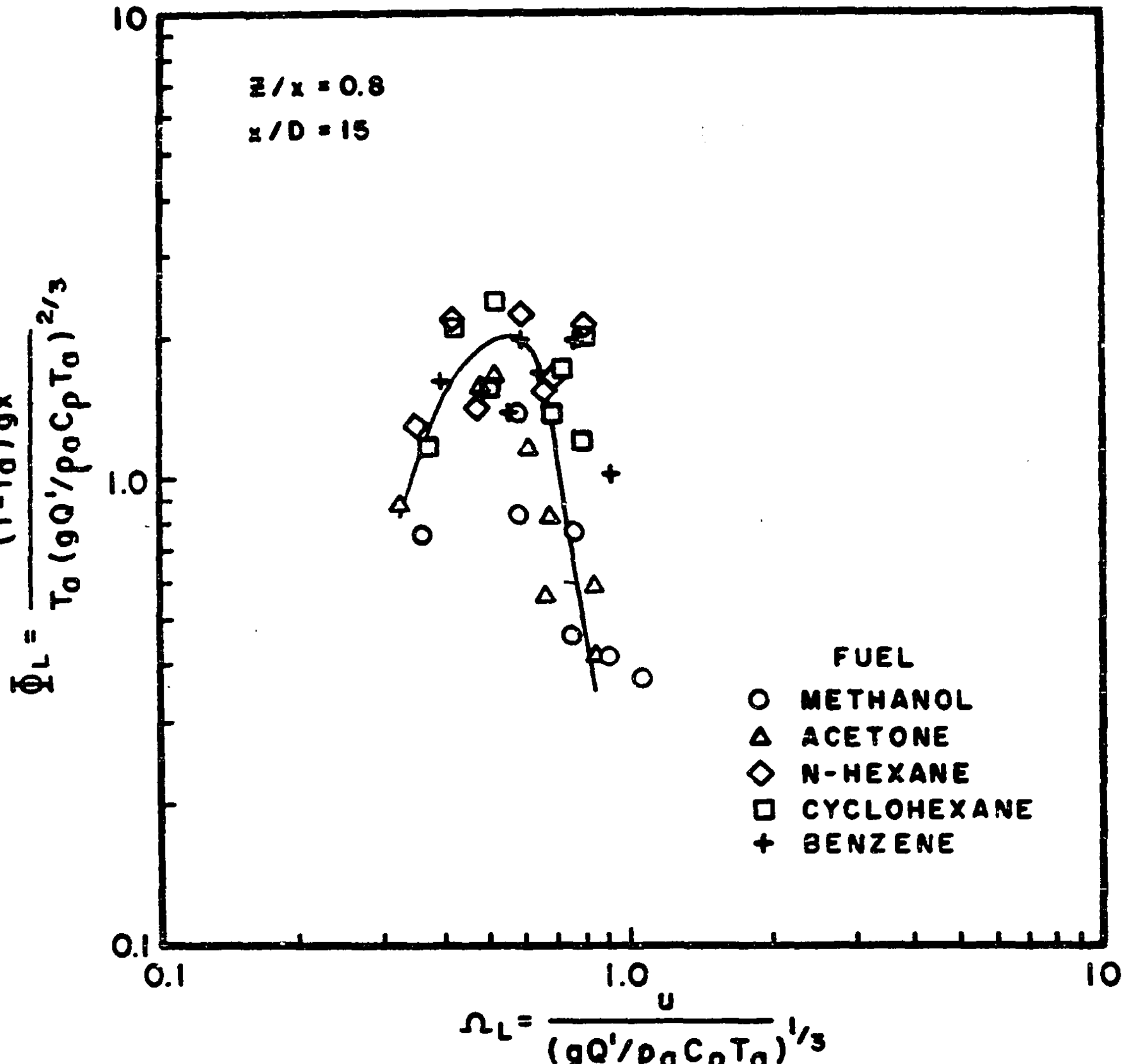


Figure 26. Temperature Rise Downstream from a Channel Burner

points are shown which were estimated from the data correlated by Thomas (56). They are apparently in about the same range as the data for liquid fires. Actually, a comparison is difficult to make since these two points were taken near the lower dimensionless velocities reported by Thomas. They do not seem unreasonable, however, in comparison with the present data. The data correlated by Thomas are for about the same wind velocities, but they are for much lower heat outputs and therefore lower temperature rises.

It is apparent from the temperature data that some refinements should be sought in techniques and equipment in order to obtain better information. In view of the difficulties involved using liquid fuels, it may well be that gaseous fuels would prove better. The temperature data used in calculating the temperature rises above are found in Tables 3 through 6 in Appendix A for circular and channel burners, respectively. Tables 7 through 10 give the $\Phi_C$ and $\Phi_L$ values calculated from the temperature data. Only a fraction of these data are represented by Figures 23 through 26. In calculating the dimensionless temperature rises of the wake gases and the dimensionless velocities of the air stream, the heat output was considered to be the total heat of combustion of the fuel. While strictly speaking this approach is not proper, it has the advantage of allowing the calculations to be made without knowledge of the amount of heat loss due to radiation. The tacit assumption is made, of course, that the fraction of energy leaving the fire due to radiation is the same in all cases. While such is not the case, it apparently does not create an inordinately large error.

Flame radiation does play an important part in heat transfer for flames. In conjunction with the other measurements made during the flame tests, radiation readings were taken at points downstream of the fires during test runs. The measurements were taken with an asymptotic radiometer, the sensing element of which was protected by a quartz window. For the smaller circular burners the data were taken with the sensing element positioned horizontally at floor level and located 5 burner diameters downstream from the center of the burner. These data are plotted in Figure 27. The data points are actually an average of the fluctuating output of the radiometer and generally appear to be approximately constant over the limited range of wind velocities. For the larger circular burners the radiometer sensing element was positioned vertically at floor level and again located 5 burner diameters downstream. Figure 28 shows the resulting data. The radiometer readings are 5 to 10 times as high as for the horizontal readings; they show a slight trend to increase at higher wind velocities except for methanol fires which seem to decrease. Some loss of accuracy is expected at lower ranges since the radiometer is

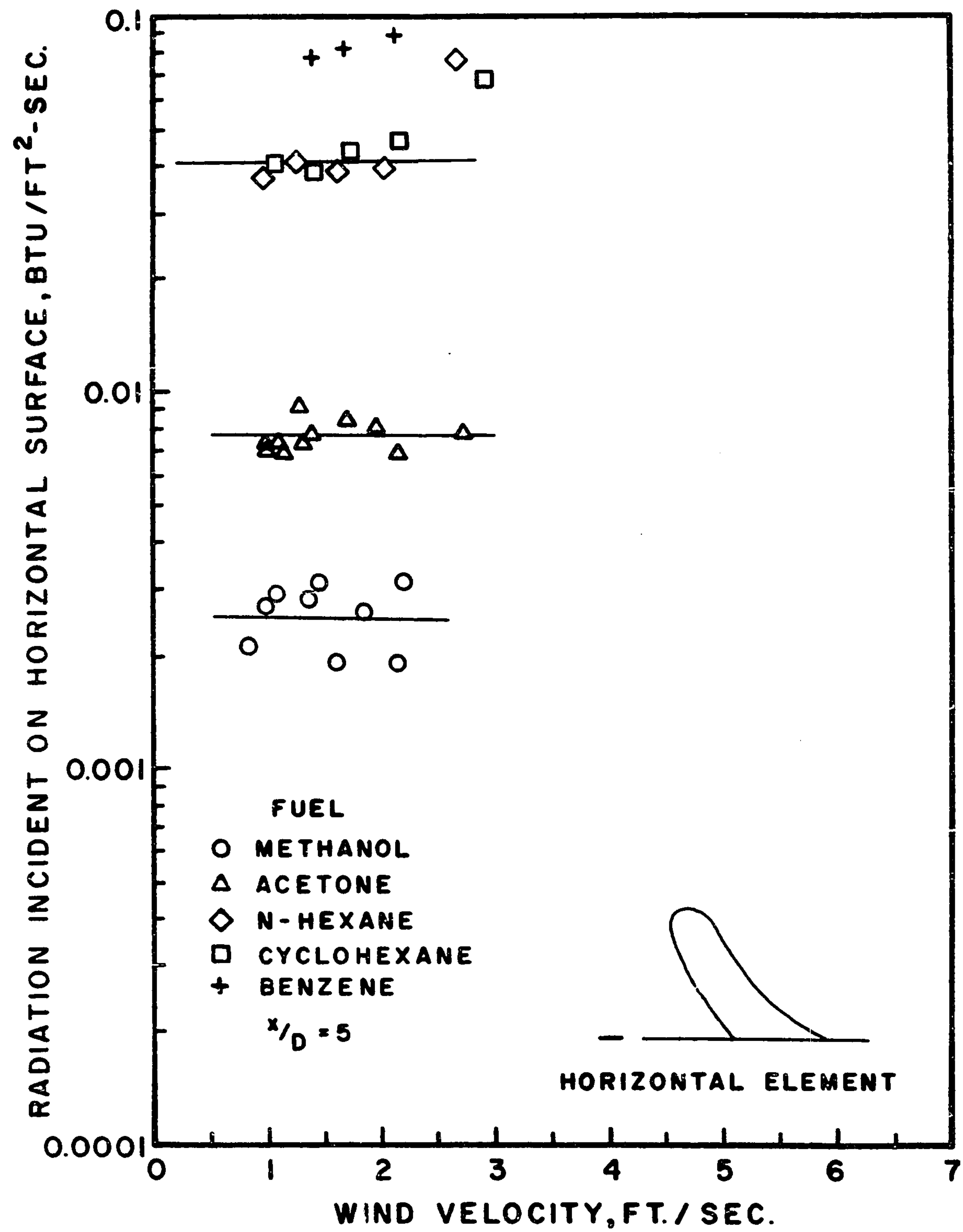


Figure 27. Radiation Incident on a Horizontal Surface Downstream from a Wind-Blown Circular Fire

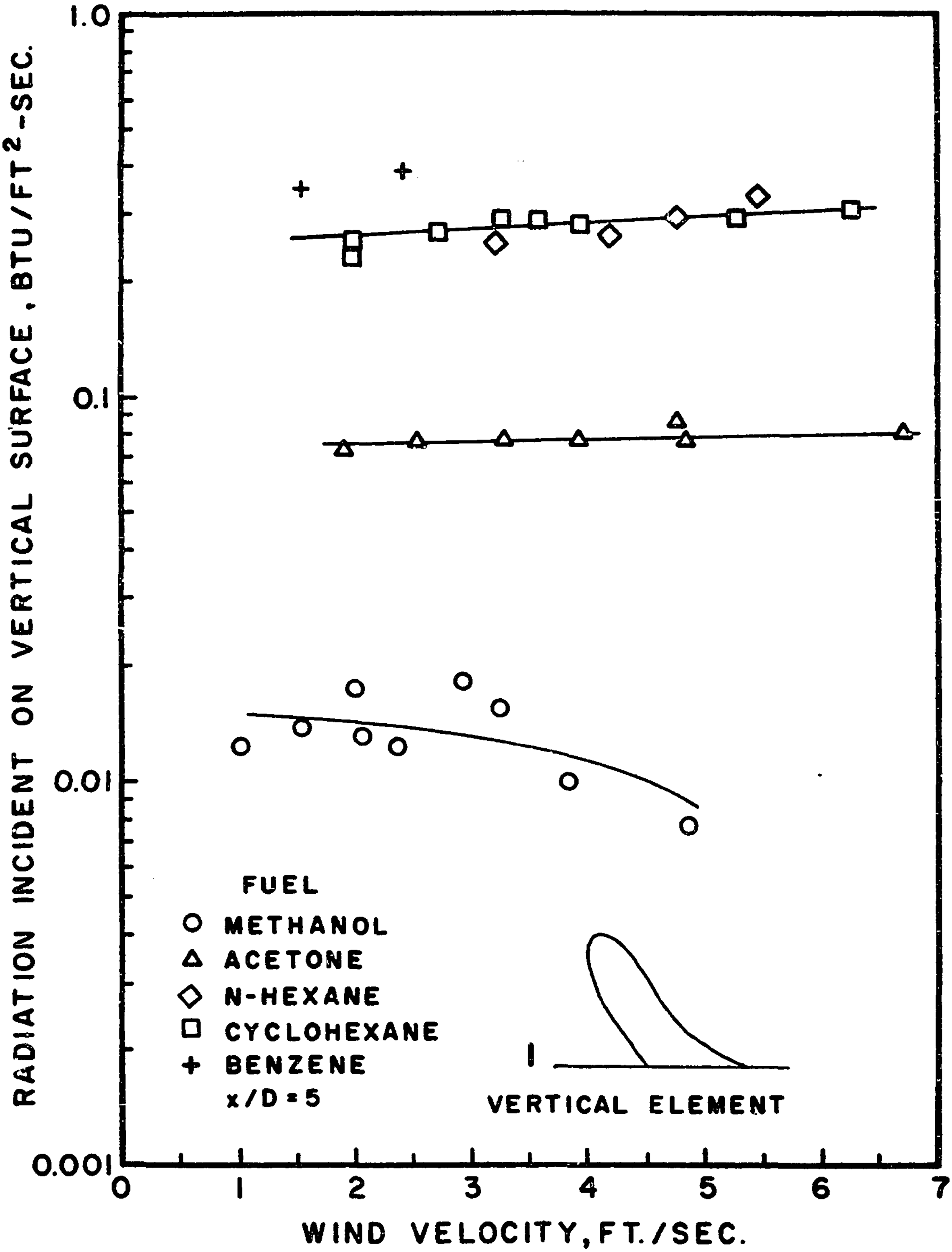


Figure 28. Radiation Incident on a Vertical Surface Downstream from a Wind-Blown Circular Fire

in the lower 5 or 10 per cent of its range and the percentage error can be larger, which helps to explain the greater data scatter for the low readings. The slight tendency of the radiation data to rise is probably due to the increased configuration factors for the larger angles of tilt.

The radiation data from the channel burner tests are shown in Figure 29. These data were taken using a vertical sensing element position and were 15 burner widths downstream. The data show a fairly sharp tendency to decrease as the wind velocity increases. Since the radiometer position is so far downstream, this decrease is probably a consequence of the decreasing configuration factor as the flame tilts. One other factor was noticed during the channel burner tests that affected the radiative output. If the fuel level in the burner dropped, the radiation decreased. If this behavior was present during circular burner tests the effect was much smaller and not noticeable. All the channel burner data were taken with the fuel level as near the top of the burner as possible; however, in some cases fuel boiling prevented keeping the fuel level too near the top of the burner. Benzene radiation data were not obtained for channel burners because of the soot which collected on the quartz window of the radiometer.

It can be seen that in general the methanol radiant output is about one-fifth that for acetone and that the cyclohexane and n-hexane outputs are about 5 times that of acetone.

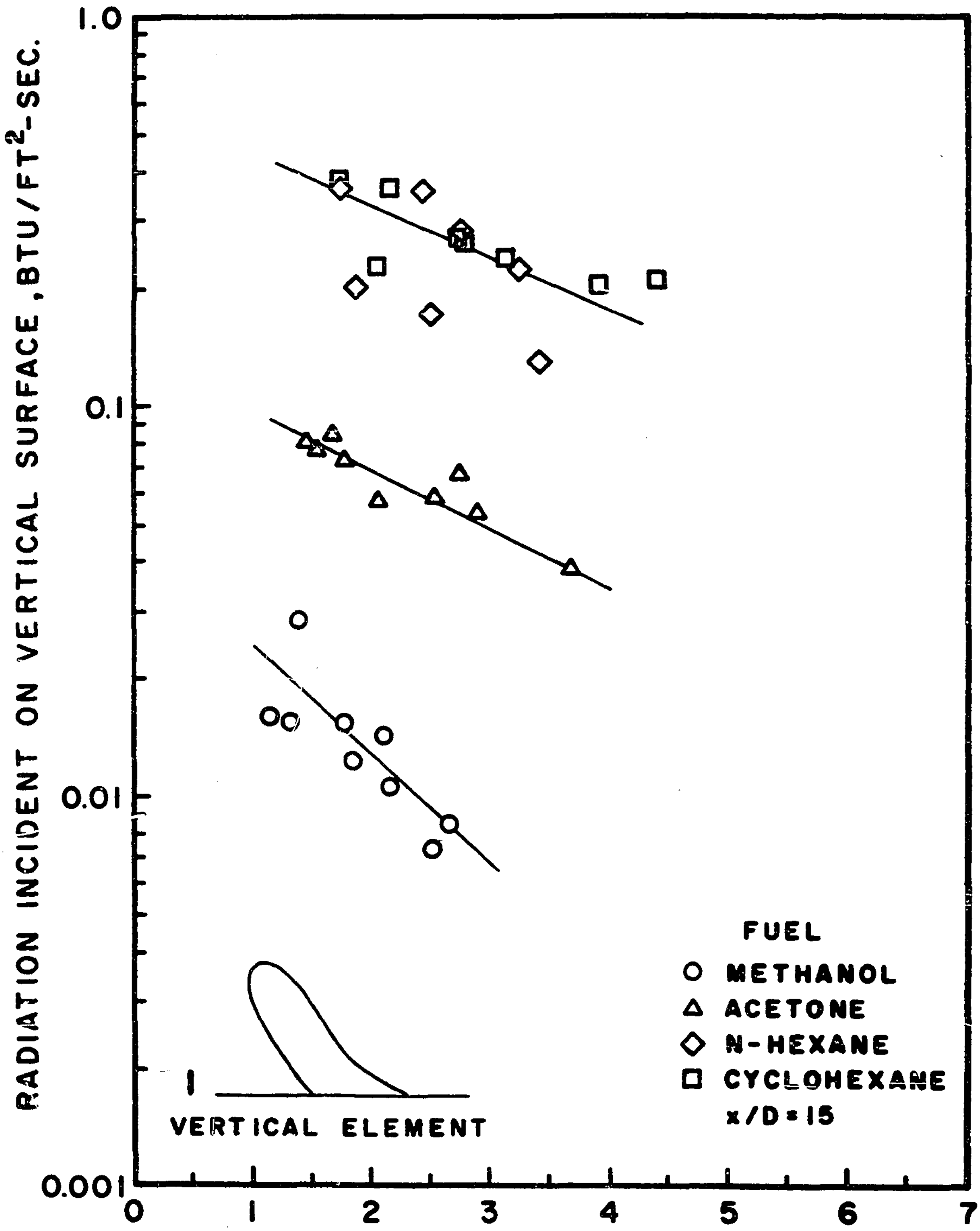


Figure 29. Radiation Incident on a Vertical Surface Downstream from a Wind-Blown Channel Fire

In practice, the behavior of cyclohexane and n-hexane were very similar. In future tests, it may prove unnecessary to use both since a duplication of results apparently occurs.

The fuel burning rates were measured by noting the consumption of fuel during each test run. The results are plotted for each of the fuels used in Figures 30 through 34 for both channel burners and circular burners. The burning rates for channel burners were approximately constant and were apparently not influenced by the wind speed as were those for circular burners. With the exception of methanol fires, there is evidence to show a decrease in burning rate as the wind speed increases. If the mechanism of heat transfer from flame to fuel is considered, this decrease is readily explained. In the case of methanol, radiative heat feedback to the fuel is smaller than for any of the other fuels, because the flame height is less and the flame is more transparent. Therefore, heat feedback probably is primarily by convection, and the convective heat transfer is not too strongly affected by changes in wind velocity. The burning rates are thus lower and are not decreased as much when wind speed increases. For the other fuels the flames are brighter and much more radiative heat feedback occurs. The burning rates are therefore higher, depending partially on how opaque the flames are. Thus acetone burns at an intermediate rate, while the hydrocarbon fuels burn at higher rates. Since the radiative heat feedback is important in determining burning rate, as the flame is tilted and the configuration factor from flame to

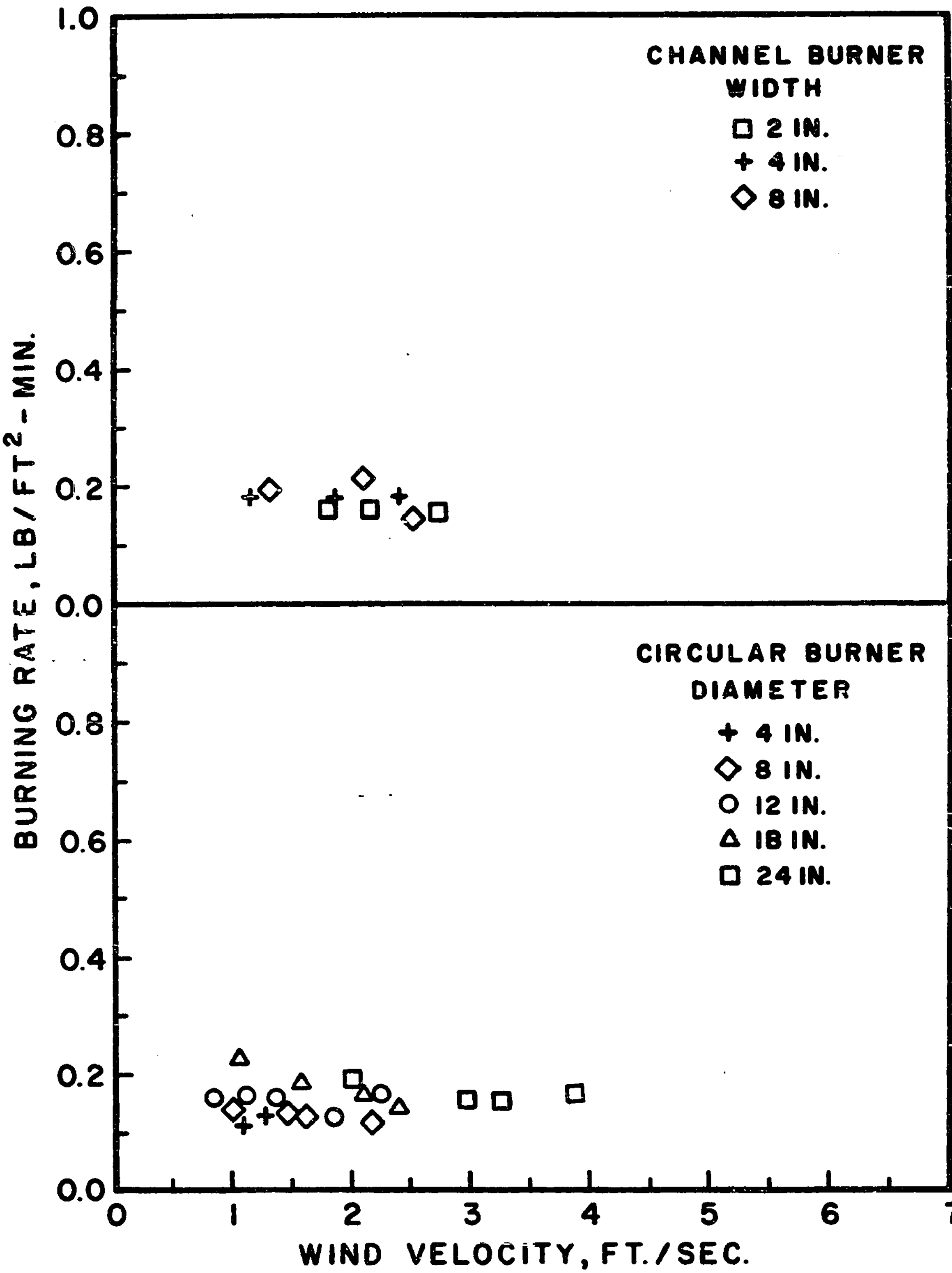


Figure 30. Burning Rates of Methanol Fires

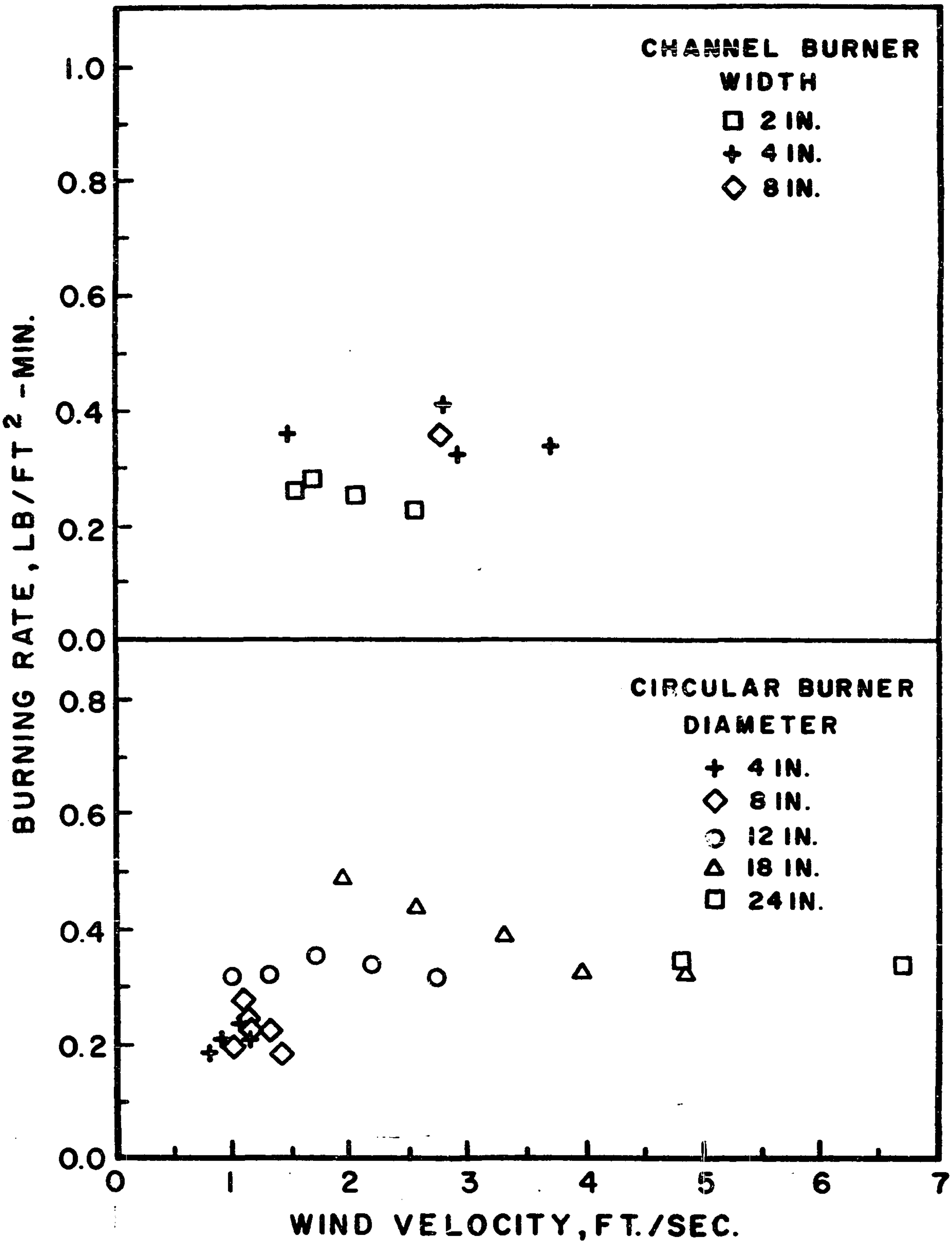


Figure 31. Burning Rates of Acetone Fires

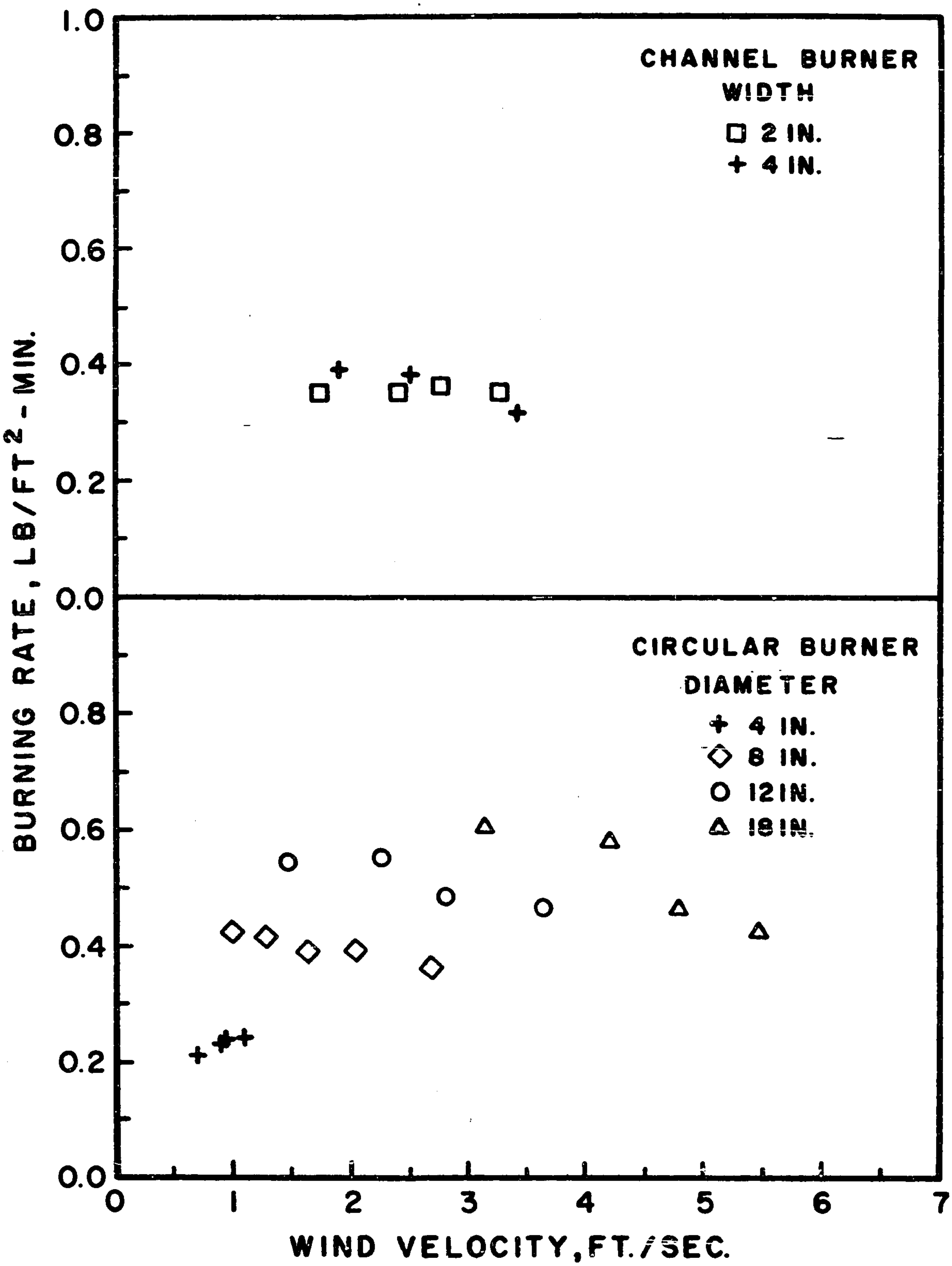


Figure 32. Burning Rates of N-Hexane Fires

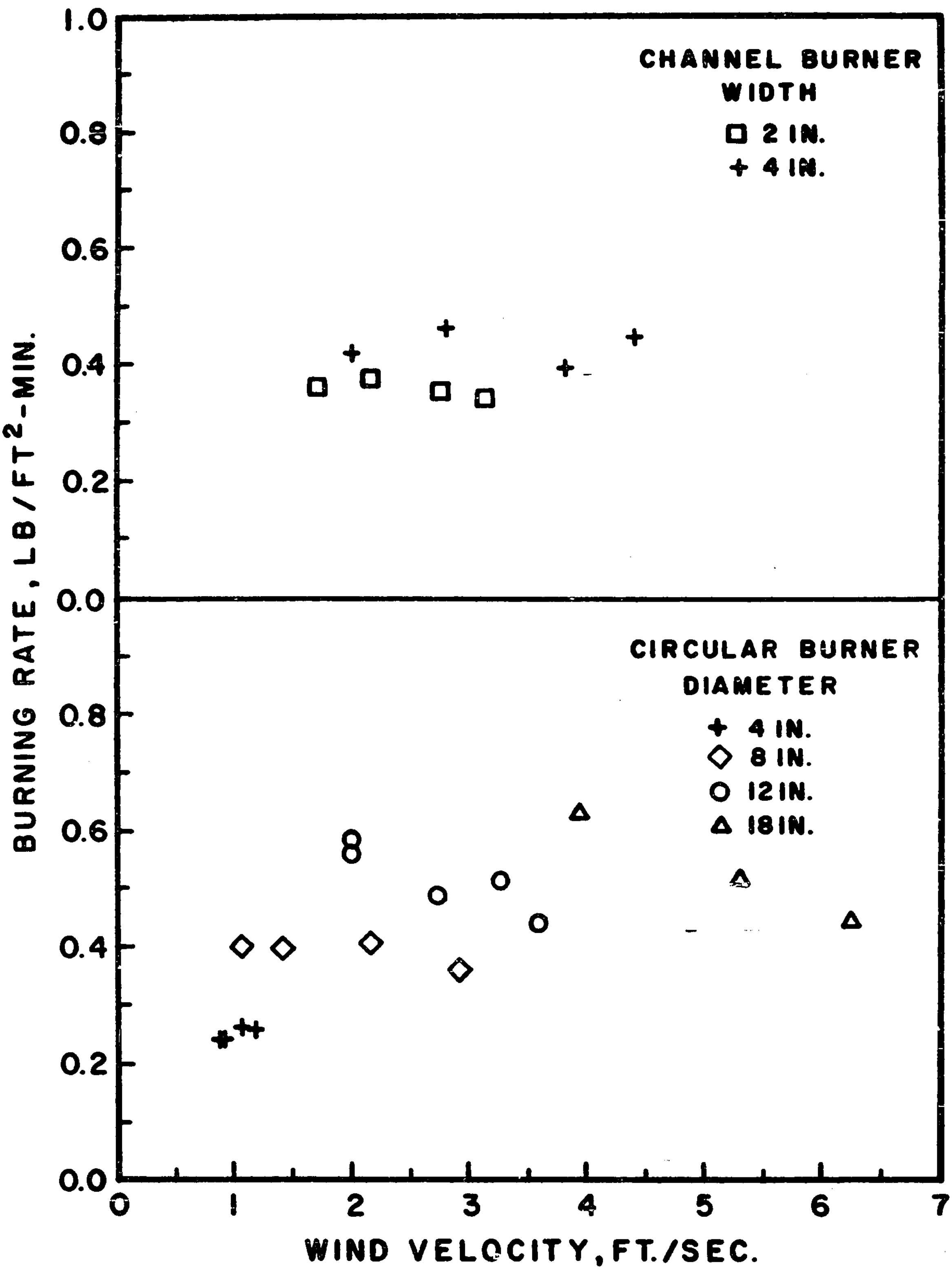


Figure 33. Burning Rates of Cyclohexane Fires

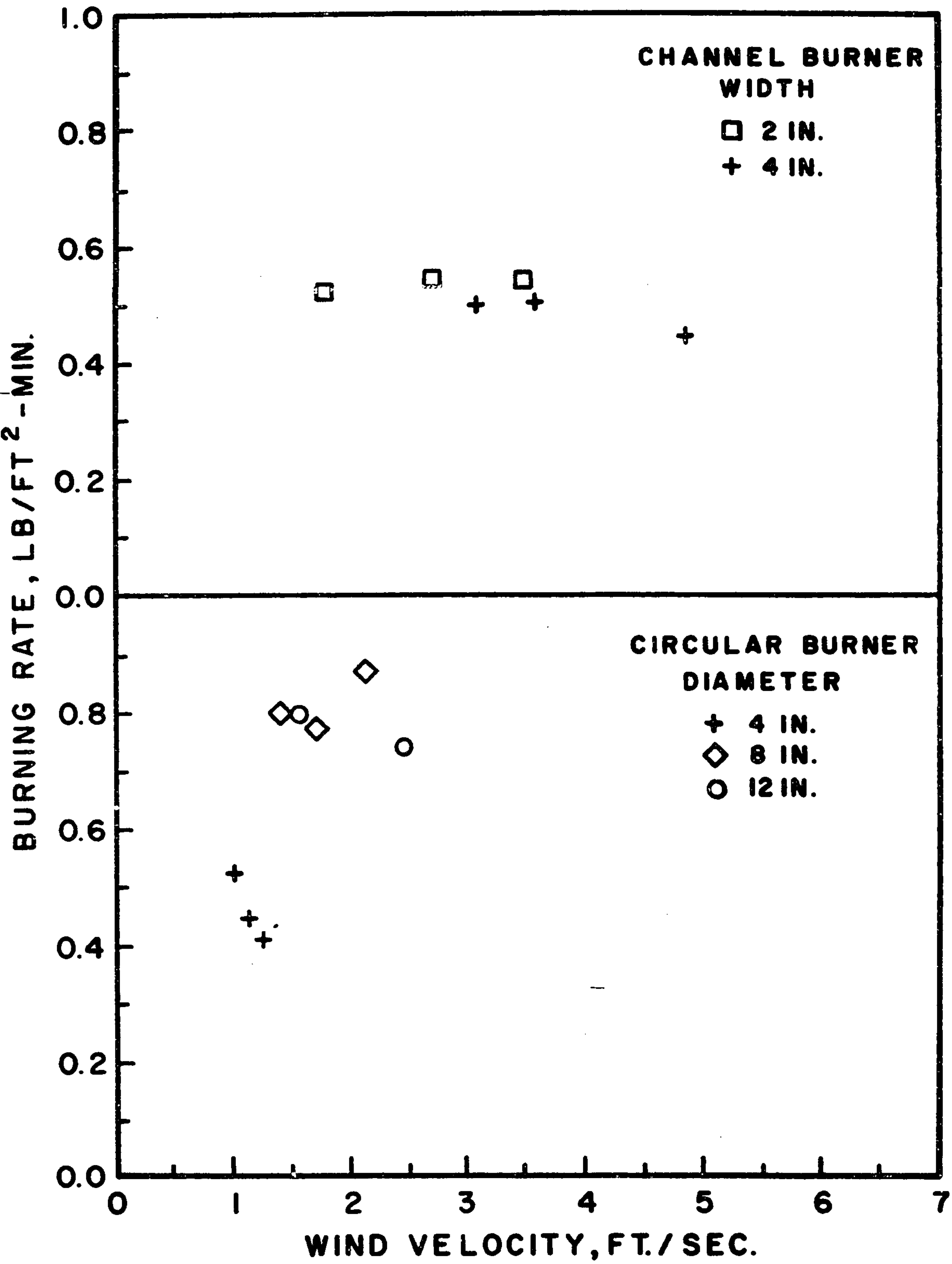


Figure 34. Burning Rates of Benzene Fires

fuel decreases, the burning rate also decreases. Although it was not done in these tests, it would be possible to increase the wind velocity to a point at which extinction would occur.

The flame lengths were measured from time exposure photographs of each of the test fires. The L/D ratios for the tests are shown in Figures 35 through 39. For circular burners the L/D ratios are approximately constant for all burner sizes and wind velocities for a particular fuel. For channel burners the L/D ratios are much larger and seem to decrease as the burner width increases. Visual observation of channel burner fires also indicated that the flame lengths were more strongly influenced by fuel level than were those for circular burners. The greater length of the channel burner flames can be partially explained by the higher burning rates for a channel burner which has the same width as the diameter of a circular burner. Calculations of the modified Froude number used by Thomas (57) to correlate flame lengths showed the present data to be in approximately the same region as those for comparable wood fires. Basic flame length data as measured from the time exposure photographs are listed in Table 1 in Appendix A.

Some comparisons of the burning rate and radiation data are made with literature data in Appendix B.

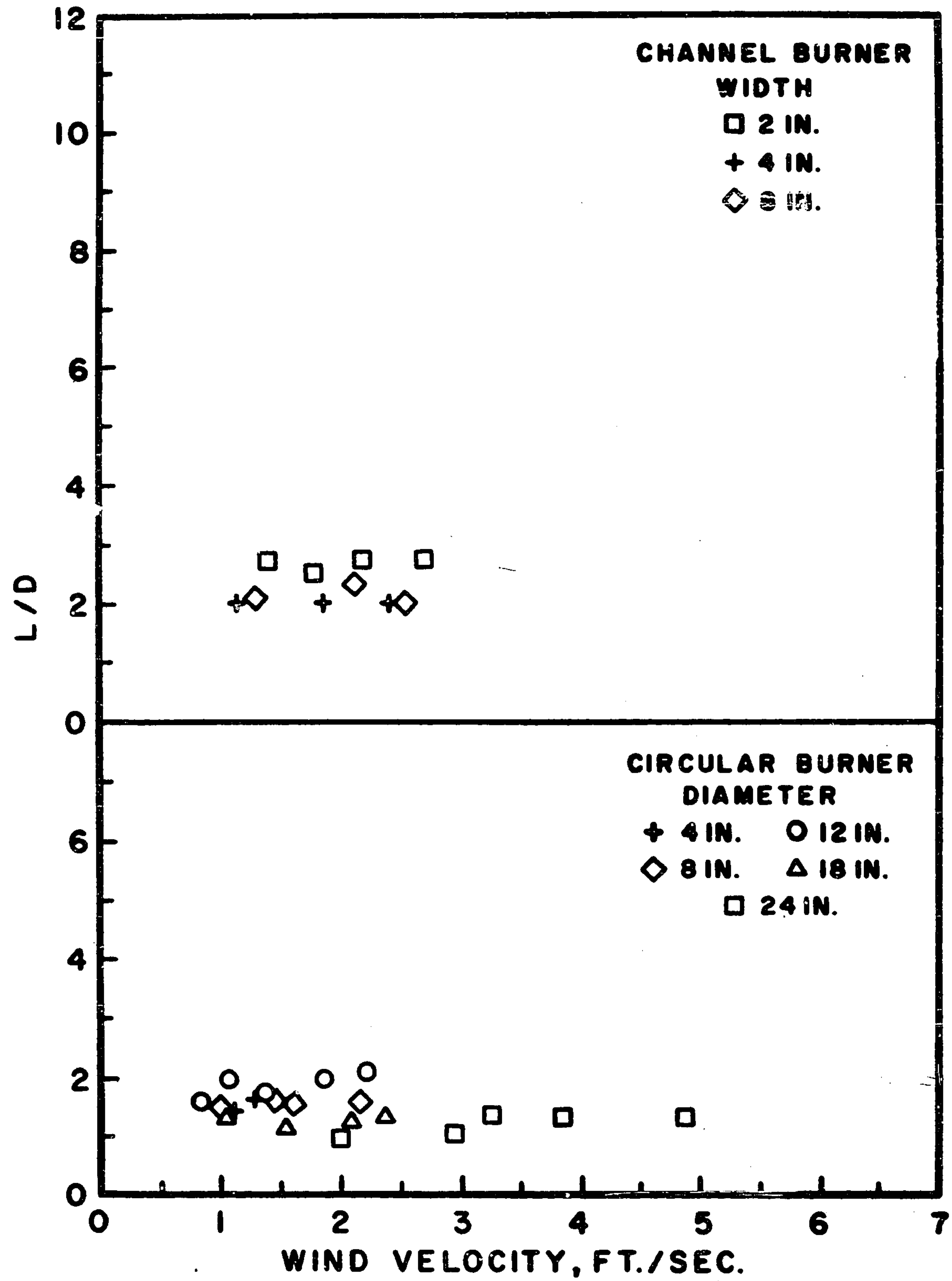


Figure 35. L/D Ratios for Methanol Fires

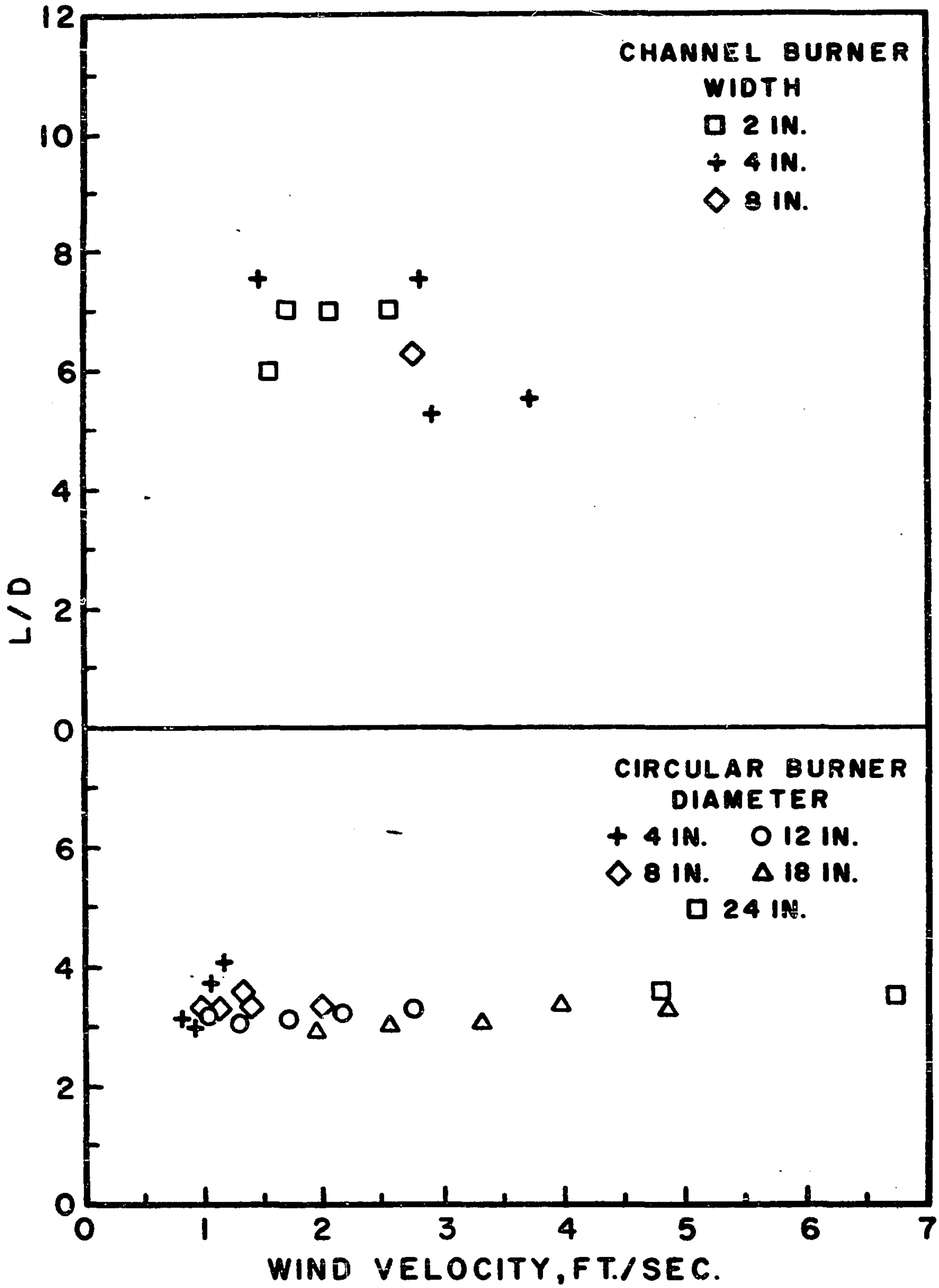


Figure 36. L/D Ratios for Acetone Fires

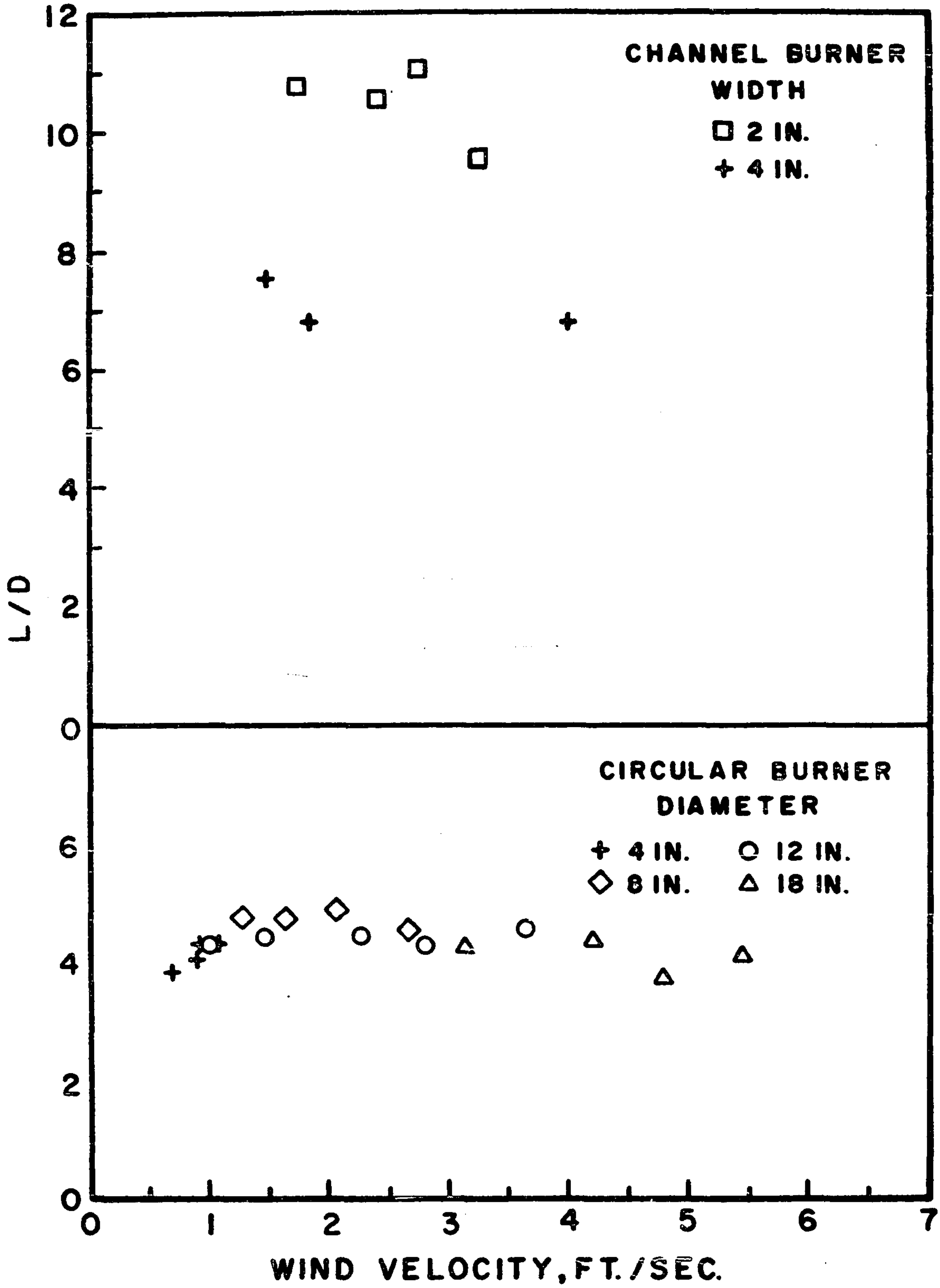


Figure 37. L/D Ratios for N-Hexane Fires

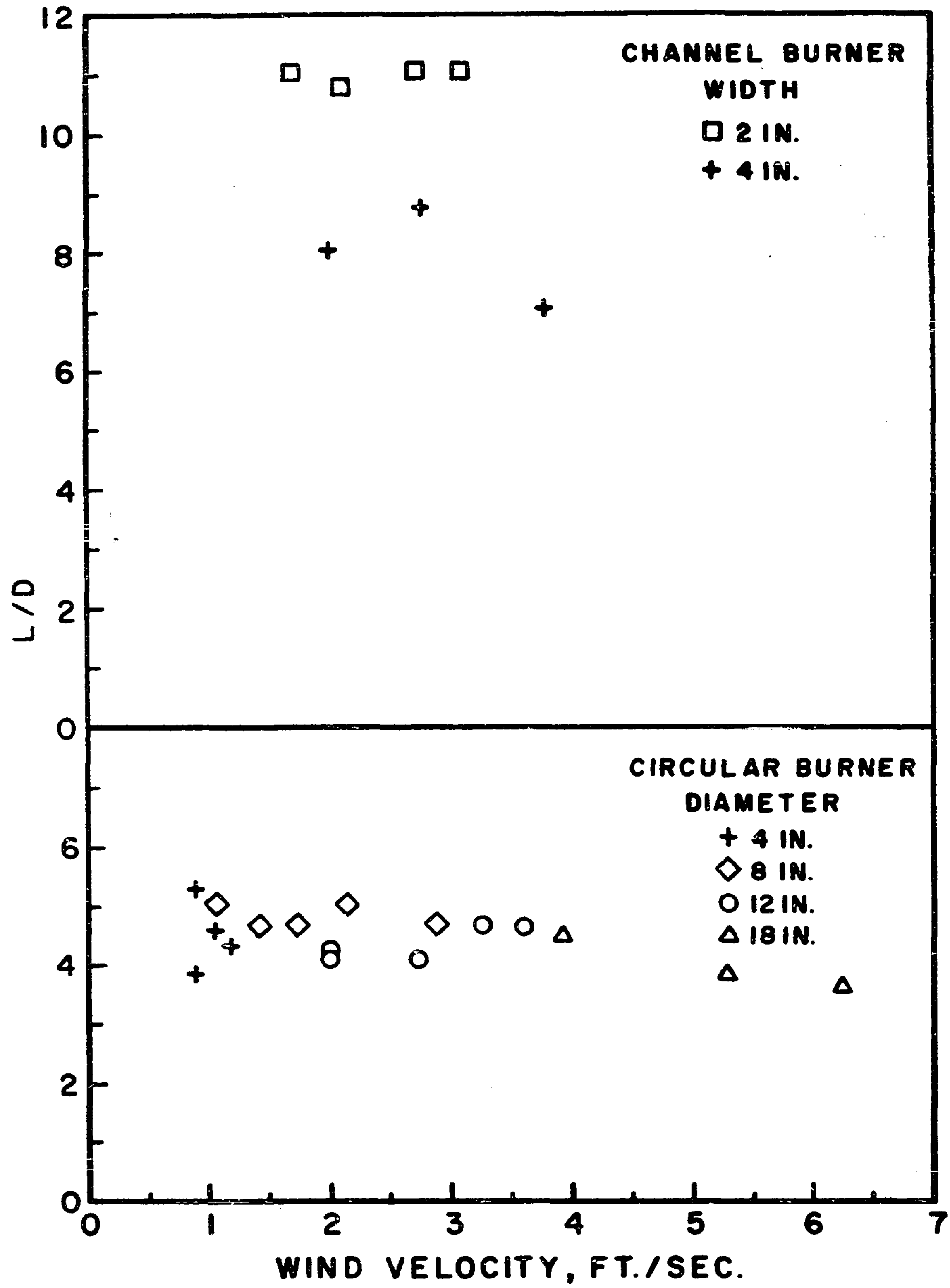


Figure 38. L/D Ratios for Cyclohexane Fires

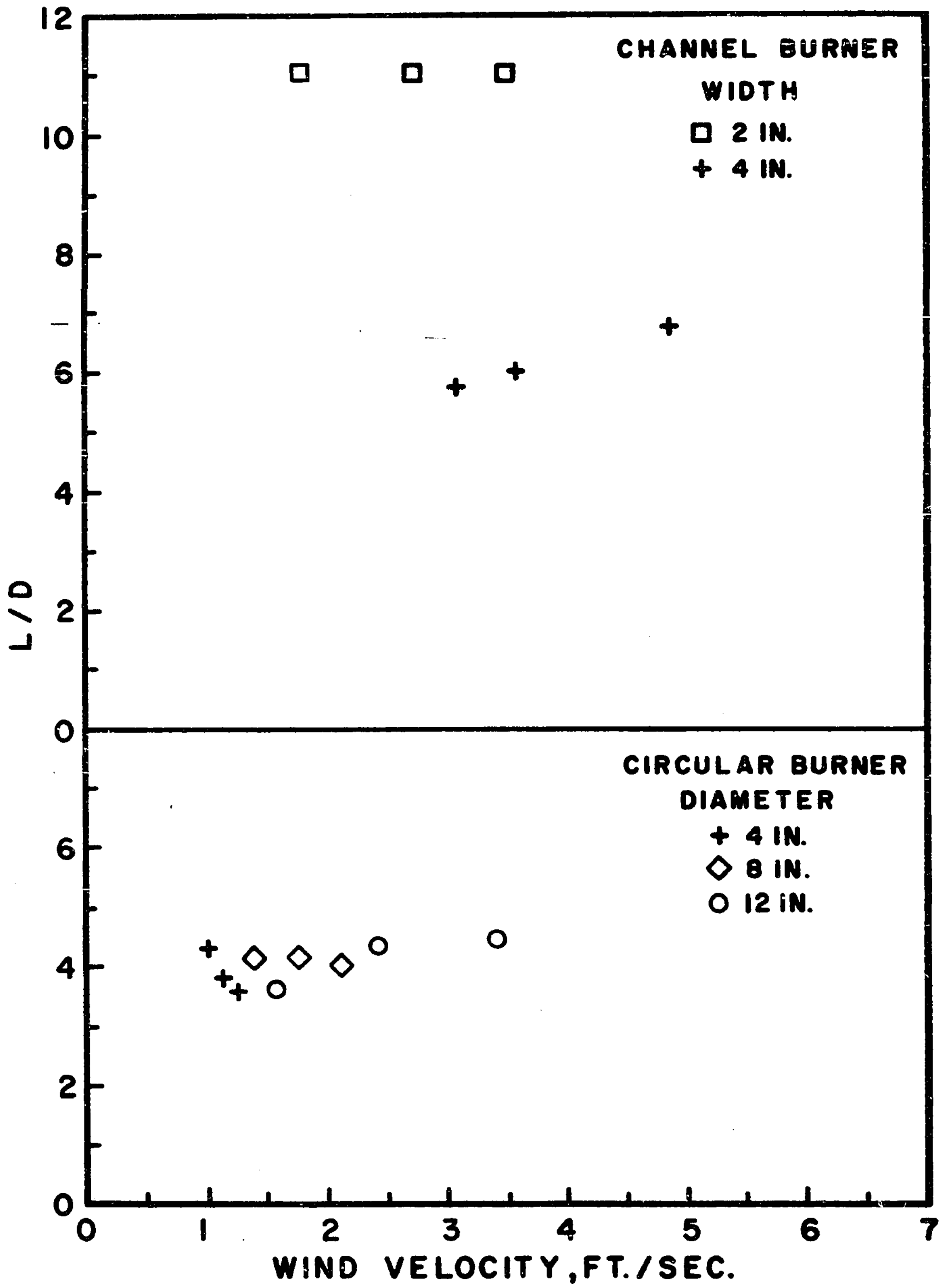


Figure 39. L/D Ratios for Benzene Fires

# CHAPTER VII

## CONCLUSIONS

This study has been the first systematic investigation of the effect of wind on buoyant diffusion flames from burning pools of liquids. The primary purpose was to study flame bending and to correlate the data in such a way as to be able to predict flame bending for large fires. It was found that the flame bending data could be expressed in terms of a flame drag coefficient and that the drag coefficient could be correlated as a function of the ReFr product and the ratio of fuel vapor density to ambient air density. Data from circular burners showed the drag coefficient to be essentially constant, but the channel burner data showed a tendency for the drag coefficient to decrease at higher wind velocities. Circular burner data can probably be used for extrapolation without too much inaccuracy, but the channel burner data should be extended to larger-scale conditions.

In the early stages of study the phenomenon of flame trailing downstream from the liquid pool was noticed. The report of Byram et al. was later received noting that they too had observed flame trailing. The flame trailing was correlated as a function of a Froude number and the fuel vapor and air densities. An estimation of the flame trailing from Byram's data showed reasonable agreement.

The temperatures measured downstream of the flames in the wind tunnel showed a fair degree of correlation, and those for channel burners were about the same as the lower range of the data reported by Thomas. The temperature measurements were not complete; they should be extended to other situations.

As a part of the bending tests, flame lengths and fuel burning rates were measured. The flame lengths were somewhat larger than those reported in the literature (3 to 4 times the diameter) and were relatively constant for each fuel burned. The burning rates decreased somewhat at higher wind velocities, a behavior which should have been anticipated. Most work reported in the literature on liquid pool burning has been run under conditions that resulted in the belief that burning rates would become constant under windy conditions. For gusty or uneven winds, or for very large fires this condition may be true, but for the smaller fires burned in the wind tunnel, the burning rate is expected to continue to decrease until extinction occurs.

## REFERENCES


1. Anderson, H. E., "Mechanisms of Fire Spread: Research Progress Report No. 1," U. S. Forest Service Research Paper INT-8 (1964).

2. Anderson, H. E., and R. C. Rothermel, "Influence of Moisture and Wind Upon the Characteristics of Free-Burning Fires," Preprint of paper presented at Tenth International Symposium on Combustion, University of Cambridge, England, August 17-21, 1964.

3. Ball, F. K., "Some Observations of Bent Plumes," Quart. Jour. Royal Met. Soc., 84, 61 (1958).

4. Blinov, V. I., and G. N. Khudiakov, "Certain Laws Governing Diffusive Burning of Liquids," Acad. Nauk. USSR Doklady, 113, 1094 (1957).

5. Bosanquet, C. H., W. F. Carey, and E. M. Halton, "Dust Deposition from Chimney Stacks," Proc. Inst. Mech. Engrs. No. 1-4, 355 (1950).

6. Broido, A., and A. W. McMasters, "Effects of Fires on Personnel in Shelters," Pacific Southwest Forest and Range Experimental Station, Berkeley, California, Technical Paper 50 (1960).

7. Brown, A. A., "Forest Fire Research in the Forest Service-USDA," Fire Research Abstracts and Reviews, 6, 216 (1964).

8. Burgess, D., and J. Grumer, "Comments on 'The Burning Rate of Liquid Fuels from Open Trays by Natural Convection' by D. B. Spalding," Fire Research Abstracts and Reviews, 4, 236 (1962).

9. Burgess, D. C., J. Grumer, and H. G. Wolfhard, "Burning Rates of Liquid Fuels in Large and Small Open Trays," The Use of Models in Fire Research, NAS-NRC Pub. 786, 68 (1961).

10. Burgess, D. S., A. Strasser, and J. Grumer, "Diffusive Burning of Liquid Fuels in Open Trays," Fire Research Abstracts and Reviews, 3, 177 (1961).

11. Burgess, D. S., and M. G. Zabetakis, "Fire and Explosion Hazards Associated with Liquefied Natural Gas," Bureau of Mines R.I. 6099, 1962.

12. Byram, G. M., H. B. Clements, E. R. Elliot, and P. M. George, "An Experimental Study of Model Fires," Technical Report No. 3, Forest Service, U. S. Department of Agriculture, Southern Forest Fire Laboratory, Macon, Georgia, June 29, 1964.

13. Combustion and Flame, Quarterly Journal of the Combustion Institute, Butterworths, London.

14. Emmons, H. W., "Some Observations on Pool Burning," The Use of Models in Fire Research, NAS-NRC Pub. 786, 50 (1961).

15. Étienne, Ct., "Rapport de Mission--Incineration de la Lande de Trensacq, April 13, 1955, Ministere de l'Intérieur, Paris, France.

16. Faure, J., "Study of Convection Currents Created by Fires of Large Area," Use of Models in Fire Research, NAS-NRC Pub. 786, 130 (1961).

17. Fire Research Abstracts and Reviews, published by Committee on Fire Research, Division of Engineering and Industrial Research, National Academy of Sciences-National Research Council, since 1958.

18. Fons, W. L., "Rate of Combustion from Free Surfaces of Liquid Hydrocarbons," Combustion and Flame, 5, 283 (1961).

19. Fons, W. L., H. D. Bruce, and W. Y. Pong, "A Steady-State Technique for Studying the Properties of Free-Burning Wood Fires," The Use of Models in Fire Research, NAS-NRC Pub. 786, 219 (1961).

20. Fons, W. L., H. D. Bruce, W. Y. Pong, and S. S. Richards, Project Fire Model, Summary Progress Report 1, November 1958-60. U. S. Department of Agriculture, Forest Service, Pacific Southwest Forest and Range Experimental Station, Berkeley, California (1960).

21. Fons, W. L., H. B. Clements, and P. M. George, "Scale Effects on Propagation Rate of Laboratory Crib Fires," Ninth International Symposium on Combustion, Academic Press, New York (1963).

22. Gaydon, A. G., and H. G. Wolfhard, Flames: Their Structure, Radiation, and Temperature, Chapman and Hall, Ltd., London (1960).

23. Gross, D. J., J. Research National Bureau of Standards, 66C, 99 (1962).

24. Halitzky, J., C. P. Randell, and M. Hackman, "Communications on Dust Deposition from Chimney Stacks," Proc. Institution Mech. Engr., 162, 366 (1950).

25. Hamada, M., "A Study of Flame Inclination Due to Wind," Bulletin of the Fire Protection Society of Japan, 1, 41 (1952).

26. Hirst, R., and D. Sutton, "The Effect of Reduced Pressure and Airflow on Liquid Surface Diffusion Flames," Combustion and Flame, 5, 319 (1961).

27. Hottel, H. C., "Fire Modeling," The Use of Models in Fire Research, NAS-NRC Pub. 786, 32 (1961).

28. Hottel, H. C., Review of Reference 4, Fire Research Abstracts and Reviews, 1, 41 (1959).

29. International Symposia on Combustion, A series of ten (currently) volumes, published by various companies, containing papers presented at meetings of the Combustion Institute over the years.

30. Kinbara, T., "A Survey of Fire Research in Japan," Fire Research Abstracts and Reviews, 3, 1 (1961).

31. Lawson, D. I., "Fire Research in the United Kingdom," Fire Research Abstracts and Reviews, 1, 149 (1959).

32. Lawson, D. I., "Research into Fire Protection," Fire Research Abstracts and Reviews, 6, 193 (1964).

33. Lewis, B., and G. von Elbe, Combustion, Flames, and Explosions of Gases, Academic Press, New York (1961).

34. McCarter, R. J., and A. Broido, "Radiative and Convective Energy From Wood Fires," Pyrodynamics, 2, 65 (1965).

35. Magnus, G., "Tests on Combustion Velocity of Liquid Fuels and Temperature Distribution in Flames and Beneath Surface of the Burning Liquid," The Use of Models in Fire Research, NAS-NRC Pub. 786, 76 (1961).

36. Milburn, R. A., "The Design and Calibration of a Very Low Speed Open Circuit Wind Tunnel," M.S. Thesis, University of Oklahoma (1965).

37. Pipkin, O. A. and C. M. Sliepcevich, "Effect of Wind on Buoyant Diffusion Flames," I. and E. C. Fundamentals, 3, 147 (1964).

38. Priestly, C. H. B., "A Working Theory of the Bent-Over Plume of Hot Gas," Quart. J. Royal Met. Soc., 82, 165 (1956).

39. Putnam, A. A., "A Model Study of Wind-Blown Free-Burning Fires," Preprint of paper presented at Tenth International Symposium on Combustion, University of Cambridge, England, August 17-21, 1964.

40. Putnam, A. A., and C. F. Speich, "A Model Study of the Interacting Effects of Mass Fires," Summary Report No. 1, Battelle Memorial Institute, Columbus, Ohio, Research Report, Nov. 9, 1961.

41. Putnam, A. A., and C. F. Speich, "A Model Study of the Interaction Effects of Mass Fires," Summary Report No. 2, Battelle Memorial Institute, Columbus, Ohio, Research Report, March 27, 1963.

42. Putnam, A. A., and C. F. Speich, "A Model Study of the Interaction of Multiple Turbulent Diffusion Flames," Ninth International Symposium on Combustion, Academic Press, New York (1963).

43. Pyrodynamics, A journal of applied thermal processes, published by Gordon and Breach Science Publishers, New York.

44. Rankine, A. O., "Experimental Studies in Thermal Convection," Proc. Phys. Soc. London, 63, Part 5 (365A), 417 (1950).

45. Rankine, A. O., "F. I. D. O. Investigations" - Wind Tunnel Experiments, Petroleum Warfare Department.

46. Rasbash, D. J., Z. E. Rogowski, and G. W. V. Stark, "Properties of Fires of Liquids," Fuel, 35, 94 (1956).

47. Robertson, A. F., "Fire Research at the National Bureau of Standards," Fire Research Abstracts and Reviews, 1, 159 (1959).

48. Rothermel, R. C., Personal Communication, October, 1964.

49. Spalding, D. B., "The Art of Partial Modeling," Ninth International Symposium on Combustion, Academic Press, New York (1963).

50. Spalding, D. B., "The Burning Rate of Liquid Fuels from Open Trays by Natural Convection," Fire Research Abstracts and Reviews, 4, 234 (1962).

51. Spalding, D. B., Some Fundamentals of Combustion, Butterworths, London (1955).

52. Stempel, F. C., and D. L. Rall, "Applications and Advancements in the Field of Direct Heat Transfer Measurements," Preprint of paper presented at Instrument Society of America 18th Annual Conference, Sept. 9-12, 1963, Chicago.

53. "A Study of Fire Problems," National Academy of Sciences-National Research Council Publication 949 (1961).

54. Sutton, O. G., "The Dispersion of Hot Gases in the Atmosphere," Jour. of Met. 7, 307 (1950).

55. Taylor, G. I., "Fire Under Influence of Natural Convection," The Use of Models in Fire Research, NAS-NRC Pub. 786, 10 (1961).

56. Thomas, P. H., "The Effect of Wind on Plumes from a Line Heat Source," Fire Research Note 572, Joint Fire Research Organization, England, November, 1964.

57. Thomas, P. H., "The Size of Flames from Natural Fires," Ninth International Symposium on Combustion, Academic Press, New York (1963).

58. Thomas, P. H., R. W. Pickard, and H. G. H. Wraight, "On the Size and Orientation of Buoyant Diffusion Flames and the Effect of Wind," Fire Research Note No. 516, Joint Fire Research Organization, England, January 1963.

59. Waterman, T. E., W. G. Labes, F. Salzberg, J. E. Tamney, and F. J. Vodvarka, "Prediction of Fire Damage to Installations and Built-up Areas from Nuclear Weapons," Final Report - Phase III, Experimental Studies - Appendices A-G, IIT Research Institute Report for National Military Command System Support Center, Contract No. DCA-8, November, 1964.

60. Zabetakis, M. G., and D. S. Burgess, "Research on the Hazards Associated with the Production and Handling of Liquid Hydrogen," Bureau of Mines R.I. 5707, 1961.

## NOMENCLATURE

$C_f$ = flame drag coefficient

$C_f'$ = uncorrected flame drag coefficient

$C_p$ = specific heat of air

$D$ = circular burner diameter or channel burner width

$D'$ = length of flame trailing

$F$ = radiation view factor

$F_b$ = body forces

$F_f$ = field forces

$Fr$ = Froude number

$g$ = gravitational acceleration

$g_c$ = gravitational constant

$H$ = flame height

$\Delta H_c$ = heat of combustion of fuel

$\Delta H_v$ = heat of vaporization of fuel

$k$ = conduction coefficient

$K$ = constant

$\ell$ = length

$L$ = flame length

$L^*$ = length of single flame

$L_{SH}$ = horizontal projection of flame length

$L_{SV}$ = vertical projection of flame length

$m$ = mass, mass flow rate

$m''$ = mass flow rate per unit area

$MV$ = momentum

$N_c$ = convection number defined by Equation (66)

$q$ = rate of heat feedback to fuel

$Q$ = rate of heat release from fire

$Q'$ = rate of heat release per unit length

$Q''$ = rate of heat release per unit area

$r$ = radius of convective plume

$Re$ = Reynolds number

$t$ = time

$T$ = temperature

$u$ = wind velocity; horizontal component of velocity

$U$ = convection coefficient

$v$ = liquid level regression rate

$v_\infty$ = liquid level regression rate for large burners

$w$ = vertical component of velocity

$x$ = horizontal distance from burner center parallel to air flow

$y$ = horizontal distance from wall perpendicular to air flow

$z$ = vertical distance from ground level

Greek

$\alpha$ = flame angle from horizontal reference

$\beta$ = correction factor for angle of tilt

$\theta$ = flame angle of tilt from vertical

$\varkappa$ = Beer's law extinction coefficient

$\mu$ = viscosity

$\rho$ = density

$\sigma$ = Stephan-Boltzmann constant

$\Phi$ = dimensionless temperature rise

$\Omega$ = dimensionless velocity

Subscripts

a = property of ambient air

b = property of liquid fuel

C = refers to circular burner

f = property of flame

g = property of fuel vapor

I = refers to quantities entering system

L = refers to channel burner or line fire

O = refers to quantities leaving system

# APPENDIX A

## TABULAR SUMMARY OF DATA

TABLE 1

SUMMARY OF FLAME BENDING DATA--CIRCULAR BURNERS

| Run Number | Fuel | Nominal Burner Diameter inches | Wind Velocity ft/sec | Air Density $lb/ft^3$ | Air Temp °F | Flame Optical Temp °F | Flame Angle degrees | Fuel Burning Rate $lb/ft^2$-min | Flame Length inches | Flame Trailing inches | Drag Coefficient |
|---|---|---|---|---|---|---|---|---|---|---|---|
| 022565-1 | H[a] | 4 | 0.68 | 0.078 | 35 | 2240 | 11 | 0.22 | 16 | 5 | 6.2 |
| 022565-2 | H | 4 | 0.90 | 0.077 | 44 | 2240 | 16 | 0.24 | 17 | 6 | 5.3 |
| 022565-3 | H | 4 | 1.08 | 0.077 | 44 | 2240 | 38 | 0.25 | 18 | 10.5 | 12.3 |
| 022565-4 | H | 4 | 0.93 | 0.077 | 44 | 2240 | 24 | 0.24 | 18 | 7.5 | 8.1 |
| 022565-5 | B | 4 | 1.13 | 0.075 | 55 | 2080 | 31 | 0.44 | 16 | 8 | 7.7 |
| 022565-6 | B | 4 | 1.25 | 0.075 | 55 | 2080 | 40 | 0.41 | 15 | 9.5 | 9.7 |
| 022565-7 | B | 4 | 1.00 | 0.074 | 57 | 2080 | 20 | 0.52 | 18 | 7 | 5.4 |
| 022565-8 | C | 4 | 0.88 | 0.076 | 50 | 2190 | 16 | 0.24 | 16 | 5 | 5.6 |
| 022565-9 | C | 4 | 1.06 | 0.076 | 50 | 2190 | 36 | 0.26 | 19 | 8 | 11.5 |
| 022565-10 | C | 4 | 1.17 | 0.076 | 50 | 2190 | 45 | 0.26 | 18 | 9 | 14.7 |
| 022565-11 | C | 4 | 0.89 | 0.076 | 50 | 2190 | 20 | 0.24 | 22 | 5.5 | 6.9 |
| 022665-1 | A | 4 | 0.78 | 0.076 | 45 | 2180 | 9 | 0.18 | 13 | 4 | 3.7 |
| 022665-2 | A | 4 | 0.90 | 0.076 | 45 | 2180 | 22 | 0.20 | 12.5 | 6.5 | 7.7 |
| 022665-3 | A | 4 | 1.03 | 0.076 | 45 | 2180 | 26 | 0.24 | 15.5 | 5 | 7.3 |
| 022665-4 | A | 4 | 1.16 | 0.076 | 45 | 2180 | 42 | 0.20 | 17 | 8 | 13.6 |
| 022665-5 | M | 4 | 1.09 | 0.074 | 58 | (c) | 41 | 0.11 | 6 | 5 | 13.7 |
| 022665-6 | M | 4 | 1.26 | 0.074 | 58 | (c) | 45 | 0.13 | 7 | 5 | 12.6 |
| 030365-1 | A | 8 | 1.00 | 0.078 | 31 | 2170 | 20 | 0.19 | 27 | 11 | 10.8 |
| 030365-2 | A | 8 | 1.10 | 0.078 | 31 | 2170 | 27 | 0.28 | 28 | 11.5 | 13.2 |
| 030365-3 | A | 8 | 1.13 | 0.078 | 31 | 2170 | 25 | 0.24 | 27 | 11.5 | 11.2 |
| 030365-4 | A | 8 | 1.32 | 0.078 | 31 | 2170 | 27 | 0.22 | 29 | 12.5 | 9.1 |
| 030365-5 | A | 8 | 1.40 | 0.078 | 31 | 2170 | 30 | 0.18 | 27 | 13.5 | 9.4 |
| 030365-6 | A | 8 | 1.97 | 0.078 | 31 | 2170 | 49 | 0.26 | 27 | 16.5 | 12.6 |
| 030365-7 | H | 8 | 0.97 | 0.077 | 33 | 2240 | 17 | 0.42 | 35 | 13 | 9.5 |
| 030365-8 | H | 8 | 1.26 | 0.077 | 33 | 2240 | 24 | 0.42 | 39 | 16 | 8.6 |
| 030365-9 | H | 8 | 1.62 | 0.077 | 33 | 2240 | 30 | 0.39 | 39 | 16 | 7.1 |
| 030365-10 | H | 8 | 2.04 | 0.077 | 33 | 2240 | 36 | 0.39 | 40 | 18.5 | 6.0 |
| 030365-11 | H | 8 | 2.68 | 0.077 | 33 | 2240 | 46 | 0.36 | 37 | 25 | 5.7 |
| 030365-12 | B | 8 | 1.38 | 0.077 | 35 | 2040 | 20 | 0.80 | 34 | 18 | 5.6 |
| 030365-13 | B | 8 | 1.72 | 0.077 | 35 | 2040 | 27 | 0.77 | 34 | 18.5 | 5.3 |
| 030365-14 | B | 8 | 2.11 | 0.077 | 35 | 2040 | 40 | 0.87 | 33 | 21 | 6.7 |
| 030465-1 | C | 8 | 1.06 | 0.078 | 28 | 2200 | 24 | 0.40 | 41 | 14 | 11.2 |
| 030465-2 | C | 8 | 1.41 | 0.078 | 28 | 2200 | 30 | 0.40 | 38 | 15.5 | 9.3 |
| 030465-3 | C | 8 | 1.73 | 0.078 | 28 | 2200 | 41 | 0.42 | 38 | 18.5 | 10.7 |
| 030465-4 | C | 8 | 2.16 | 0.078 | 28 | 2200 | 49 | 0.41 | 41 | 20 | 10.5 |
| 030465-5 | C | 8 | 2.90 | 0.078 | 28 | 2200 | 55 | 0.36 | 38 | 25 | 8.3 |
| 030465-6 | M | 8 | 1.00 | 0.077 | 32 | (c) | 21 | 0.14 | 12.5 | 8.5 | 11.4 |
| 030465-7 | M | 8 | 1.45 | 0.077 | 32 | (c) | 40 | 0.13 | 13 | 9.5 | 14.4 |
| 030465-8 | M | 8 | 1.60 | 0.077 | 32 | (c) | 49 | 0.12 | 13 | 10.5 | 19.1 |
| 030465-9 | M | 8 | 2.14 | 0.077 | 32 | (c) | 62 | 0.12 | 13 | 11 | 24.4 |
| 030465-10 | M | 12 | 0.84 | 0.076 | 38 | (c) | 11 | 0.16 | 13 | 12.5 | 11.8 |
| 030465-11 | M | 12 | 1.08 | 0.076 | 38 | (c) | 24 | 0.16 | 16 | 13.5 | 17.4 |
| 030465-12 | M | 12 | 1.36 | 0.076 | 38 | (c) | 29 | 0.16 | 14 | 15 | 14.3 |
| 030465-13 | M | 12 | 1.85 | 0.076 | 38 | (c) | 47 | 0.12 | 16 | 16 | 19.2 |
| 030465-14 | M | 12 | 2.21 | 0.076 | 38 | (c) | 54 | 0.17 | 17 | 17.5 | 20.0 |

TABLE 1 (CONTINUED)

| Run Number | Fuel | Nominal Burner Diameter inches | Wind Velocity ft/sec | Air Density $lb/ft^3$ | Air Temp °F | Flame Optical Temp °F | Flame Angle degrees | Fuel Burning Rate $lb/ft^2$-min | Flame Length inches | Flame Trailing inches | Drag Coefficient |
|---|---|---|---|---|---|---|---|---|---|---|---|
| 030565-1 | A | 12 | 1.00 | 0.076 | 36 | 2180 | 8 | 0.32 | 39 | 14 | 5.9 |
| 030565-2 | A | 12 | 1.29 | 0.076 | 36 | 2180 | 25 | 0.32 | 37 | 20.5 | 12.8 |
| 030565-3 | A | 12 | 1.70 | 0.076 | 36 | 2160 | 34 | 0.35 | 38 | 21 | 11.7 |
| 030565-4 | A | 12 | 2.16 | 0.076 | 36 | 2180 | 39 | 0.33 | 39 | 22 | 9.3 |
| 030565-5 | A | 12 | 2.73 | 0.076 | 36 | 2180 | 53 | 0.31 | 40 | 29.5 | 12.3 |
| 032565-1 | H | 12 | 1.45 | 0.078 | 31 | 2200 | 16 | 0.55 | 54 | 31 | 5.9 |
| 032565-2 | H | 12 | 2.26 | 0.078 | 31 | 2200 | 35 | 0.55 | 54 | 30 | 7.0 |
| 032565-3 | H | 12 | 2.79 | 0.078 | 31 | 2200 | 38 | 0.48 | 52 | 33 | 5.3 |
| 032565-4 | H | 12 | 3.63 | 0.078 | 31 | 2200 | 46 | 0.47 | 55 | 38 | 4.7 |
| 032965-1 | C | 12 | 1.99 | 0.076 | 44 | 2160 | 23 | 0.56 | 51 | 29.5 | 4.8 |
| 032965-2 | C | 12 | 2.73 | 0.076 | 44 | 2160 | 39 | 0.48 | 49 | 35 | 5.8 |
| 032965-3 | C | 12 | 3.58 | 0.076 | 44 | 2160 | 46 | 0.44 | 56 | 41.5 | 4.8 |
| 032965-4 | C | 12 | 3.26 | 0.076 | 44 | 2160 | 43 | 0.51 | 57 | 37.5 | 5.0 |
| 032965-5 | C | 12 | 1.99 | 0.076 | 44 | 2160 | 27 | 0.59 | 50 | 31.5 | 6.0 |
| 032965-6 | B | 12 | 1.54 | 0.075 | 50 | 2020 | 26 | 0.79 | 44 | 29 | 9.3 |
| 032965-7 | B | 12 | 2.41 | 0.075 | 50 | 2020 | 37 | 0.74 | 53 | 40 | 6.6 |
| 032965-8 | B | 12 | 3.40 | 0.075 | 50 | 2020 | 54 | --- | 54 | 44.5 | 8.2 |
| 033165-1 | M | 18 | 1.03 | 0.075 | 39 | (c) | 13 | 0.23 | 24 | 18 | 13.7 |
| 033165-2 | M | 18 | 1.55 | 0.075 | 39 | (c) | 27 | 0.19 | 21 | 18 | 14.8 |
| 033165-3 | M | 18 | 2.38 | 0.075 | 39 | (c) | 52 | 0.15 | 25 | 26 | 22.7 |
| 033165-4 | M | 18 | 2.08 | 0.075 | 39 | (c) | 36 | 0.17 | 23 | 21 | 12.9 |
| 033165-5 | A | 18 | 1.92 | 0.072 | 67 | 2260 | 19 | 0.49 | 53 | 31 | 6.1 |
| 033165-6 | A | 18 | 2.54 | 0.072 | 67 | 2260 | 39 | 0.43 | 55 | 34 | 10.0 |
| 033165-7 | A | 18 | 3.30 | 0.072 | 67 | 2260 | 45 | 0.39 | 56 | 31.5 | 8.1 |
| 033165-8 | A | 18 | 3.94 | 0.072 | 67 | 2260 | 59 | 0.32 | 62 | 38.5 | 12.8 |
| 033165-9 | A | 18 | 4.84 | 0.072 | 67 | 2260 | 63 | 0.33 | 60 | 38 | 11.5 |
| 040265-1 | H | 18 | 3.12 | 0.072 | 66 | 2220 | 27 | 0.60 | 77 | 36.5 | 3.6 |
| 040265-2 | H | 18 | 4.18 | 0.072 | 66 | 2220 | 42 | 0.58 | 80 | 42 | 4.3 |
| 040265-3 | H | 18 | 4.77 | 0.072 | 66 | 2220 | 47 | 0.47 | 68 | 47 | 4.3 |
| 040265-4 | H | 18 | 5.45 | 0.072 | 66 | 2220 | 55 | 0.43 | 75 | 49.5 | 7.2 |
| 040265-5 | C | 18 | 3.93 | 0.072 | 66 | 2200 | 41 | 0.63 | 82 | 39 | 4.6 |
| 040265-6 | C | 18 | 5.29 | 0.072 | 66 | 2200 | 55 | 0.52 | 70 | 43.5 | 5.5 |
| 040265-7 | C | 18 | 6.24 | 0.072 | 66 | 2200 | 56 | 0.45 | 66 | 48.5 | 4.2 |
| 040665-1 | M | 24 | 2.00 | 0.071 | 70 | (c) | 26 | 0.19 | 23 | 23.5 | 10.7 |
| 040665-2 | M | 24 | 2.93 | 0.071 | 70 | (c) | 42 | 0.15 | 25 | 30 | 11.2 |
| 041365-1 | M | 24 | 3.25 | 0.071 | 70 | (c) | 59 | 0.15 | 32 | 35 | 18.0 |
| 041365-2 | M | 24 | 3.85 | 0.071 | 70 | (c) | 62 | 0.16 | 31 | 36 | 18.5 |
| 041365-3 | M | 24 | 4.86 | 0.071 | 70 | (c) | 72 | 0.17 | 31 | 37 | 15.6 |
| 041465-1 | A | 24 | 4.78 | 0.071 | 70 | 2300 | 57 | 0.34 | 85 | 42 | 9.8 |
| 041465-2 | A | 24 | 6.71 | 0.071 | 70 | 2300 | 65 | --- | 83 | 52 | 8.9 |

(a) Fuels are denoted as follows: A - acetone, B - benzene, C - cyclohexane, H - n-hexane, M - methanol.

(b) The burner diameters are nominal values. Actual diameters are:

| Nominal Diameter, Inches | Actual Diameter, Feet |
|---|---|
| 4 | 0.349 |
| 8 | 0.677 |
| 12 | 1.016 |
| 18 | 1.526 |
| 24 | 1.968 |

(c) Methanol flames were too dim to read the optical temperature. The flame temperature was assumed to be 2600°R for use in calculations.

TABLE 2

SUMMARY OF FLAME BENDING DATA--CHANNEL BURNERS

| Run Number | Fuel | Burner Diameter<br>inches | Wind Velocity<br>ft/sec | Air Density<br>$lb/ft^3$ | Air Temp<br>°F | Flame Optical Temp<br>°F | Flame Angle<br>degrees | Fuel Burning Rate<br>$lb/ft^2$-min | Flame Length<br>inches | Drag Coefficient |
|---|---|---|---|---|---|---|---|---|---|---|
| 041565-1 | A[a] | 2 | 1.52 | 0.072 | 64 | 2280 | 63 | 0.26 | 12 | 16.2 |
| 041565-2 | A | 2 | 2.04 | 0.072 | 64 | 2280 | 70 | 0.25 | 14 | 16.8 |
| 041565-3 | A | 2 | 2.54 | 0.072 | 64 | 2280 | 67 | 0.23 | 14 | 8.1 |
| 041565-4 | A | 2 | 1.68 | 0.072 | 64 | 2280 | 52 | 0.27 | 14 | 6.4 |
| 041565-5 | M | 2 | 1.38 | 0.072 | 64 | (b) | 69 | 0.15 | 5.5 | 32.8 |
| 041565-6 | M | 2 | 1.78 | 0.072 | 64 | (b) | 69 | 0.16 | 5 | 19.7 |
| 041565-7 | M | 2 | 2.16 | 0.072 | 64 | (b) | 70 | 0.16 | 5.5 | 14.8 |
| 041565-8 | M | 2 | 2.68 | 0.072 | 64 | (b) | 72 | 0.16 | 5.5 | 11.9 |
| 041665-1 | C | 2 | 1.71 | 0.073 | 60 | 2180 | 53 | 0.36 | 22 | 6.5 |
| 041665-2 | C | 2 | 2.14 | 0.073 | 60 | 2180 | 61 | 0.37 | 21.5 | 7.0 |
| 041665-3 | C | 2 | 2.74 | 0.073 | 60 | 2180 | 71 | 0.35 | 22 | 10.2 |
| 041665-4 | C | 2 | 3.11 | 0.073 | 60 | 2180 | 69 | 0.34 | 22 | 6.5 |
| 041665-5 | H | 2 | 1.72 | 0.073 | 64 | 2200 | 56 | 0.35 | 21 | 7.7 |
| 041665-6 | H | 2 | 2.41 | 0.073 | 64 | 2200 | 56 | 0.35 | 21 | 3.9 |
| 041665-7 | H | 2 | 2.76 | 0.073 | 64 | 2200 | 70 | 0.36 | 22 | 9.1 |
| 041665-8 | H | 2 | 3.24 | 0.073 | 64 | 2200 | 70 | 0.35 | 19 | 6.6 |
| 041665-9 | B | 2 | 1.77 | 0.071 | 75 | 1880 | 54 | 0.52 | 22 | 6.2 |
| 041665-10 | B | 2 | 2.69 | 0.071 | 75 | 1880 | 65 | 0.54 | 22 | 5.8 |
| 041665-11 | B | 2 | 3.46 | 0.071 | 75 | 1880 | 68 | 0.54 | 22 | 4.6 |
| 042365-1 | M | 4 | 1.15 | 0.071 | 75 | (b) | 48 | 0.18 | 8 | 22.6 |
| 042365-2 | M | 4 | 1.85 | 0.071 | 75 | (b) | 64 | 0.18 | 8 | 23.2 |
| 042365-3 | M | 4 | 2.40 | 0.071 | 75 | (b) | 66 | 0.18 | 8 | 16.3 |
| 042365-4 | A | 4 | 1.44 | 0.070 | 85 | 2200 | 37 | 0.35 | 30 | 7.8 |
| 042365-5 | A | 4 | 2.79 | 0.070 | 85 | 2200 | 68 | 0.40 | 30 | 14.5 |
| 042365-6 | A | 4 | 2.88 | 0.070 | 85 | 2200 | 67 | 0.32 | 21 | 12.4 |
| 042365-7 | A | 4 | 3.69 | 0.070 | 85 | 2200 | 63 | 0.33 | 22 | 5.4 |
| 042665-1 | C | 4 | 2.01 | 0.074 | 50 | 2180 | 57 | 0.42 | 32 | 12.1 |
| 042665-2 | C | 4 | 3.80 | 0.074 | 50 | 2180 | 68 | 0.40 | 28 | 7.9 |
| 042665-3 | C | 4 | 2.79 | 0.074 | 50 | 2180 | 54 | 0.46 | 35 | 5.2 |
| 042665-4 | C | 4 | 4.40 | 0.074 | 50 | 2180 | -- | 0.44 | -- | --- |
| 042665-5 | H | 4 | 1.87 | 0.074 | 55 | 2200 | 46 | 0.39 | 30 | 7.4 |
| 042665-6 | H | 4 | 3.40 | 0.074 | 55 | 2200 | 62 | 0.32 | 27 | 6.0 |
| 042665-7 | H | 4 | 2.50 | 0.074 | 55 | 2200 | 50 | 0.38 | 31 | 5.1 |
| 042665-8 | B | 4 | 4.85 | 0.074 | 55 | 1880 | 68 | 0.44 | 27 | 4.8 |
| 042665-9 | B | 4 | 3.06 | 0.074 | 55 | 1880 | 59 | 0.50 | 23 | 5.7 |
| 042665-10 | B | 4 | 3.57 | 0.074 | 55 | 1880 | 62 | 0.50 | 24 | 5.2 |
| 042865-1 | M | 8 | 2.52 | 0.074 | 58 | (b) | 62 | 0.14 | 16 | 21.7 |
| 042865-2 | M | 8 | --- | 0.074 | 58 | (b) | 73 | --- | 20 | --- |
| 042865-3 | M | 8 | 1.30 | 0.074 | 58 | (b) | 40 | 0.20 | 17 | 22.3 |
| 042865-4 | M | 8 | 2.11 | 0.074 | 58 | (b) | 47 | 0.22 | 19 | 12.1 |
| 042865-5 | A | 8 | 2.75 | 0.073 | 66 | 2270 | 47 | 0.36 | 50 | 7.2 |
| 042865-6 | A | 8 | 3.95 | 0.073 | 66 | 2270 | 66 | --- | 34 | 8.7 |

(a) Fuels are denoted as follows: A - acetone, B - benzene, C - cyclohexane, H - n-hexane, M - methanol.

(b) Methanol flames were too dim to read the optical temperature. The flame temperature was assumed to be 2600°R for use in calculations.

TABLE 3

SUMMARY OF TEMPERATURES DOWNSTREAM FROM CIRCULAR FIRES
IRON-CONSTANTAN THERMOCOUPLES

| Run No. | Distance Downstream ft | Thermocouple Number and (y,z) coordinate 1 (0.5,2) | 2 (2,3) | 3 (2,4) | 4 (2,5) | 5 (2,6) | 6 (6,6) | 7 (6,5) | 8 (6,4) | 9 Fuel | 10 (6,2) |
|---|---|---|---|---|---|---|---|---|---|---|---|
| 032565-1 | 5 | 78 | 106 | 107 | 105 | 142 | 136 | 100 | 98 | 51 | 84 |
| 032565-2 | 5 | 65 | 99 | 110 | 175 | 173 | 172 | 147 | 124 | 44 | 69 |
| 032565-3 | 5 | 62 | 90 | 111 | 136 | 163 | 186 | 176 | 168 | 44 | 64 |
| 032565-4 | 5 | 56 | 69 | 121 | 150 | 190 | 196 | 194 | 171 | 47 | 60 |
| 032965-1 | 5 | 88 | 115 | 122 | 124 | 149 | 161 | 135 | 138 | 61 | 89 |
| 032965-2 | 5 | 70 | 103 | 122 | 140 | 172 | 205 | 203 | 190 | 63 | 72 |
| 032965-3 | 5 | 66 | 83 | 137 | 155 | 202 | 200 | 193 | 174 | 57 | 63 |
| 032965-4 | 5 | 70 | 95 | 131 | 160 | 203 | 215 | 222 | 213 | 58 | 70 |
| 032965-5 | 5 | 96 | 126 | 137 | 144 | 192 | 202 | 178 | 170 | 60 | 98 |
| 032965-6 | 5 | 98 | 129 | 134 | 146 | 189 | 192 | 168 | 165 | 58 | 108 |
| 032965-7 | 5 | 77 | 120 | 172 | 200 | 238 | 232 | 219 | 200 | 58 | 78 |
| 033165-1 | 7.5 | 58 | 62 | 62 | 63 | 79 | 82 | 64 | 63 | 60 | 59 |
| 033165-2 | 7.5 | 60 | 63 | 64 | 65 | 82 | 80 | 66 | 65 | 61 | 61 |
| 033165-3 | 7.5 | 60 | 102 | 107 | 108 | 108 | 105 | 101 | 101 | 62 | 68 |
| 033165-4 | 7.5 | 63 | 66 | 66 | 69 | 87 | 87 | 71 | 67 | 63 | 64 |
| 033165-5 | 7.5 | 101 | 127 | 128 | 123 | 172 | 172 | 135 | 131 | 64 | 102 |
| 033165-6 | 7.5 | 96 | 113 | 121 | 127 | 174 | 158 | 139 | 129 | 65 | 97 |
| 033165-7 | 7.5 | 93 | 109 | 122 | 131 | 174 | 167 | 144 | 134 | 65 | 90 |
| 033165-8 | 7.5 | 77 | 125 | 158 | 167 | 187 | 189 | 178 | 164 | 65 | 80 |
| 033165-9 | 7.5 | 73 | 92 | 88 | 84 | 85 | 91 | 94 | 95 | 56 | 78 |
| 040265-1 | 7.5 | 122 | 183 | 207 | 215 | 280 | 292 | 242 | 226 | 66 | 144 |
| 040265-2 | 7.5 | 114 | 172 | 197 | 207 | 290 | 256 | 227 | 211 | 65 | 122 |
| 040265-3 | 7.5 | 94 | 204 | 232 | 265 | 307 | 339 | 346 | 374 | 66 | 128 |
| 040265-4 | 7.5 | 81 | 117 | 164 | 210 | 258 | 272 | 242 | 184 | 66 | 120 |
| 040265-5 | 7.5 | 133 | 202 | 227 | 250 | 326 | 312 | 274 | 258 | 66 | 188 |
| 040265-6 | 7.5 | 103 | 138 | 220 | 254 | 294 | 311 | 315 | 336 | 67 | 138 |
| 040265-7 | 7.5 | 86 | 137 | 231 | 270 | 307 | 308 | 304 | 261 | 67 | 125 |
| 040665-1 | 10 | 84 | 87 | 87 | 88 | 119 | 116 | 90 | 88 | 66 | 86 |
| 040665-2 | 10 | 83 | 84 | 84 | 90 | 111 | 108 | 90 | 86 | 66 | 85 |
| 041365-1 | 10 | 87 | 140 | 143 | 146 | 147 | 147 | 150 | 148 | 68 | 115 |
| 041365-2 | 10 | 80 | 128 | 121 | 111 | 121 | 114 | 103 | 115 | 69 | 117 |
| 041365-3 | 10 | 80 | 106 | 99 | 85 | 81 | 82 | 84 | 101 | 70 | 115 |
| 041465-1 | 10 | 87 | 86 | 110 | 168 | 210 | 167 | 160 | 151 | 67 | 76 |
| 041465-2 | 10 | 72 | 139 | 107 | 86 | 80 | 82 | 81 | 115 | 67 | 142 |

TABLE 4

SUMMARY OF TEMPERATURES DOWNSTREAM FROM CIRCULAR FIRES
CHROMEL-ALUMEL THERMOCOUPLES

| Run No. | Distance Downstream | Thermocouple Number and (y,z) Coordinate | | | | | | | | | | | |
|---|---|---|---|---|---|---|---|---|---|---|---|---|---|
| | | 1 | 2 | 3 | 4 | 5 | 6 | 7 | 8 | 9 | 10 | 11 | 12 |
| | ft | (4,1) | (4,2) | (4,3) | (4,4) | (4,5) | (4,6) | (4,7) | (3,6) | (3,5) | (3,4) | (3,3) | (3,2) |
| 032565-1 | 5 | 101 | 115 | 116 | 117 | 118 | 120 | 150 | 120 | 120 | 115 | 110 | 116 |
| 032565-2 | 5 | 101 | 143 | 144 | 156 | 174 | 174 | 202 | 168 | 166 | 158 | 142 | 130 |
| 032565-3 | 5 | 106 | 138 | 149 | 161 | 180 | 187 | 200 | 174 | 169 | 184 | 170 | 101 |
| 032565-4 | 5 | 100 | 139 | 181 | 226 | 216 | 216 | 216 | 194 | 188 | 200 | 224 | 189 |
| 032965-1 | 5 | 165 | 152 | 150 | 163 | 160 | 171 | 205 | 164 | 150 | 162 | 157 | 149 |
| 032965-2 | 5 | 142 | 150 | 161 | 175 | 183 | 188 | 198 | 178 | 176 | 193 | 205 | 150 |
| 032965-3 | 5 | 145 | 185 | 267 | 248 | 220 | 221 | 220 | 215 | 201 | 208 | 242 | 236 |
| 032965-4 | 5 | 157 | 185 | 214 | 239 | 222 | 217 | 221 | 212 | 198 | 207 | 233 | 185 |
| 032965-5 | 5 | 174 | 176 | 191 | 194 | 185 | 198 | 225 | 192 | 170 | 185 | 188 | 186 |
| 032965-6 | 5 | 187 | 185 | 188 | 186 | 180 | 194 | 215 | 184 | 165 | 181 | 194 | 200 |
| 032965-7 | 5 | 200 | 220 | 274 | 286 | 259 | 246 | 243 | 232 | 229 | 249 | 316 | 300 |
| 033165-1 | 7.5 | 72 | 75 | 76 | 76 | 77 | 99 | 115 | 97 | 77 | 77 | 77 | 75 |
| 033165-2 | 7.5 | 75 | 76 | 76 | 78 | 79 | 93 | 116 | 98 | 80 | 80 | 79 | 78 |
| 033165-3 | 7.5 | 75 | 75 | 85 | 113 | 119 | 120 | 119 | 120 | 123 | 123 | 125 | 111 |
| 033165-4 | 7.5 | 77 | 79 | 79 | 81 | 81 | 100 | 121 | 95 | 81 | 80 | 80 | 80 |
| 033165-5 | 7.5 | 137 | 150 | 150 | 160 | 162 | 208 | 236 | 204 | 153 | 158 | 153 | 150 |
| 033165-6 | 7.5 | 125 | 131 | 132 | 146 | 159 | 190 | 215 | 195 | 159 | 150 | 139 | 137 |
| 033165-7 | 7.5 | 130 | 132 | 130 | 143 | 150 | 170 | 207 | 174 | 153 | 149 | 138 | 132 |
| 033165-8 | 7.5 | 116 | 123 | 200 | 222 | 212 | 212 | 210 | 207 | 207 | 216 | 230 | 249 |
| 033165-9 | 7.5 | 110 | 136 | 205 | 155 | 122 | 110 | 118 | 104 | 111 | 145 | 217 | 244 |
| 040265-1 | 7.5 | 192 | 198 | 198 | 235 | 256 | 281 | 341 | 279 | 250 | 241 | 220 | 219 |
| 040265-2 | 7.5 | 199 | 220 | 214 | 243 | 256 | 282 | 330 | 291 | 252 | 248 | 263 | 250 |
| 040265-3 | 7.5 | 180 | 208 | 240 | 285 | 310 | 325 | 343 | 318 | 302 | 324 | 350 | 297 |
| 040265-4 | 7.5 | 208 | 347 | 345 | 236 | 260 | 310 | 313 | 294 | 252 | 210 | 191 | 300 |
| 040265-5 | 7.5 | 213 | 230 | 232 | 264 | 288 | 306 | 357 | 315 | 288 | 278 | 253 | 260 |
| 040265-6 | 7.5 | 196 | 224 | 258 | 285 | 292 | 310 | 334 | 300 | 300 | 310 | 295 | 230 |
| 040265-7 | 7.5 | 190 | 273 | 345 | 295 | 318 | 337 | 348 | 337 | 306 | 273 | 260 | 374 |
| 040665-1 | 10 | 96 | 100 | 100 | 103 | 105 | 135 | 160 | 140 | 104 | 103 | 102 | 101 |
| 040665-2 | 10 | 98 | 99 | 100 | 102 | 107 | 135 | 154 | 122 | 102 | 100 | 100 | 100 |
| 041365-1 | 10 | 98 | 98 | 105 | 135 | 162 | 165 | 165 | 166 | 165 | 160 | 160 | 138 |
| 041365-2 | 10 | 98 | 98 | 112 | 133 | 125 | 135 | 142 | 135 | 128 | 145 | 152 | 169 |
| 041365-3 | 10 | 95 | 100 | 125 | 132 | 112 | 99 | 95 | 97 | 105 | 138 | 160 | 187 |
| 041465-1 | 10 | 98 | 95 | 98 | 126 | 173 | 190 | 219 | 225 | 210 | 145 | 105 | 100 |
| 041465-2 | 10 | 102 | 102 | 172 | 175 | 123 | 100 | 102 | 100 | 125 | 185 | 250 | 288 |

TABLE 5

SUMMARY OF TEMPERATURES DOWNSTREAM FROM CHANNEL FIRES
IRON-CONSTANTAN THERMOCOUPLES

| Run No. | Distance Downstream ft | Thermocouple Number and (y,z) Coordinate | | | | | | | | | |
|---|---|---|---|---|---|---|---|---|---|---|---|
| | | 1 (0.5,2) | 2 (2,3) | 3 (2,4) | 4 (2,5) | 5 (2,6) | 6 (6,6) | 7 (6,5) | 8 (6,4) | 9 Fuel | 10 (6,2) |
| 041565-1 | 2.5 | 85 | 112 | 110 | 120 | 115 | 117 | 114 | 114 | 66 | 125 |
| 041565-2 | 2.5 | 74 | 83 | 104 | 116 | 108 | 109 | 104 | 105 | 65 | 75 |
| 041565-3 | 2.5 | 73 | 79 | 81 | 83 | 78 | 82 | 77 | 82 | 67 | 78 |
| 041565-4 | 2.5 | 92 | 140 | 118 | 132 | 129 | 130 | 125 | 118 | 68 | 111 |
| 041565-5 | 2.5 | 77 | 81 | 98 | 101 | 97 | 98 | 96 | 98 | 70 | 79 |
| 041565-6 | 2.5 | 74 | 77 | 78 | 79 | 85 | 82 | 86 | 78 | 70 | 75 |
| 041565-7 | 2.5 | 73 | 76 | 76 | 78 | 76 | 77 | 75 | 76 | 70 | 75 |
| 041565-8 | 2.5 | 72 | 73 | 74 | 75 | 74 | 75 | 72 | 74 | 69 | 72 |
| 041665-1 | 2.5 | 102 | 154 | 155 | 180 | 170 | 178 | 162 | 149 | 64 | 244 |
| 041665-2 | 2.5 | 103 | 151 | 155 | 188 | 176 | 179 | 167 | 154 | 64 | 247 |
| 041665-3 | 2.5 | 100 | 179 | 186 | 195 | 178 | 180 | 167 | 187 | 66 | 144 |
| 041665-4 | 2.5 | 90 | 118 | 119 | 158 | 144 | 146 | 134 | 122 | 68 | 123 |
| 041665-5 | 2.5 | 110 | 167 | 167 | 192 | 182 | 182 | 175 | 168 | 65 | 263 |
| 041665-6 | 2.5 | 110 | 160 | 176 | 201 | 188 | 190 | 182 | 174 | 66 | 220 |
| 041665-7 | 2.5 | 107 | 200 | 203 | 212 | 191 | 194 | 182 | 198 | 66 | 163 |
| 041665-8 | 2.5 | 95 | 122 | 109 | 119 | 141 | 143 | 117 | 111 | 69 | 139 |
| 041665-9 | 2.5 | 123 | 209 | 191 | 209 | 200 | 199 | 198 | 196 | 70 | 277 |
| 041665-10 | 2.5 | 137 | 242 | 242 | 250 | 229 | 233 | 233 | 247 | 70 | 283 |
| 041665-11 | 2.5 | 134 | 267 | 254 | 254 | 232 | 238 | 234 | 270 | 70 | 270 |
| 042365-1 | 5 | 91 | 100 | 108 | 114 | 118 | 118 | 117 | 115 | 71 | 89 |
| 042365-2 | 5 | 122 | 126 | 117 | 118 | 122 | 123 | 120 | 121 | 74 | 124 |
| 042365-3 | 5 | 89 | 93 | 93 | 93 | 94 | 95 | 91 | 93 | 74 | 101 |
| 042365-4 | 5 | 124 | 124 | 134 | 150 | 168 | 174 | 150 | 139 | 82 | 114 |
| 042365-5 | 5 | 120 | 149 | 156 | 174 | 182 | 180 | 173 | 170 | 83 | 196 |
| 042365-6 | 5 | 104 | 112 | 134 | 152 | 154 | 153 | 146 | 138 | 83 | 110 |
| 042365-7 | 5 | 100 | 108 | 111 | 110 | 108 | 110 | 105 | 112 | 64 | 111 |
| 042665-1 | 5 | 153 | 145 | 154 | 173 | 192 | 194 | 173 | 164 | 60 | 125 |
| 042665-2 | 5 | 127 | 185 | 200 | 229 | 238 | 224 | 220 | 210 | 61 | 251 |
| 042665-3 | 5 | 196 | 216 | 222 | 226 | 230 | 232 | 224 | 217 | 61 | 176 |
| 042665-4 | 5 | 110 | 198 | 236 | 263 | 260 | 257 | 248 | 251 | 60 | 158 |
| 042665-5 | 5 | 156 | 148 | 158 | 174 | 195 | 198 | 177 | 166 | 61 | 141 |
| 042665-6 | 5 | 142 | 179 | 184 | 204 | 212 | 208 | 205 | 196 | 63 | 175 |
| 042665-7 | 5 | 172 | 177 | 192 | 207 | 214 | 200 | 188 | 182 | 63 | 146 |
| 042665-8 | 5 | 96 | 126 | 154 | 191 | 196 | 198 | 183 | 152 | 64 | 114 |
| 042665-9 | 5 | 198 | 210 | 210 | 208 | 213 | 215 | 204 | 196 | 64 | 183 |
| 042665-10 | 5 | 164 | 211 | 227 | 242 | 248 | 248 | 238 | 229 | 64 | 213 |
| 042865-1 | 10 | 85 | 102 | 102 | 103 | 106 | 107 | 106 | 104 | 58 | 113 |
| 042865-3 | 10 | 82 | 85 | 90 | 111 | 117 | 116 | 110 | 88 | 62 | 81 |
| 042865-4 | 10 | 84 | 97 | 92 | 109 | 126 | 126 | 107 | 92 | 62 | 83 |
| 042865-5 | 10 | 126 | 134 | 145 | 155 | 185 | 207 | 181 | 152 | 67 | 117 |

TABLE 6

SUMMARY OF TEMPERATURES DOWNSTREAM FROM CHANNEL FIRES
CHROMEL-ALUMEL THERMOCOUPLES

| Run No. | Distance Downstream ft | Thermocouple Number and (y,z) Coordinate | | | | | | | | | | | |
|---|---|---|---|---|---|---|---|---|---|---|---|---|---|
| | | 1 (4,1) | 2 (4,2) | 3 (4,3) | 4 (4,4) | 5 (4,5) | 6 (4,6) | 7 (4,7) | 8 (3,6) | 9 (3,5) | 10 (3,4) | 11 (3,3) | 12 (3,2) |
| 041565-1 | 2.5 | 151 | 165 | 121 | 119 | 126 | 130 | 130 | 130 | 130 | 120 | 123 | 153 |
| 041565-2 | 2.5 | 120 | 99 | 100 | 116 | 121 | 122 | 125 | 125 | 125 | 115 | 104 | 99 |
| 041565-3 | 2.5 | 112 | 99 | 95 | 95 | 83 | 85 | 86 | 86 | 86 | 86 | 98 | 100 |
| 041565-4 | 2.5 | 154 | 184 | 93 | 127 | 188 | 190 | 190 | 190 | 190 | 130 | 153 | 168 |
| 041565-5 | 2.5 | 122 | 94 | 105 | 110 | 110 | 110 | 109 | 109 | 110 | 109 | 107 | 92 |
| 041565-6 | 2.5 | 95 | 81 | 80 | 80 | 79 | 87 | 90 | 86 | 80 | 80 | 80 | 80 |
| 041565-7 | 2.5 | 85 | 80 | 78 | 78 | 77 | 77 | 80 | 79 | 79 | 79 | 80 | 80 |
| 041565-8 | 2.5 | 78 | 78 | 77 | 76 | 76 | 76 | 77 | 76 | 77 | 76 | 78 | 78 |
| 041665-1 | 2.5 | 187 | 283 | 224 | 178 | 181 | 180 | 180 | 181 | 188 | 118 | 210 | 311 |
| 041665-2 | 2.5 | 265 | 304 | 201 | 170 | 186 | 185 | 182 | 187 | 193 | 161 | 185 | 295 |
| 041665-3 | 2.5 | 283 | 203 | 207 | 205 | 190 | 184 | 186 | 190 | 195 | 195 | 208 | 200 |
| 041665-4 | 2.5 | 219 | 174 | 154 | 145 | 150 | 150 | 166 | 153 | 153 | 130 | 151 | 174 |
| 041665-5 | 2.5 | 230 | 300 | 242 | 189 | 192 | 188 | 187 | 191 | 195 | 183 | 240 | 326 |
| 041665-6 | 2.5 | 343 | 307 | 203 | 190 | 202 | 195 | 194 | 198 | 205 | 185 | 204 | 291 |
| 041665-7 | 2.5 | 371 | 232 | 232 | 228 | 204 | 201 | 202 | 205 | 212 | 215 | 232 | 223 |
| 041665-8 | 2.5 | 241 | 291 | 163 | 129 | 125 | 143 | 157 | 148 | 125 | 120 | 159 | 186 |
| 041665-9 | 2.5 | 270 | 292 | 270 | 222 | 215 | 215 | 210 | 215 | 216 | 220 | 268 | 333 |
| 041665-10 | 2.5 | 437 | 344 | 285 | 279 | 270 | 252 | 248 | 249 | 266 | 276 | 282 | 313 |
| 041665-11 | 2.5 | 400 | 347 | 326 | 303 | 266 | 261 | 249 | 254 | 260 | 293 | 310 | 312 |
| 042365-1 | 5 | 90 | 91 | 97 | 100 | 110 | 120 | 126 | 122 | 114 | 105 | 98 | 100 |
| 042365-2 | 5 | 124 | 146 | 132 | 124 | 124 | 129 | 129 | 129 | 127 | 127 | 135 | 147 |
| 042365-3 | 5 | 164 | 112 | 102 | 100 | 100 | 100 | 112 | 103 | 100 | 100 | 99 | 107 |
| 042365-4 | 5 | 117 | 120 | 133 | 142 | 150 | 171 | 190 | 170 | 145 | 135 | 124 | 120 |
| 042365-5 | 5 | 229 | 221 | 178 | 168 | 171 | 180 | 177 | 177 | 170 | 154 | 145 | 198 |
| 042365-6 | 5 | 202 | 126 | 120 | 135 | 147 | 155 | 159 | 156 | 150 | 136 | 114 | 123 |
| 042365-7 | 5 | 203 | 122 | 117 | 112 | 107 | 110 | 116 | 111 | 110 | 112 | 110 | 121 |
| 042665-1 | 5 | 130 | 140 | 166 | 158 | 177 | 200 | 217 | 197 | 174 | 158 | 137 | 134 |
| 042665-2 | 5 | 193 | 234 | 210 | 200 | 210 | 226 | 228 | 228 | 215 | 206 | 237 | 248 |
| 042665-3 | 5 | 148 | 160 | 190 | 203 | 214 | 226 | 235 | 227 | 219 | 207 | 190 | 170 |
| 042665-4 | 5 | 283 | 174 | 197 | 240 | 250 | 260 | 257 | 259 | 255 | 236 | 196 | 204 |
| 042665-5 | 5 | 138 | 149 | 166 | 171 | 182 | 201 | 215 | 196 | 176 | 167 | 160 | 150 |
| 042665-6 | 5 | 230 | 200 | 176 | 185 | 205 | 212 | 208 | 210 | 200 | 189 | 210 | 230 |
| 042665-7 | 5 | 143 | 157 | 175 | 182 | 190 | 205 | 214 | 210 | 195 | 178 | 165 | 154 |
| 042665-8 | 5 | 200 | 128 | 141 | 147 | 180 | 199 | 212 | 198 | 185 | 157 | 145 | 139 |
| 042665-9 | 5 | 165 | 165 | 182 | 190 | 198 | 207 | 218 | 211 | 207 | 204 | 190 | 169 |
| 042665-10 | 5 | 201 | 228 | 206 | 220 | 239 | 247 | 261 | 243 | 236 | 225 | 210 | 231 |
| 042865-1 | 10 | 95 | 119 | 119 | 110 | 109 | 110 | 111 | 110 | 109 | 109 | 117 | 125 |
| 042865-3 | 10 | 84 | 86 | 88 | 95 | 115 | 136 | 153 | 132 | 115 | 97 | 88 | 86 |
| 042865-4 | 10 | 86 | 88 | 89 | 96 | 115 | 131 | 150 | 130 | 113 | 100 | 91 | 88 |
| 042865-5 | 10 | 114 | 122 | 128 | 152 | 173 | 198 | 225 | 188 | 165 | 155 | 130 | 122 |

TABLE 7

CALCULATED DIMENSIONLESS TEMPERATURE RISE AND DIMENSIONLESS VELOCITY DATA FOR CIRCULAR BURNERS--IRON-CONSTANTAN THERMOCOUPLES

| Run Number | $\Omega_C$ | $\Phi_C$ For Thermocouple Number and (y,z) Coordinate | | | | | | | | |
|---|---|---|---|---|---|---|---|---|---|---|
| | | 1 | 2 | 3 | 4 | 5 | 6 | 7 | 8 | 10 |
| | | (0.5,2) | (2,3) | (2,4) | (2,5) | (2,6) | (6,6) | (6,5) | (6,4) | (6,2) |
| 032565-1 | 0.075 | 0.041 | 0.066 | 0.066 | 0.064 | 0.097 | 0.092 | 0.060 | 0.059 | 0.046 |
| 032565-2 | 0.11 | 0.029 | 0.059 | 0.068 | 0.12 | 0.12 | 0.12 | 0.10 | 0.080 | 0.033 |
| 032565-3 | 0.16 | 0.035 | 0.067 | 0.098 | 0.12 | 0.15 | 0.18 | 0.16 | 0.16 | 0.037 |
| 032565-4 | 0.22 | 0.030 | 0.045 | 0.11 | 0.14 | 0.19 | 0.20 | 0.19 | 0.17 | 0.035 |
| 032965-1 | 0.10 | 0.038 | 0.061 | 0.068 | 0.069 | 0.091 | 0.10 | 0.079 | 0.081 | 0.039 |
| 032965-2 | 0.16 | 0.030 | 0.068 | 0.090 | 0.11 | 0.15 | 0.19 | 0.18 | 0.17 | 0.032 |
| 032965-3 | 0.24 | 0.030 | 0.054 | 0.13 | 0.15 | 0.22 | 0.22 | 0.21 | 0.18 | 0.026 |
| 032965-4 | 0.19 | 0.027 | 0.053 | 0.090 | 0.15 | 0.16 | 0.18 | 0.18 | 0.18 | 0.027 |
| 032965-5 | 0.099 | 0.041 | 0.064 | 0.073 | 0.12 | 0.12 | 0.12 | 0.10 | 0.099 | 0.042 |
| 032965-6 | 0.061 | 0.024 | 0.039 | 0.042 | 0.078 | 0.069 | 0.071 | 0.059 | 0.057 | 0.029 |
| 032965-7 | 0.103 | 0.016 | 0.041 | 0.071 | 0.048 | 0.109 | 0.11 | 0.098 | 0.087 | 0.016 |
| 033165-1 | 0.34 | 0.31 | 0.46 | 0.46 | 0.087 | 1.06 | 1.16 | 0.53 | 0.49 | 0.35 |
| 033165-2 | 0.52 | 0.59 | 0.76 | 0.81 | 0.49 | 1.78 | 1.67 | 0.29 | 0.86 | 0.65 |
| 033165-3 | 1.03 | 0.98 | 4.72 | 5.17 | 0.86 | 5.26 | 4.99 | 4.63 | 4.63 | 1.69 |
| 033165-4 | 0.79 | 0.96 | 1.16 | 1.16 | 5.26 | 2.59 | 2.59 | 1.50 | 1.23 | 1.02 |
| 033165-5 | 1.91 | 0.16 | 0.27 | 0.28 | 1.36 | 0.48 | 0.48 | 0.31 | 0.29 | 0.16 |
| 033165-6 | 0.26 | 0.14 | 0.22 | 0.26 | 0.26 | 0.51 | 0.44 | 0.35 | 0.30 | 0.14 |
| 033165-7 | 0.38 | 0.16 | 0.25 | 0.33 | 0.29 | 0.64 | 0.60 | 0.46 | 0.40 | 0.14 |
| 033165-8 | 0.54 | 0.088 | 0.50 | 0.79 | 0.38 | 1.04 | 1.06 | 0.96 | 0.84 | 0.11 |
| 033165-9 | 0.65 | 0.050 | 0.21 | 0.18 | 0.87 | 0.15 | 0.20 | 0.22 | 0.23 | 0.092 |
| 040265-1 | 0.14 | 0.056 | 0.12 | 0.14 | 0.14 | 0.21 | 0.22 | 0.18 | 0.16 | 0.078 |
| 040265-2 | 0.20 | 0.052 | 0.12 | 0.14 | 0.15 | 0.24 | 0.21 | 0.17 | 0.16 | 0.061 |
| 040265-3 | 0.29 | 0.046 | 0.23 | 0.27 | 0.15 | 0.40 | 0.45 | 0.46 | 0.51 | 0.10 |
| 040265-4 | 0.36 | 0.030 | 0.10 | 0.20 | 0.33 | 0.38 | 0.41 | 0.29 | 0.24 | 0.11 |
| 040265-5 | 0.18 | 0.074 | 0.13 | 0.16 | 0.29 | 0.25 | 0.24 | 0.20 | 0.19 | 0.12 |
| 040265-6 | 0.30 | 0.054 | 0.10 | 0.22 | 0.18 | 0.33 | 0.36 | 0.36 | 0.39 | 0.10 |
| 040265-7 | 0.40 | 0.038 | 0.14 | 0.32 | 0.27 | 0.46 | 0.46 | 0.46 | 0.38 | 0.11 |
| 040665-1 | 0.66 | 0.93 | 1.13 | 1.13 | 0.39 | 3.26 | 3.06 | 1.33 | 1.20 | 1.06 |
| 040665-2 | 1.21 | 1.35 | 1.45 | 1.45 | 1.20 | 4.25 | 3.94 | 2.07 | 1.66 | 1.55 |
| 041365-1 | 1.34 | 1.75 | 7.20 | 7.51 | 2.07 | 7.92 | 8.00 | 8.23 | 8.03 | 4.63 |
| 041365-2 | 1.48 | 0.90 | 5.21 | 4.58 | 7.82 | 4.58 | 3.95 | 2.97 | 4.04 | 4.22 |
| 041365-3 | 1.82 | 0.86 | 3.09 | 2.49 | 3.68 | 0.94 | 1.03 | 1.20 | 2.66 | 3.86 |
| 041465-1 | 0.61 | 0.17 | 0.16 | 0.40 | 1.29 | 1.41 | 0.97 | 0.90 | 0.81 | 0.060 |
| 041465-2 | 0.86 | 0.020 | 0.69 | 0.37 | 0.98 | 0.10 | 0.12 | 0.11 | 0.45 | 0.72 |

TABLE 8

CALCULATED DIMENSIONLESS TEMPERATURE RISE AND DIMENSIONLESS VELOCITY DATA FOR CIRCULAR BURNERS--CHROMEL-ALUMEL THERMOCOUPLES

| Run No. | $\Omega_C$ | $\Phi_C$ For Thermocouple Number and (y,z) Coordinate | | | | | | | | | | | |
|---|---|---|---|---|---|---|---|---|---|---|---|---|---|
| | | 1 | 2 | 3 | 4 | 5 | 6 | 7 | 8 | 9 | 10 | 11 | 12 |
| | | (4,1) | (4,2) | (4,3) | (4,4) | (4,5) | (4,6) | (4,7) | (3,6) | (3,5) | (3,4) | (3,3) | (3,2) |
| 032565-1 | 0.075 | 0.061 | 0.074 | 0.074 | 0.075 | 0.076 | 0.078 | 0.10 | 0.078 | 0.078 | 0.074 | 0.069 | 0.074 |
| 032565-2 | 0.11 | 0.061 | 0.097 | 0.098 | 0.11 | 0.12 | 0.12 | 0.15 | 0.12 | 0.12 | 0.11 | 0.096 | 0.086 |
| 032565-3 | 0.16 | 0.085 | 0.12 | 0.13 | 0.15 | 0.17 | 0.18 | 0.19 | 0.16 | 0.16 | 0.17 | 0.16 | 0.079 |
| 032565-4 | 0.22 | 0.082 | 0.13 | 0.18 | 0.23 | 0.22 | 0.22 | 0.22 | 0.19 | 0.19 | 0.20 | 0.23 | 0.19 |
| 032965-1 | 0.10 | 0.10 | 0.093 | 0.092 | 0.10 | 0.10 | 0.11 | 0.14 | 0.10 | 0.092 | 0.10 | 0.08 | 0.098 |
| 032965-2 | 0.16 | 0.11 | 0.12 | 0.14 | 0.15 | 0.16 | 0.17 | 0.18 | 0.16 | 0.15 | 0.17 | 0.19 | 0.12 |
| 032965-3 | 0.24 | 0.14 | 0.20 | 0.31 | 0.28 | 0.26 | 0.24 | 0.24 | 0.24 | 0.22 | 0.23 | 0.27 | 0.27 |
| 032965-4 | 0.19 | 0.12 | 0.14 | 0.18 | 0.20 | 0.18 | 0.18 | 0.18 | 0.17 | 0.16 | 0.17 | 0.20 | 0.14 |
| 032965-5 | 0.098 | 0.10 | 0.10 | 0.12 | 0.12 | 0.11 | 0.12 | 0.14 | 0.12 | 0.099 | 0.11 | 0.11 | 0.11 |
| 032965-6 | 0.061 | 0.068 | 0.067 | 0.069 | 0.068 | 0.065 | 0.072 | 0.082 | 0.067 | 0.057 | 0.065 | 0.072 | 0.074 |
| 032965-7 | 0.10 | 0.087 | 0.099 | 0.13 | 0.14 | 0.12 | 0.11 | 0.112 | 0.11 | 0.10 | 0.12 | 0.16 | 0.14 |
| 033165-1 | 0.34 | 0.81 | 0.92 | 0.95 | 0.95 | 0.99 | 1.76 | 2.33 | 1.69 | 0.99 | 0.99 | 0.99 | 0.92 |
| 033165-2 | 0.52 | 1.66 | 1.45 | 1.45 | 1.56 | 1.62 | 2.37 | 3.61 | 2.64 | 1.67 | 1.67 | 1.62 | 1.51 |
| 033165-3 | 1.03 | 2.32 | 2.32 | 3.21 | 5.70 | 6.24 | 6.33 | 6.24 | 6.33 | 6.59 | 6.59 | 6.77 | 5.52 |
| 033165-4 | 0.79 | 1.91 | 2.05 | 2.05 | 2.18 | 2.10 | 3.48 | 4.91 | 3.14 | 2.18 | 2.11 | 2.11 | 2.11 |
| 033165-5 | 0.19 | 0.32 | 0.38 | 0.38 | 0.42 | 0.43 | 0.64 | 0.77 | 0.62 | 0.39 | 0.41 | 0.39 | 0.38 |
| 033165-6 | 0.26 | 0.28 | 0.31 | 0.31 | 0.38 | 0.44 | 0.59 | 0.71 | 0.61 | 0.44 | 0.40 | 0.35 | 0.34 |
| 033165-7 | 0.38 | 0.38 | 0.39 | 0.38 | 0.46 | 0.50 | 0.62 | 0.84 | 0.64 | 0.52 | 0.49 | 0.42 | 0.39 |
| 033165-8 | 0.54 | 0.42 | 0.49 | 1.15 | 1.34 | 1.26 | 1.26 | 1.24 | 1.21 | 1.21 | 1.29 | 1.41 | 1.58 |
| 033165-9 | 0.65 | 0.36 | 0.58 | 1.15 | 0.73 | 0.46 | 0.36 | 0.42 | 0.31 | 0.37 | 0.65 | 1.25 | 1.48 |
| 040265-1 | 0.14 | 0.12 | 0.13 | 0.13 | 0.17 | 0.19 | 0.21 | 0.27 | 0.21 | 0.19 | 0.17 | 0.15 | 0.15 |
| 040265-2 | 0.20 | 0.14 | 0.17 | 0.16 | 0.19 | 0.21 | 0.23 | 0.29 | 0.24 | 0.20 | 0.20 | 0.21 | 0.20 |
| 040265-3 | 0.29 | 0.19 | 0.24 | 0.29 | 0.36 | 0.40 | 0.43 | 0.46 | 0.42 | 0.39 | 0.43 | 0.47 | 0.38 |
| 040265-4 | 0.36 | 0.28 | 0.50 | 0.50 | 0.34 | 0.39 | 0.49 | 0.49 | 0.46 | 0.37 | 0.29 | 0.25 | 0.47 |
| 040265-5 | 0.18 | 0.14 | 0.16 | 0.16 | 0.19 | 0.22 | 0.14 | 0.28 | 0.24 | 0.22 | 0.20 | 0.18 | 0.19 |
| 040265-6 | 0.30 | 0.19 | 0.23 | 0.28 | 0.32 | 0.33 | 0.36 | 0.39 | 0.34 | 0.34 | 0.36 | 0.33 | 0.24 |
| 040265-7 | 0.40 | 0.24 | 0.40 | 0.48 | 0.44 | 0.48 | 0.52 | 0.48 | 0.52 | 0.46 | 0.40 | 0.37 | 0.59 |
| 040665-1 | 0.66 | 1.73 | 2.00 | 2.00 | 2.20 | 2.33 | 4.33 | 5.99 | 4.66 | 2.26 | 2.19 | 2.13 | 2.06 |
| 040665-2 | 1.21 | 2.90 | 3.00 | 3.11 | 3.31 | 3.83 | 6.73 | 8.70 | 5.39 | 3.31 | 3.11 | 3.11 | 3.11 |
| 041365-1 | 1.34 | 2.88 | 2.88 | 3.60 | 6.69 | 9.47 | 9.87 | 9.87 | 9.88 | 9.77 | 9.26 | 9.26 | 7.00 |
| 041365-2 | 1.48 | 2.52 | 2.52 | 3.77 | 5.66 | 4.94 | 5.84 | 6.47 | 5.84 | 5.21 | 6.74 | 7.37 | 8.90 |
| 041365-3 | 1.82 | 2.15 | 2.58 | 4.72 | 5.32 | 3.61 | 2.49 | 2.15 | 2.32 | 3.01 | 3.26 | 7.73 | 10.00 |
| 041465-1 | 0.61 | 0.28 | 0.25 | 0.28 | 0.56 | 1.04 | 1.21 | 1.50 | 1.56 | 1.41 | 0.75 | 0.35 | 0.30 |
| 041465-2 | 0.86 | 0.32 | 0.32 | 1.03 | 1.06 | 0.53 | 0.30 | 0.32 | 0.30 | 0.55 | 1.16 | 1.81 | 2.19 |

TABLE 9

CALCULATED DIMENSIONLESS TEMPERATURE RISE AND DIMENSIONLESS VELOCITY DATA FOR CHANNEL BURNERS--IRON-CONSTANTAN THERMOCOUPLES

| Run No. | $\Omega_L$ | $\Phi_L$ For Thermocouple Number and (y,z) Coordinate | | | | | | | | |
|---|---|---|---|---|---|---|---|---|---|---|
| | | 1 | 2 | 3 | 4 | 5 | 6 | 7 | 8 | 10 |
| | | (0.5,2) | (2,3) | (2,4) | (2,5) | (2,6) | (6,6) | (6,5) | (6,4) | (6,2) |
| 041565-1 | 0.49 | 0.33 | 0.75 | 0.72 | 0.87 | 0.80 | 0.83 | 0.78 | 0.78 | 0.95 |
| 041565-2 | 0.65 | 0.16 | 0.30 | 0.63 | 0.82 | 0.69 | 0.71 | 0.63 | 0.65 | 0.17 |
| 041565-3 | 0.84 | 0.15 | 0.25 | 0.28 | 0.32 | 0.23 | 0.30 | 0.22 | 0.30 | 0.23 |
| 041565-4 | 0.52 | 0.41 | 1.12 | 0.80 | 1.00 | 0.96 | 0.98 | 0.90 | 0.80 | 0.70 |
| 041565-5 | 0.58 | 0.36 | 0.47 | 0.94 | 1.02 | 0.91 | 0.94 | 0.88 | 0.94 | 0.41 |
| 041565-6 | 0.74 | 0.27 | 0.35 | 0.38 | 0.40 | 0.56 | 0.48 | 0.59 | 0.38 | 0.52 |
| 041565-7 | 0.90 | 0.24 | 0.32 | 0.32 | 0.38 | 0.32 | 0.35 | 0.30 | 0.32 | 0.30 |
| 041565-8 | 1.12 | 0.21 | 0.24 | 0.27 | 0.29 | 0.27 | 0.29 | 0.21 | 0.27 | 0.21 |
| 041665-1 | 0.42 | 0.40 | 0.89 | 0.90 | 1.14 | 1.04 | 1.12 | 1.06 | 0.84 | 1.74 |
| 041665-2 | 0.52 | 0.42 | 0.89 | 0.93 | 1.26 | 1.14 | 1.16 | 1.05 | 0.92 | 1.83 |
| 041665-3 | 0.68 | 0.38 | 1.14 | 1.21 | 1.29 | 1.13 | 1.15 | 1.02 | 1.21 | 0.80 |
| 041665-4 | 0.78 | 0.29 | 0.56 | 0.57 | 0.95 | 0.82 | 0.84 | 0.92 | 0.60 | 0.61 |
| 041665-5 | 0.42 | 0.43 | 0.95 | 0.95 | 1.18 | 1.09 | 1.09 | 1.06 | 0.96 | 1.84 |
| 041665-6 | 0.59 | 0.43 | 0.89 | 0.89 | 1.27 | 1.15 | 1.17 | 1.09 | 1.01 | 1.44 |
| 041665-7 | 0.68 | 0.39 | 1.24 | 1.24 | 1.35 | 1.17 | 1.19 | 1.08 | 1.23 | 0.91 |
| 041665-8 | 0.80 | 0.29 | 0.54 | 0.54 | 0.52 | 0.72 | 0.74 | 0.50 | 0.44 | 0.70 |
| 041665-9 | 0.40 | 0.36 | 1.00 | 0.87 | 1.00 | 0.94 | 0.93 | 0.92 | 0.91 | 1.51 |
| 041665-10 | 0.59 | 0.45 | 1.22 | 1.22 | 1.28 | 1.12 | 1.15 | 1.15 | 1.26 | 1.51 |
| 041665-11 | 0.76 | 0.43 | 1.40 | 1.31 | 1.31 | 1.31 | 1.15 | 1.19 | 1.17 | 1.43 |
| 042365-1 | 0.36 | 0.48 | 0.67 | 1.00 | 1.18 | 1.30 | 1.30 | 1.27 | 1.21 | 0.42 |
| 042365-2 | 0.59 | 1.42 | 1.55 | 1.27 | 1.30 | 1.42 | 1.46 | 1.36 | 1.39 | 1.48 |
| 042365-3 | 0.76 | 0.42 | 0.54 | 0.54 | 0.54 | 0.58 | 0.61 | 0.48 | 0.54 | 0.79 |
| 042365-4 | 0.33 | 0.59 | 0.59 | 0.74 | 0.99 | 1.26 | 1.35 | 0.99 | 0.82 | 0.44 |
| 042365-5 | 0.60 | 0.48 | 0.89 | 0.98 | 1.23 | 1.34 | 1.32 | 1.22 | 1.18 | 1.54 |
| 042365-6 | 0.68 | 0.31 | 0.44 | 0.80 | 1.10 | 1.13 | 1.11 | 1.00 | 0.87 | 0.41 |
| 042365-7 | 0.86 | 0.24 | 0.36 | 0.41 | 0.40 | 0.36 | 0.40 | 0.32 | 0.43 | 0.41 |
| 042665-1 | 0.37 | 1.12 | 1.03 | 1.13 | 1.34 | 1.54 | 1.56 | 1.34 | 1.24 | 0.81 |
| 042665-2 | 0.72 | 0.87 | 1.53 | 1.70 | 2.03 | 2.13 | 1.97 | 1.93 | 1.81 | 2.28 |
| 042665-3 | 0.50 | 1.50 | 1.70 | 1.76 | 1.81 | 1.85 | 1.87 | 1.78 | 1.71 | 1.29 |
| 042665-4 | 0.80 | 0.63 | 1.56 | 1.96 | 2.25 | 2.61 | 2.18 | 2.09 | 2.12 | 1.14 |
| 042665-5 | 0.35 | 1.12 | 1.03 | 1.15 | 1.32 | 1.56 | 1.59 | 1.36 | 1.24 | 0.96 |
| 042665-6 | 0.69 | 1.11 | 1.59 | 1.65 | 1.91 | 2.01 | 1.96 | 1.92 | 1.81 | 1.54 |
| 042665-7 | 0.48 | 1.33 | 1.38 | 1.55 | 1.72 | 1.57 | 1.64 | 1.51 | 1.44 | 1.03 |
| 042665-8 | 0.91 | 0.45 | 0.78 | 1.09 | 1.50 | 1.56 | 1.58 | 1.42 | 1.07 | 0.65 |
| 042665-9 | 0.56 | 1.48 | 1.60 | 1.60 | 1.58 | 1.63 | 1.65 | 1.54 | 1.47 | 1.32 |
| 042665-10 | 0.64 | 1.11 | 1.58 | 1.75 | 1.90 | 1.96 | 1.96 | 1.86 | 1.77 | 1.60 |
| 042865-1 | 0.69 | 1.24 | 2.03 | 2.03 | 2.08 | 2.21 | 2.26 | 2.21 | 2.12 | 2.54 |
| 042865-3 | 0.32 | 0.90 | 1.01 | 1.19 | 1.98 | 2.20 | 2.16 | 1.94 | 1.27 | 0.86 |
| 042865-4 | 0.50 | 0.91 | 1.01 | 1.19 | 1.78 | 2.38 | 2.38 | 1.71 | 1.19 | 0.87 |
| 042865-5 | 0.50 | 1.19 | 1.35 | 1.56 | 1.76 | 2.38 | 2.79 | 2.28 | 1.70 | 1.01 |

TABLE 10

CALCULATED DIMENSIONLESS TEMPERATURE RISE AND DIMENSIONLESS VELOCITY DATA FOR CHANNEL BURNERS--CHROMEL-ALUMEL THERMOCOUPLES

| Run No. | $\Omega_L$ | $\theta_L$ For Thermocouple Number and (y,z) Coordinate | | | | | | | | | | | |
|---|---|---|---|---|---|---|---|---|---|---|---|---|---|
| | | 1 | 2 | 3 | 4 | 5 | 6 | 7 | 8 | 9 | 10 | 11 | 12 |
| | | (4,1) | (4,2) | (4,3) | (4,4) | (4,5) | (4,6) | (4,7) | (3,6) | (3,5) | (3,4) | (3,3) | (3,2) |
| 041565-1 | 0.48 | 1.36 | 1.57 | 0.89 | 0.86 | 0.97 | 1.03 | 1.03 | 1.03 | 1.03 | 0.87 | 0.92 | 1.39 |
| 041565-2 | 0.65 | 0.88 | 0.55 | 0.57 | 0.82 | 0.90 | 0.91 | 0.96 | 0.96 | 0.96 | 0.80 | 0.63 | 0.55 |
| 041565-3 | 0.84 | 0.86 | 0.58 | 0.52 | 0.52 | 0.35 | 0.35 | 0.37 | 0.37 | 0.37 | 0.37 | 0.57 | 0.60 |
| 041565-4 | 0.52 | 1.33 | 1.77 | 0.43 | 0.93 | 1.83 | 1.87 | 1.87 | 1.87 | 1.87 | 0.98 | 1.32 | 1.54 |
| 041565-5 | 0.58 | 1.60 | 0.83 | 1.13 | 1.27 | 1.27 | 1.27 | 1.24 | 1.24 | 1.27 | 1.24 | 1.18 | 0.77 |
| 041565-6 | 0.74 | 0.83 | 0.46 | 0.43 | 0.43 | 0.40 | 0.62 | 0.70 | 0.59 | 0.43 | 0.43 | 0.43 | 0.43 |
| 041565-7 | 0.90 | 0.56 | 0.43 | 0.38 | 0.38 | 0.35 | 0.35 | 0.43 | 0.40 | 0.40 | 0.40 | 0.43 | 0.43 |
| 041565-8 | 1.12 | 0.37 | 0.37 | 0.35 | 0.32 | 0.32 | 0.32 | 0.35 | 0.32 | 0.35 | 0.32 | 0.37 | 0.37 |
| 041665-1 | 0.42 | 1.20 | 2.11 | 1.56 | 1.12 | 1.15 | 1.14 | 1.14 | 1.15 | 1.21 | 0.55 | 1.42 | [illegible].52 |
| 041665-2 | 0.52 | 2.00 | 2.39 | 1.38 | 1.08 | 1.23 | 1.22 | 1.19 | 1.25 | 1.30 | 0.99 | 1.22 | 2.30 |
| 041665-3 | 0.68 | 2.13 | 1.37 | 1.41 | 1.38 | 1.25 | 1.19 | 1.21 | 1.25 | 1.29 | 1.29 | 1.42 | 1.34 |
| 041665-4 | 0.78 | 1.55 | 1.20 | 0.91 | 0.83 | 0.87 | 0.87 | 1.03 | 0.90 | 0.90 | 0.68 | 0.88 | 1.20 |
| 041665-5 | 0.42 | 1.54 | 2.18 | 1.65 | 1.16 | 1.18 | 1.15 | 1.14 | 1.17 | 1.21 | 1.10 | 1.62 | 2.43 |
| 041665-6 | 0.59 | 2.59 | 2.25 | 1.28 | 1.17 | 1.28 | 1.21 | 1.20 | 1.24 | 1.31 | 1.12 | 1.29 | 2.10 |
| 041665-7 | 0.68 | 2.82 | 1.54 | 1.54 | 1.50 | 1.28 | 1.26 | 1.27 | 1.29 | 1.35 | 1.38 | 1.54 | 1.45 |
| 041665-8 | 0.80 | 1.66 | 2.12 | 0.93 | 0.61 | 0.57 | 0.74 | 0.87 | 0.79 | 0.57 | 0.52 | 0.89 | 1.14 |
| 041665-9 | 0.40 | 1.46 | 1.63 | 1.46 | 1.08 | 1.05 | 1.05 | 1.01 | 1.05 | 1.05 | 1.08 | 1.44 | 1.93 |
| 041665-10 | 0.59 | 2.65 | 1.96 | 1.53 | 1.49 | 1.43 | 1.29 | 1.26 | 1.27 | 1.39 | 1.47 | 1.51 | 1.74 |
| 041665-11 | 0.76 | 2.38 | 1.99 | 1.84 | 1.67 | 1.40 | 1.36 | 1.28 | 1.31 | 1.36 | 1.60 | 1.72 | 1.74 |
| 042365-1 | 0.36 | 0.46 | 0.48 | 0.67 | 0.76 | 1.06 | 1.36 | 1.54 | 1.42 | 1.18 | 0.91 | 0.70 | 0.76 |
| 042365-2 | 0.59 | 1.48 | 2.15 | 1.73 | 1.48 | 1.48 | 1.64 | 1.64 | 1.64 | 1.58 | 1.58 | 1.82 | 2.18 |
| 042365-3 | 0.76 | 2.70 | 1.12 | 0.82 | 0.76 | 0.76 | 0.76 | 1.12 | 0.85 | 0.76 | 0.76 | 0.73 | 0.97 |
| 042365-4 | 0.33 | 0.49 | 0.53 | 0.73 | 0.86 | 0.99 | 1.31 | 1.59 | 1.29 | 0.91 | 0.76 | 0.58 | 0.53 |
| 042365-5 | 0.60 | 2.00 | 1.88 | 1.29 | 1.15 | 1.19 | 1.32 | 1.28 | 1.28 | 1.18 | 0.96 | 0.83 | 1.57 |
| 042365-6 | 0.68 | 1.91 | 0.67 | 0.57 | 0.82 | 1.01 | 1.14 | 1.21 | 1.16 | 1.06 | 0.83 | 0.47 | 0.62 |
| 042365-7 | 0.86 | 1.88 | 0.59 | 0.51 | 0.43 | 0.35 | 0.40 | 0.49 | 0.41 | 0.40 | 0.43 | 0.40 | 0.57 |
| 042665-1 | 0.37 | 0.87 | 0.98 | 1.26 | 1.17 | 1.38 | 1.63 | 1.81 | 1.60 | 1.34 | 1.17 | 0.94 | 0.91 |
| 042665-2 | 0.72 | 1.62 | 2.08 | 1.01 | 1.70 | 1.81 | 2.00 | 2.02 | 2.02 | 1.87 | 1.77 | 2.12 | 2.24 |
| 042665-3 | 0.50 | 1.00 | 1.13 | 1.44 | 1.57 | 1.68 | 1.81 | 1.90 | 1.82 | 1.73 | 1.61 | 1.44 | 1.23 |
| 042665-4 | 0.80 | 2.45 | 1.31 | 1.55 | 2.00 | 2.11 | 2.21 | 2.18 | 2.20 | 2.16 | 1.96 | 1.54 | 1.62 |
| 042665-5 | 0.35 | 0.92 | 1.04 | 1.24 | 1.29 | 1.41 | 1.62 | 1.78 | 1.57 | 1.35 | 1.25 | 1.07 | 1.06 |
| 042665-6 | 0.69 | 2.24 | 1.86 | 1.55 | 1.66 | 1.92 | 2.01 | 1.96 | 1.98 | 1.86 | 1.72 | 1.98 | 2.24 |
| 042665-7 | 0.48 | 1.00 | 1.16 | 1.36 | 1.44 | 1.53 | 1.70 | 1.80 | 1.76 | 1.59 | 1.39 | 1.25 | 1.12 |
| 042665-8 | 0.91 | 1.60 | 0.81 | 0.95 | 1.01 | 1.38 | 1.59 | 1.74 | 1.58 | 1.44 | 1.13 | 1.00 | 0.93 |
| 042665-9 | 0.56 | 1.14 | 1.14 | 1.31 | 1.39 | 1.48 | 1.57 | 1.68 | 1.61 | 1.57 | 1.49 | 1.39 | 1.18 |
| 042665-10 | 0.64 | 1.48 | 1.76 | 1.53 | 1.68 | 1.87 | 1.95 | 2.09 | 1.91 | 1.84 | 1.73 | 1.57 | 1.79 |
| 042865-1 | 0.69 | 1.72 | 2.81 | 2.81 | 2.40 | 2.35 | 2.40 | 2.44 | 2.40 | 2.35 | 2.35 | 2.72 | 3.09 |
| 042865-3 | 0.32 | 0.97 | 1.04 | 1.12 | 1.38 | 2.13 | 2.91 | 3.54 | 2.76 | 3.13 | 1.46 | 1.19 | 1.04 |
| 042865-4 | 0.50 | 0.98 | 1.05 | 1.07 | 1.14 | 1.99 | 2.55 | 3.21 | 2.52 | 1.92 | 1.48 | 1.10 | 1.05 |
| 042865-5 | 0.50 | 0.95 | 1.11 | 1.23 | 1.70 | 2.12 | 2.62 | 3.15 | 2.42 | 1.96 | 1.76 | 1.27 | 1.11 |

# APPENDIX B

## FURTHER CONSIDERATION OF BURNING RATE AND RADIATION DATA

Some of the information obtained from the wind tunnel studies can be manipulated in such a way as to compare it with data from the literature. These comparisons lead to the conclusion that more data should be obtained for fires burning under calm conditions, with careful attention being paid to the burning rates and heat transfer mechanisms.

According to the results of work at the Bureau of Mines, (9, 10, 11, 60) the regression rate of liquids burning in large diameter pans is

$$v_\infty = 0.0076 \frac{\Delta H_c}{\Delta H_v} \qquad \text{(B-1)}$$

where $v_\infty$ is in cm/min. Rearranging Equation (B-1) gives

$$\frac{(\Delta H_c/\Delta H_v)}{v_\infty} = 132 \qquad \text{(B-2)}$$

It might be expected that the burning rate function $(\Delta H_c/\Delta H_v)/v$ would be constant for wind-blown pool fires under a constant wind velocity. A plot of liquid regression rates for circular burners modified to take into account the ratio of heats of combustion and vaporization is shown in Figure 40. The data for methanol are not included because methanol flames are non-luminous, and the burning rate mechanism of methanol is thought to be different from that of the other fuels. Although some data scatter is evident, lines have been drawn through the data and extrapolated to calm conditions. A cross-plot of the data is shown in Figure 41, where the burning rate function has been plotted as a function of the reciprocal of the burner diameter, with parameters of velocity. Extrapolation of the curves of Figure 41 to intercept the ordinate then gives the burning rate function for large diameter burners.

Two major differences appear when the results are compared with the Bureau of Mines data. The first is that the burning rates for large liquid fires obtained by extrapolating the present data are more than twice those found previously. The second is that the burning rate apparently increases until the pan diameter is larger than was previously expected. Indeed, an estimate based on Figures 40 and 41 shows that the pan diameter must be about 15 feet for the maximum burning rate to be reached. Even though these results are based on extrapolation of wind-blown fire data, they strongly indicate that further investigation of burning rates should be made, with particular emphasis on careful burner design and steady state burning techniques.

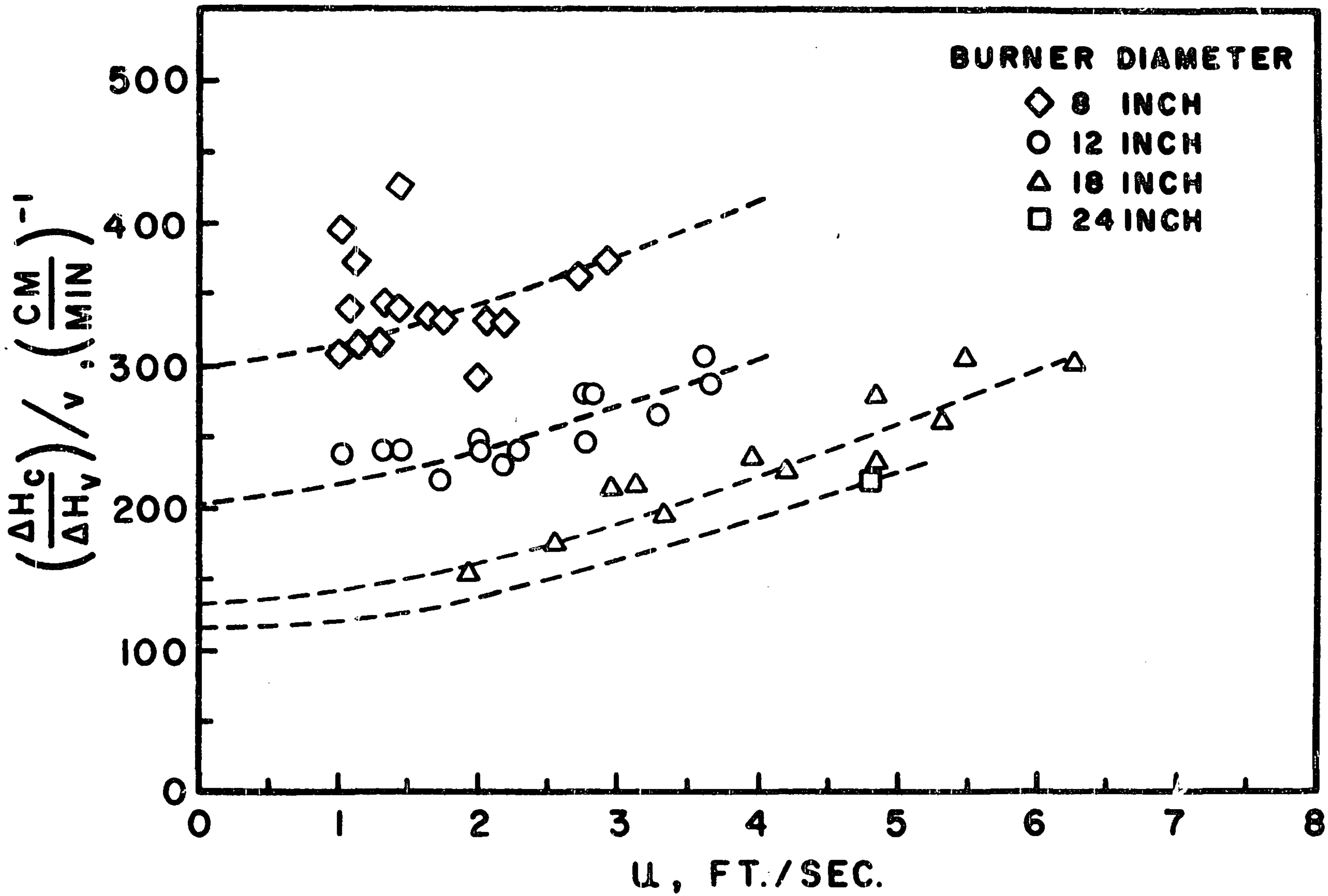


Figure 40. Burning Rate Functions for Liquid Fuels

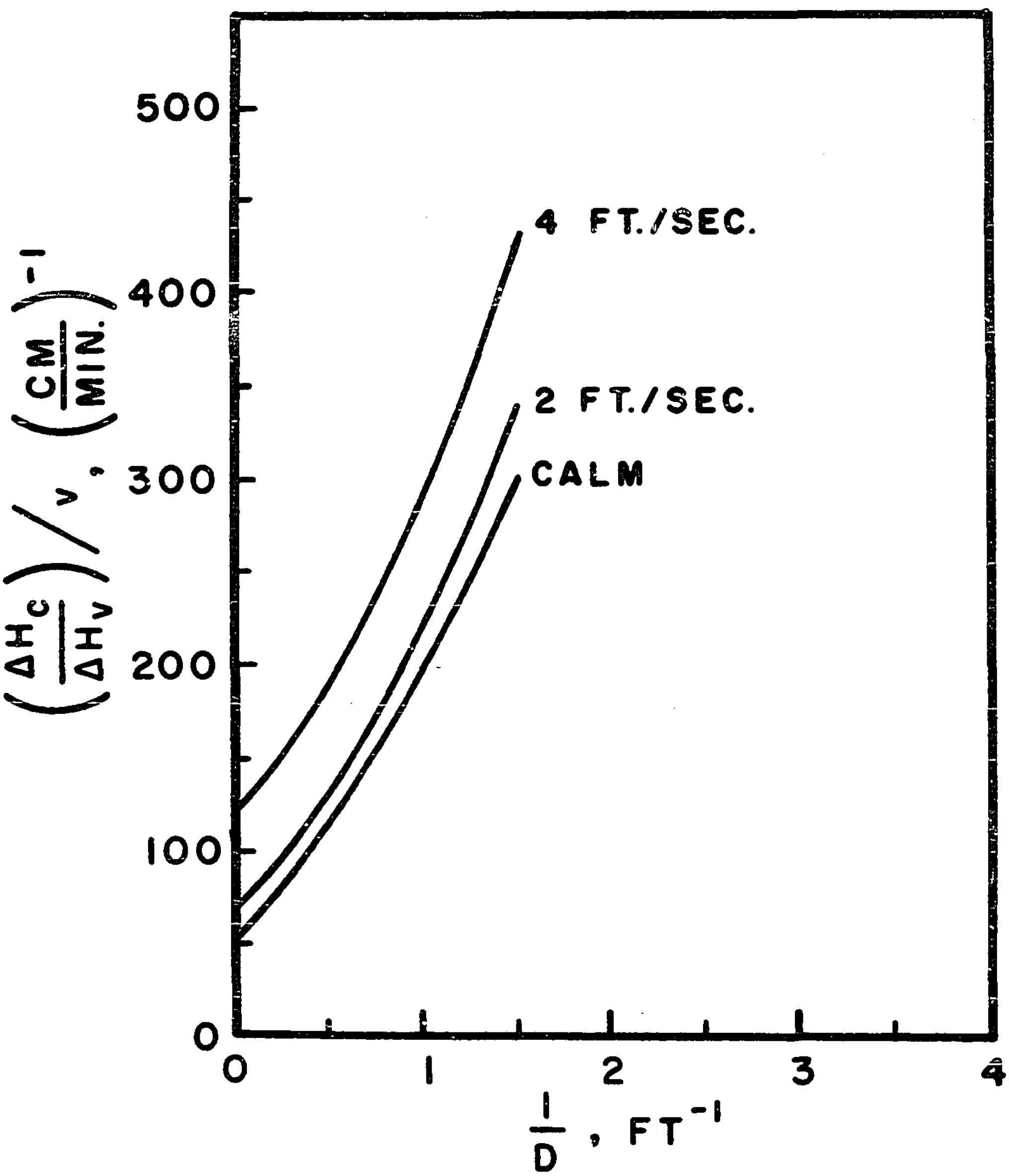


Figure 41. Extrapolation of Burning Rate Function

The amount of energy leaving a fire due to thermal radiation has often been expressed as a function of the total heat released from the fire. The radiation data from the present tests were used to estimate the ratio $Q_R/Q$, where $Q_R$ is the rate of energy release from the fire by radiation. In calculating $Q_R$, it was assumed that radiation received from the flame over a hemispherical shell was constant and equal to that at the single point where radiation measurements were made. For flames tilted by the wind such an assumption is obviously in error, but it does give an indication of the amount of radiation from a flame. The results showed about the same percentage of heat transfer from the flame as did the Bureau of Mines work. About 10 per cent of the energy from methanol fires was radiative, and 30 to 40 per cent of the energy released from hydrocarbon fires was in the form of radiation. The radiation data point out the need for obtaining more complete information on radiative heat transfer. Most work up to the present time has used spotty data from a few radiation measurements to estimate flame radiation. Tests should be made using a number of sensing elements located at different points around the flame in order to measure more accurately flame radiation. More comprehensive data would result in much better understanding of flame heat transfer mechanisms.